

Huh7.5 Cells Grown in Human Serum as a Model to Study the Effects of Hepatitis C
Virus Infection on Lipid Catabolism

by

Wilson Tat

A thesis submitted in partial fulfillment of the requirements for the degree of

Master of Science

in

Virology

Department of Medical Microbiology and Immunology
University of Alberta

© Wilson Tat, 2018

Abstract

Our goal is to study the additional elements of the mechanism of steatosis underlying hepatitis C virus (HCV) infection. Human hepatoma Huh7.5 cells cultured in human serum (HS) were used as a model to study the development of steatosis.

Huh7.5 cells grown in HS media were chosen to study the effects of HCV infection on lipid catabolism due to the increased expression of transcription factors associated with lipid catabolism compared to cells grown in fetal bovine serum (FBS) media. Here we show that cells grown in HS media have increased degradation of fatty acids through β -oxidation compared to cells grown in FBS media. This result was reflected by the increase in protein levels of carnitine palmitoyltransferase 1 (CPT-1), the rate limiting step of β -oxidation. Additionally, there was significantly higher production of ketone bodies in cells grown in HS media relative to FBS media. These ketone bodies are generated from the ketogenesis pathway that is downstream of β -oxidation. Finally, when these cells were grown in HS media compared to FBS media, there were larger lipid droplets and significantly more triglyceride. These results show that Huh7.5 cells cultured in HS have increased lipid metabolism compared to cells grown in FBS media.

During HCV infection, we showed that the rate of β -oxidation was significantly decreased. This reduction in β -oxidation was associated with the reduction of CPT-1 and reduction of ketone body production. The reduction in lipid catabolism observed during HCV infection was reflected with the increased lipid content in HCV infected

cells compared to uninfected cells. These results indicate that HCV infection leads to lower β -oxidation, potentially contributing to lipid accumulation and steatosis during HCV infection.

Acknowledgements

First and foremost, I would like to thank my mentor Dr. Lorne Tyrrell. Without his consistent help, dedicated support and guidance, this work would not have been possible. He is a visionary and inspiring mentor who is a constant reminder that behind every obstacle stands something even greater. Behind all his accomplishments stands an even more extraordinary individual who is always compassionate. Learning from Dr. Tyrrell has been a truly rewarding experience and a once in a lifetime opportunity.

I would like to thank Michael Houghton and Edan Foley for serving on my committee and providing me with critical suggestions to improve my thesis.

I am grateful to have Rineke Steenbergen as my lab supervisor. Without her guidance, I would have been completely lost. Also, I am grateful for her in helping me strive to work harder and become a better person.

I would like to thank Karl Fisher and Aviad Levin, both of whom have been extremely valuable in answering any questions I have, no matter how ridiculous they were. I would also like to thank both these wonderful individuals for putting up with my antics in the lab and making the time spent in the lab so much more enjoyable.

Darci Loewn-Dobler as the ‘lab mom’ and somebody whom I could talk to when I needed advice or a listener.

Tiing Tiing Chua, for all her help in the lab when I was busy or away. I am grateful for all the great conversations we’ve had and for putting up with my antics in the lab. I am truly lucky to be able to call her a friend.

There are a number of people around the lab with whom I would like to specifically thank. Chao Chen, for introducing me to research. Justin Shields and Karyn Berry-Wynne, for their technical help, without them I would have no idea how to complete half the assays in this thesis. Suellen Lamb, for her help with histology. Michael Joyce, for his very helpful advice. Bill Addison, for ordering all the materials I need no matter how expensive they were. Bonnie Bock, for fitting me into Dr. Tyrrell’s busy schedule. Cory Ebeling, Deanna Santer and Gillian Minty, for their help with my FACS experiments. John Law and Darren Hockman, for providing me with reagents. Evangelos Michelakis, Vikram Gurtu and Sotirios Zervopoulos for their help with the XFe24 analyzer.

Finally, I would like to thank my family for their continual support and encouragement throughout my studies.

Table of Contents

Chapter 1 – Introduction

1.1 Hepatitis C Virus Overview	
1.1.1 Global Health Burden of Hepatitis C Virus.....	2
1.1.2 The Discovery of HCV.....	3
1.1.3 Transmission.....	5
1.1.4 Clinical Course of HCV Infection.....	5
1.1.5 Therapies and Limitations.....	7
1.1.6 HCV Vaccines.....	9
1.2 Hepatitis C Virus Molecular Biology	
1.2.1 Virion Structure.....	10
1.2.2 Genome Characteristics.....	11
1.2.3 Protein Overview.....	12
1.2.4 Life Cycle	
1.2.4.1 Entry.....	16
1.2.4.2 Uncoating and Fusion.....	17
1.2.4.3 Replication.....	17
1.2.4.4 Assembly and Egress.....	18
1.3 Metabolism and the Effects of HCV Infection	
1.3.1 Metabolism of Glucose through Glycolysis.....	20
1.3.2 Disturbances of glucose Metabolism During HCV Infection.....	23
1.3.3 Lipid Metabolism.....	26
1.3.4 Formation of Lipid Droplets	26
1.3.5 Consumption of Lipid Droplets through Lipolysis.....	27
1.3.6 Disturbances of Lipid Metabolism during HCV Infection	
1.3.6.1 Increase Lipogenesis	30
1.3.6.2 Decrease Lipid Catabolism.....	32
1.3.6.3 Decrease Lipoprotein Secretion	32
1.3.7 The Warburg Effect: The Relationship between Glycolysis and Synthetic Pathways	33
1.4 Huh7.5 Cells as an <i>in vitro</i> Model to Study HCV.....	35
1.5 Objective and Hypothesis	
1.5.1 Objective.....	37
1.5.2 Hypothesis.....	37

Chapter 2 – Materials and Methods

2.1 Huh7.5 Standard Culture Conditions	
2.1.1 Huh7.5 FBS Cultured Cells.....	39
2.1.2 Huh7.5 HS Cultured Cells.....	40
2.1.3 Infection of Huh7.5 Cells.....	40
2.1.4 Treatment of HCV Infected Cells with Sofosbuvir to Determine Dose Response.....	41
2.1.5 Lipoprotein Depletion of Human Serum and Fetal Bovine Serum.....	41
2.2 Testing for Differentiation	
2.2.1 Determining VLDL Secretion with Fast Lipoprotein Liquid Chromatography (FPLC).....	42
2.2.2 Quantifying Albumin Secretion.....	42
2.3 HCV Quantification	
2.3.1 Production of HCV.....	44
2.3.2 HCV RNA Isolation.....	46
2.3.3 HCV RNA Quantification via qRT-PCR	46
2.3.4 Titering by Limiting Dilutions (50% Tissue Culture Infective Dose).....	48
2.3.5 Immunofluorescence Staining of HCV Core Protein.....	49
2.4 Coating Plates	
2.4.1 Coating Plates and Coverslips with Poly L Lysine.....	50
2.4.2 Plates with Collagen.....	50
2.5 Testing for Lipid Content	
2.5.1 BCA Protein Assay.....	51
2.5.2 Total Lipid Class Analysis by HPLC.....	52
2.5.3 Oil Red O Staining.....	53
2.5.4 Flow Cytometry.....	54
2.6 Assessment of Metabolism	
2.6.1 NMR Analysis of End Product Metabolites.....	55
2.6.2 Testing the Dependency of Glycolysis, β -oxidation and Glutaminolysis.....	55
2.6.3 Measuring Oxidation of Endogenous Fatty Acids.....	57
2.7 Western Blot Analysis.....	60
2.8 Statistical Analysis.....	62

Chapter 3 – Huh7.5 Cells Cultured in HS as a Model to Study HCV Infection

3.1 Culturing Huh7.5 Cells in HS Leads to Differentiation.....	64
3.2 Assessment of Metabolism	
3.2.1 Assessment of Metabolomic Profile of Huh7.5 Cells Cultured in HS or FBS Media.....	67
3.2.1.1 Arginine, Glycine and Proline Metabolism	68
3.2.1.2 Branched Carbon Amino Acid Metabolism.....	70
3.2.1.2.1 Isoleucine Degradation.....	70
3.2.1.2.2 Leucine Degradation.....	72
3.2.1.3 Methionine Metabolism.....	73
3.2.1.4 Phospholipid Metabolism.....	75
3.2.1.5 Glycolysis.....	77
3.2.1.6 Ketogenesis.....	79
3.2.2 Assessment of Metabolic Flux.....	80
3.2.3 Assessment of the Rate of β -oxidation.....	84
3.3 Assessment of Rate Limiting Step of β -oxidation.....	86
3.4 Assessment of Lipids	
3.4.1 Assessment of Lipid Droplets.....	88
3.4.2 Assessment of Total Lipid Content.....	88
3.4.2.1 Triglycerides and Fatty Acid Content.....	89
3.4.2.2 Phospholipid and Cholesterol Content.....	90
3.5 HS Differentiated Cells As a Model to Study HCV	
3.5.1 Assessment of HCV Production.....	94
3.5.2 Assessment of Specific Infectivity of HCV.....	95
3.5.3 Assessment of Proportion of HCV Infected Cells.....	97
3.6 Summary of Differences in Huh7.5 Cells Cultured in HS and FBS.....	101

Chapter 4 – The Effects of HCV Infection on Lipid Metabolism

4.1 Assessment of Metabolism during HCV Infection	
4.1.1 Assessment of Metabolomic Profile.....	104
4.1.1.1 Amino Acid Metabolism	
4.1.1.1.1 Arginine, Glycine and Proline Metabolism.....	105
4.1.1.1.2 Tryptophan Metabolism.....	106
4.1.1.1.3 Methionine Metabolism.....	107
4.1.1.1.4 Alanine Metabolism.....	109
4.1.1.1.5 Phenylalanine Metabolism.....	111
4.1.1.1.6 Leucine Metabolism.....	112
4.1.1.2 Phospholipid Metabolism.....	113
4.1.1.3 Glycolysis.....	114
4.1.1.4 Ketogenesis.....	117
4.1.2 Assessing the Metabolic Flux of Huh7.5 Cells during HCV Infection.....	118
4.1.3 Assessment of the Rate of β -oxidation.....	120
4.2 Assessment of CPT-1 Levels.....	122
4.3 Assessment of Lipid Content.....	123
4.3.1 Assessment of Total Lipid Content.....	124
4.3.1.1 Triglycerides and Fatty Acid Content.....	124
4.3.1.2 Phospholipid and Cholesterol Content.....	125
4.3.2 Assessment of Lipid Droplets using Flow Cytometry.....	129
4.4 Effects of Antiviral Therapy on Metabolism in HCV Infected Cells	
4.4.1 Assessment of HCV RNA following Sofosbuvir Treatment.....	131
4.4.2 Assessment of Ketone Body Production after Sofosbuvir Treatment.....	134
4.5 Summary of the Effects of HCV Infection.....	136

Chapter 5 – Discussion and Future Directions

5.1 Discussion and Future Directions.....	177
---	-----

Reference

Reference.....	153
----------------	-----

Appendix.....197

List of Figures

Figure 1.1 – Epidemiology of HCV Infection.....	3
Figure 1.2 - Clinical Course of HCV Infection.....	7
Figure 1.3 - The HCV Virion.....	11
Figure 1.4 – HCV Genome.....	12
Figure 1.5 – HCV Lifecycle.....	19
Figure 1.6 – The Glycolysis Pathway.....	22
Figure 1.7 – Mechanism of Insulin Resistance due to HCV Infection.....	25
Figure 1.8 – The Mechanism of HCV Induced Steatosis.....	29
Figure 3.1 – Albumin Secretion in Cells Grown in 2% HS and 10% FBS Supplemented Media.....	65
Figure 3.2 – Lipoprotein Profile of Huh7.5 Cells Cultured in 2% HS or 10% FBS Supplemented Media.....	66
Figure 3.3 – Arginine, Glycine and Proline Metabolism in Cells Cultured in Huh7.5 Cells Cultured Using 2% HS Supplemented or 10% FBS Media.....	69
Figure 3.4 – Isoleucine Metabolism in Cells Cultured in Huh7.5 Cells Cultured Using 2% HS Supplemented or 10% FBS Media.....	71
Figure 3.5 – Leucine Metabolism in Cells Cultured in Huh7.5 Cells Cultured Using 2% HS Supplemented or 10% FBS Media.....	73
Figure 3.6 – Methionine Metabolism in Cells Cultured in Huh7.5 Cells Cultured Using 2% HS Supplemented or 10% FBS Media.....	75
Figure 3.7 –Phospholipid Metabolism in Cells Cultured in Huh7.5 Cells Cultured Using 2% HS Supplemented or 10% FBS Media.....	76
Figure 3.8 – Glycolysis in Cells Cultured in Huh7.5 Cells Cultured Using 2% HS Supplemented or 10% FBS Media.....	78
Figure 3.9 –Ketogenesis in Cells Cultured in Huh7.5 Cells Cultured Using 2% HS Supplemented or 10% FBS Media.....	80

Figure 3.10 – Dependency of β -oxidation, Glycolysis and Glutaminolysis in Cells Cultured in Huh7.5 Cells Cultured Using 2% HS Supplemented or 10% FBS Media.....	83
Figure 3.11 – Endogenous β -oxidation, Maximum β -oxidation and Spare Capacity for β oxidation in Huh7.5 Cells Cultured using 2% HS Supplemented or 10% FBS Media.....	85
Figure 3.12 – CPT-1 Production in Huh7.5 Cells.....	87
Figure 3.13 – Lipid Droplets in Cells Cultured in Huh7.5 Cells Cultured Using 2% HS Supplemented or 10% FBS Media.....	88
Figure 3.14 –Triglyceride and Fatty Acid Content in Cells Cultured in 2% HS Media or 10% FBS Media.....	90
Figure 3.15 – Phospholipid Content in Cells Cultured in 2% HS Media or 10% FBS Media.....	92
Figure 3.16 –Cholesterol Content in Cells Cultured in 2% HS Media or 10% FBS Media.....	93
Figure 3.17 – HCV Production in Huh7.5 Cells in Two Different Culture Systems.....	95
Figure 3.18 – Specific Infectivity of HCV Produced in Huh7.5 Cells.....	96
Figure 3.19 – Proportion of Huh7.5 Cells Cultured in 2% HS Media Infected with HCV after 7 Days.....	98
Figure 3.20 – Proportion of Huh7.5 Cells Cultured in 2% HS Media Infected with HCV after 21 Days	99
Figure 3.21 – Proportions of Huh7.5 Cells Grown in 10% FBS Media Infected with HCV in the two Culture Systems.....	100
Figure 4.1 – Arginine, Glycine and Proline Metabolism in Huh7.5 Cells Cultured in 2% HS with or without HCV Infection.....	105
Figure 4.2 – Tryptophan Metabolism in Huh7.5 Cells Cultured in 2% HS with or without HCV Infection.....	107

Figure 4.3 – Methionine Metabolism in Huh7.5 Cells Cultured in 2% HS with or without HCV Infection.....	109
Figure 4.4 – Alanine Metabolism in Huh7.5 Cells Cultured in 2% HS with or without HCV.....	110
Figure 4.5 – Phenylalanine Metabolism in Huh7.5 Cells Cultured in 2% HS with or without HCV Infection.....	111
Figure 4.6 – Leucine Metabolism in Huh7.5 Cells Cultured in 2% HS with or without HCV Infection.....	112
Figure 4.7 – O-phosphocholine Metabolism in Huh7.5 Cells Cultured in 2% HS with or without HCV Infection.....	114
Figure 4.8 – Glucose Metabolism in Huh7.5 Cells Cultured in 2% HS with or without HCV Infection.....	116
Figure 4.9 – Ketogenesis in Huh7.5 Cells Cultured in 2% HS with or without HCV Infection.....	117
Figure 4.10 – HCV Infected and Uninfected Cells Cultured in 2% HS dependency on Glycolysis, β -oxidation and Glutaminolysis.....	119
Figure 4.11 – Endogenous β -oxidation, Maximum β -oxidation and Spare Capacity for β -oxidation in Huh7.5 Cells Cultured using 2% HS Supplemented Media with or without HCV Infection.....	121
Figure 4.11 – CPT-1 Protein Levels in Huh7.5 Cells Cultured in 2% HS media with or without HCV Infection.....	123
Figure 4.12 – Triglyceride and Fatty Acids Content in Huh7.5 Cells Cultured in 2% HS media with or without HCV Infection.....	125
Figure 4.13 – Phospholipid Content in Huh7.5 Cells Cultured in 2% HS media with or without HCV Infection.....	127
Figure 4.14 –Cholesterol Content in Huh7.5 Cells Cultured in 2% HS media with or without HCV Infection.....	128
Figure 4.14 – Bodioy493/503 Staining in Huh7.5 Cells Cultured in 2% HS media with or without HCV Infection.....	130

Figure 4.16 – HCV Production during Sofosbuvir Treatment in HCV Infected Huh7.5 Cells Cultured in 2% HS.....	133
Figure 4.17 – HCV RNA and Acetoacetate Production after 3µg/mL Sofosbuvir Treatment for 14 days in Infected Huh7.5 Cells Cultured in 2% HS.....	135
Figure 5.1 – Mechanism of HCV Induced Steatosis.....	146

List of Tables

Table 2.1 – JFH-1 Tissue Culture Adapted Virus Mutations.....	44
Table 2.2 – Concentration of Drugs Loaded onto Sensor Cartridges to Measure the Dependency of Glycolysis, β -oxidation and Glutaminolysis.....	57
Table 2.3 – The Instrument Run Protocol for Measuring the Dependency of Glycolysis, β -oxidation and Glutaminolysis.....	57
Table 2.4 – Concentration and Volume of Inhibitors used in Measuring Endogenous Fatty Acid Oxidation using the XF Analyzer.....	59
Table 2.5 – The Instrument Run Protocol for Measuring Endogenous Oxidation of Fatty Acids using the XFe24 Analyzer.....	59
Table 2.6 – Calculating the different aspects of β -oxidation.....	60
Table A.1 – Metabolites Secreted by Huh7.5 Cells Cultured in 2% HS Supplemented or 10% FBS Supplemented Media.....	197
Table A.2 – Metabolites Secreted by Huh7.5 Cells Cultured in 2% HS Supplemented or 10% FBS Supplemented Media.....	208

Last of Abbreviation

3HB	3-hydroxybutyrate
3PG	3-phosphoglycerate
aa	Amino acid
ACC	Acetyl-CoA carboxylase
ALT	Alanine aminotransferase
Apo	Apolipoprotein
ANGPTL3	Angiopoietin related protein 3
ATGL	Adipose triglyceride lipase
BCA	Bicinchoninic acid
BCAA	Branched carbon amino acid
BCKDH	Branched-chain alpha-keto acid dehydrogenase
CCT	CTP- phosphocholine cytidyltransferase
CDC	Centre for Disease Control and Prevention
cDNA	Copy deoxynucleic acid
C/EPT	Choline/ethanolamine phosphotransferase
CLDN1	Claudin 1
CMV	Cytomegalovirus
CPT-1	Carnitine palmitoyltransferase I
D1/D2	Domain 1/ Domain 2

DAA	Direct acting antiviral
DG	Diglyceride
DGAT1	Diglyceride acyltransferase
dFBS	Delipidated Fetal Bovine Serum
dHS	Delipidated Human Serum
dNTP	Deoxynucleotide triphosphate
DMEM	Dulbecco's modified eagle's medium
EBV	Epstein Barr virus
EGFR	Endothelial growth factor receptor
eIF	Eukaryotic initiation factor
ELISA	Enzyme-linked immunosorbent assay
ER	Endoplasmic reticulum
ERR α	Estrogen-related receptor alpha
ESC-RT	Endosomal sorting complexes required for transport
ESLD	End stage liver disease
F6P	Fructose 6 phosphate
F16P	Fructose 1,6 bisphosphate
FA	Fatty acid
FAT	Fatty acid translocase
FAS	Fatty acid synthase
FAM	6-carboxyfluorescein

FAO	Fatty acid oxidation
FBS	Fetal bovine serum
FOXO1	Forkhead box protein O1
FPLC	Fast protein liquid chromatography
G3P	Glyceraldehyde 3-phosphate dehydrogenase
G5S	Glutamate 5-semialdehyde
G6P	Glucose 6 phosphate
GAG	Glycosaminoglycans
GE	Genome equivalence
GLUT	Glucose Transporter
GLS	Glutaminase
HAV	Hepatitis A virus
HBV	Hepatitis B virus
HCC	Hepatocellular carcinoma
HCV	Hepatitis C virus
HDL	High density lipoprotein
HMB	β -hydroxy β -methylbutyrate
HMG-CoA	3-hydroxy-3-methylglutaryl-coenzyme A
HPLC	High Performance Liquid Chromatography
HS	Human serum
HSL	Hormone sensitive lipase

HVR	Hypervariable region
IF	Immunofluorescence
IFN	Interferon
Insig	Insulin signalling
IR	Insulin resistance
IRES	Internal ribosomal entry site
IR1	Insulin receptor 1
IRS	Insulin response substrate
IS-1	Internal standard 1
IVDU	Intravenous drug use
JFH	Japanese fulminant hepatitis
Kb	Kilobase
kDa	Kilodalton
LDL	Low density lipoprotein
LVP	Lipoviral particle
LXR	Liver X receptor
MAM	Mitochondrial associated membranes
MCM	Methylmalonyl CoA mutase
MPC	Mitochondrial pyruvate carrier
MG	Monoglyceride
mTOR	Mammalian target of rapamycin complex

MTP	Microsomal transfer protein
NANBH	NonA-nonB Hepatitis
NEAA	Non-essential amino acid
NLS	Nuclear localization signal
NMR	Nuclear magnetic resonance
NPC1L1	Niemann-Pick C1-Like 1
NS	Non-structural proteins
NTR	Nontranslated region
OAT	Ornithine aminotransferase
OCN	Occludin
OCR	Oxygen Consumption Rate
ORF	Open reading frame
OXPHOS	Oxidative phosphorylation
P5C	1-pyrroline-5-carboxylate
PCR	Polymerase chain reaction
PBS	Phosphate buffered saline
PBST	Phosphate buffered saline and 0.1% tween-20
PC	Phosphatidylcholine
PDC	Pyruvate dehydrogenase complex
PDME	Dipalmitoyl-phosphatidylmethylethanolamine
PE	Phosphatidylethanolamine

PEP	Phosphoenolpyruvate
PGC-1 α	Peroxisome proliferator-activated receptor gamma coactivator 1 α
PHH	Primary Hepatocyte
PI3K-AKT	Phosphatidylinositol-4,5-bisphosphate 3-kinase-protein kinase B
PLA2G4	Phospholipase A2
PLL	Poly L lysine
PPAR	Peroxisome proliferating activated receptor
PPP	Pentose phosphate pathway
PRR	Pattern recognition receptor
PTEN	Phosphatase and tensin homolog
qPCR	Quantitative polymerase chain reaction
qRT	Quantitative reverse transcription
RIPA	Radioimmunoprecipitation assay
RXR	Retinoid X receptor
SAM	S-adenosyl methionine
SCAP	Sterol regulatory element binding protein cleavage activating protein
SCID/ ALb-uPA	Severe Combine immunodeficient disease/ Albumin- urokinase-type plasminogen activator

SD	Standard deviation
SDS PAGE	Sodium dodecyl sulfate polyacrylamide gel electrophoresis
SER	Serine
SIRT1	Sirtuin 1
SOCS	Suppressor of cytokine signaling
SPP	Signal peptide peptidase
SRB1	Scavenger receptor B1
SRE	Sterol regulatory element binding protein response element
SREBP	Sterol regulatory element binding protein
SVR	Sustained virological response
TBST	Tris-buffered saline + 0.1% Tween20
TCID ₅₀	Tissue culture infectious dose 50
TEP	Triethyl phosphate
TEMED	Tetramethylethylenediamine
TG	Triglyceride
THF	Tetrahydrofolate
TIP47	Tail interacting protein 47
TMD	Transmembrane membrane domain
TSC	Tuberous sclerosis complex
VLDL	Very low density low lipoprotein

CHAPTER 1: Introduction

Chapter 1: Introduction

1.1 Hepatitis C Virus Overview

1.1.1 Global Health Burden of Hepatitis C virus

Hepatitis C virus (HCV) currently infects an estimated 71 million people worldwide according to the World Health Organization in 2015 with 3-4 million new individuals being infected each year (1–4). The percentage of infected individuals within a given country ranges from less than 2% of the total population in countries within North America and Western Europe, to more than 10% in Egypt (3,5,6). Presently, there are 7 genotypes of HCV that have been characterized, with more than 100 known subtypes. The prevalence of genotypes present in each country also varies. In North America and Western Europe, genotype 1 predominates while Egypt and the Middle Eastern countries predominantly have genotype 4 (Figure 1.1) (7–11).

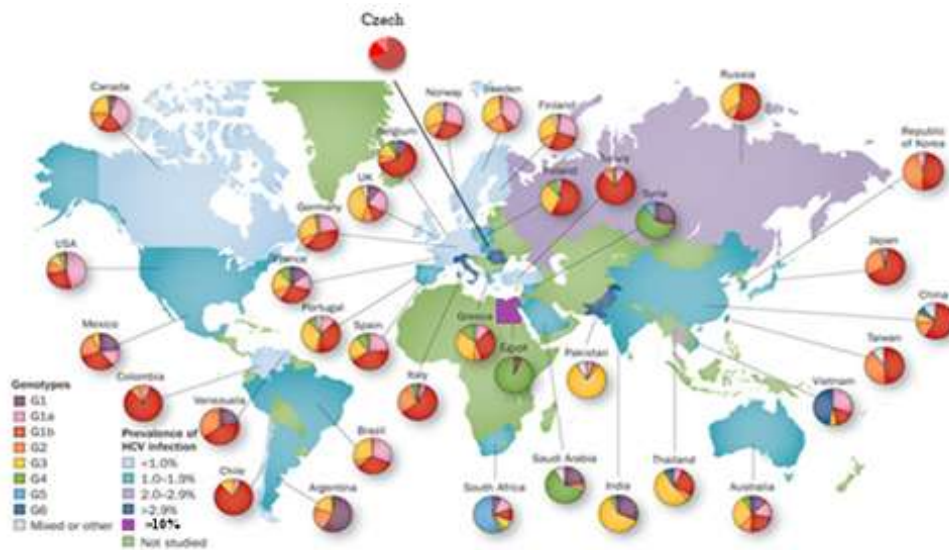


Figure 1.1 – Epidemiology of HCV Infection: The different colors found on each country depict the percentage of individuals infected with HCV. In North America, less than 2% of the population is infected with HCV, other countries such as Egypt have more than 10% of its population infected with HCV. The pie charts indicate the prevalence of each genotype within the respective country. Genotype 1a is especially prevalent in North America whereas genotype 1b is more prevalent in European countries. A total of 130-170 million people or 2-3% of the world’s population is infected with HCV worldwide. Adapted from Hajarizadeh *et al.* 2013 (6).

1.1.2 The Discovery of HCV

Prior to the early 1970s, there were only two known causes for viral hepatitis, hepatitis A virus (HAV) and hepatitis B virus (HBV) (12). However, some patients who received blood transfusion during this period developed post transfusion associated hepatitis that could not be linked to either HAV or HBV infections. Additionally, the patients who developed post-transfusion associated hepatitis did not develop antibodies specific to either HAV or HBV (13,14). In order to confirm the post transfusion hepatitis was not a consequence of other viral infections such as cytomegalovirus (CMV) and Epstein Barr virus (EBV) infections, sera of infected

patients were tested for antibodies against both these viruses (13,15–18). Their results showed that some patients were exposed to EBV prior to transfusion. Therefore, the post transfusion hepatitis did not arise from EBV infection. Furthermore, the exposure of some but not all patients to CMV after transfusion fails to explain post transfusion hepatitis in the unexposed patients. Thus, it was postulated that the causative agent was not HAV, HBV, CMV or EBV (13). This causative agent was given the name non-A,non-B hepatitis (NANBH) and it wasn't until over a decade later that the virus was characterized and termed HCV by a team led by Michael Houghton at Chiron Corporation(19).

A number of laboratories had tried unsuccessfully to identify a viral cause of NANBH. Dr. Houghton began the search for the agent in 1982 at Chiron Corporation by leading a team of co-investigators including Qui-Lim Choo and George Kuo. The team used NANBH infected chimpanzee sera provided by Daniel Bradley from the Center for Disease Control and Prevention (CDC). By creating a cDNA library from liver and plasma samples of NANBH infected chimpanzees and immunoscreening the cDNA library, eventually a single cDNA clone was isolated with the ability to hybridize a large single strand RNA approximately 10kb in size. The RNA strand possessed some sequence similarity with flaviviruses suggesting that it was of viral origin (20). It was termed HCV and assays were developed to detect HCV antibodies in biological fluids (21). This not only improved blood safety but also enabled epidemiology and allowed many studies to further characterize the virus.

1.1.3 Transmission

HCV is primarily transmitted through blood to blood contact. Blood transfusions were the primary cause for new infections before 1990 prior to implementation of screening programs. Another major form of transmission is intravenous drug use (IVDU) in countries within North America and Western Europe (22–26). In Asian countries such as China, Korea, Taiwan; Eastern European countries such as Romania and Hungary; and Middle Eastern countries such as Syria, unsafe medical procedures or improper sterilization of medical equipment remains a cause for new infections (8,27).

Additional methods of transmission include cultural practices such as bloodletting in Saudi Arabia and body modification procedures such as tattoos and piercings. In general, sexual transmission for HCV is uncommon but having multiple sexual partners or male to male sexual relations leads to increased chances of infection (16, 30). Furthermore, in Egypt, household transmission has been proposed to be a major cause of new infections (28–30). HCV can also be transmitted vertically from mother to child in 5% of all cases (31).

1.1.4 Clinical Course of HCV Infection

Often infections remain asymptomatic with only 20-30% of infected individuals presenting clinical symptoms such as malaise, nausea and jaundice 3-12 weeks post infection (32–34). However, within 2 weeks of infection, serum alanine aminotransferase (ALT), a marker of hepatocyte necrosis, and HCV RNA are present in the blood of infected individuals (32,33,35). In rare cases patients develop acute

fulminant hepatitis (36). Alternatively, 15-25% of infected individuals clear the infection, with production of HCV specific antibodies, loss of HCV RNA and normalization of ALT. However, 75-85% of the infected individuals progress to chronic HCV infection, meaning that the infected individual fails to clear the virus within 6 months (37,38). Less than 1% of chronically infected individuals with HCV will clear the virus spontaneously each year (39,40) .

The majority of chronically infected patients will develop some degree of liver fibrosis and approximately 55% will progress to more severe liver diseases such as steatosis, cirrhosis and hepatocellular carcinoma (HCC). After decades of chronic HCV infection, liver cirrhosis occurs in 10-20% of infected individuals (38,41). Often individuals do not realize they are infected with HCV due to the lack of clinical symptoms until the severity of the disease has progressed and complications of end stage liver disease (ESLD) or HCC arise. Generally, HCC occurs in a small proportion of those infected, usually if they have liver cirrhosis. Between 1-4% of patients with ESLD will develop HCC per year (38). Despite HCV primarily targeting hepatocytes, extrahepatic conditions such as autoimmune diseases, lymphoproliferative diseases, metabolic disorders and insulin resistance can occur (41-43) in HCV infected patients. Each year, conditions associated with chronic HCV infection lead to approximately 350 000 deaths worldwide (44).

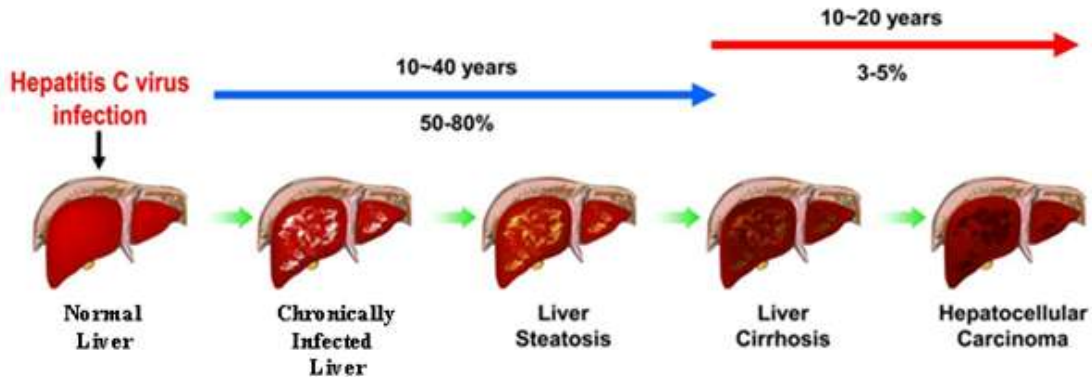


Figure 1.2 - Clinical Course of HCV Infection: When HCV infects hepatocytes, 50-80% of the infected individuals fail to clear the virus. After decades of infection, chronic HCV can result in steatosis, cirrhosis and HCC in 3-5% of the people that are infected. Adapted from Ke & Chan 2012 (38).

1.1.5 Therapies and their Limitations

The goal of treatment of HCV infection is to cure chronically infected patients. This is defined as being unable to detect HCV RNA in patient sera post therapy, in other words, achieving a sustained virological response (SVR). Initially, treatment of patients with chronic HCV was monotherapy with interferon α (IFN α) for 24 weeks. The rates of SVR with this therapy ranged from 5-20%. With the introduction of a combination therapy of the antiviral drug, ribavirin in conjunction with IFN α , SVR became 40-50% (45-49). Next, with the development of pegylated IFN α along with ribavirin, the rates of SVR increased to 54-63% depending on the genotype (45,48,50). This was standard treatment for patients who were chronically infected with HCV until 2013. Treatment with pegylated IFN α and ribavirin often led to

significant adverse effects including mild influenza-like symptoms, hemolysis, cardiotoxicity and central nervous system symptoms such as depression and aggression. Thus, treatment with IFN α and ribavirin required close monitoring for adverse effects. Poor tolerance of adverse effects and possible patient harm led to low adherence and frequent discontinuation of therapy (41).

Over the past few years, there has been a rapid evolution of therapy from the use of IFN α to the use of direct acting antivirals (DAAs). DAAs target multiple HCV proteins with improved effectiveness and reduced side effects compared to previous treatment regimens. Additionally, many of the new treatment regimens are delivered in a single tablet once per day for 8-12 weeks with a SVR greater than 95% depending regardless of the genotype that infected the patient. Moreover, these DAAs pose a high barrier to resistance, leading to a very low rate of relapse. Examples of new drugs that target HCV include Harvoni which was licensed in 2014 to treat patients that are infected with genotype 1, 4, 5 or 6 with 86-100% success. Harvoni is a combination of Ledipasvir and Sofosbuvir which are NS5a and NS5b inhibitors respectively (51). NS5a is a phosphoprotein that is involved in the regulation of the HCV lifecycle. On the other hand, NS5a is a RNA dependent RNA polymerase that is functions to replicate the HCV genome (52). Ledipasvir functions by binding to NS5a and preventing the interaction with other HCV proteins and host proteins (53). Sofosbuvir, alternatively, inhibits HCV replication by functioning as a nucleoside analogue leading to premature termination of the HCV RNA replication (51). Another DAA recently developed is Epclusa, a combination of Sofosbuvir and Velpatasvir, which are also NS5b and NS5a inhibitors used to treat patients infected with genotypes 1-6 with greater than 95% success (54). Other recently licensed DAAs for HCV include Technivie, Zepatier and Sunvepra (55–57).

One limitation of these contemporary treatments is accessibility. Factors such as cost and restriction of treatment to patients who have more advanced liver disease limits access to therapy. For example, 12 week treatments with DAAs may cost more than \$60,000, a prohibitive cost to patients lacking insurance coverage. Additionally, patients who are eligible to receive treatment are required to have moderately severe liver disease as indicated through a fibroscan score of at least F2 according to the METAVIR scoring system based on the degree of liver inflammation and liver fibrosis (51,58). Patients who achieve SVR do not have protective immunity and, consequently, are at risk of reinfection.

1.1.6 HCV Vaccines

A major medical need is a HCV vaccine. An estimated 3-4 million new infections occur each year and treated patients who achieve SVR may be reinfected with HCV. A prophylactic vaccine could prevent many of these new infections from occurring. An ideal vaccine would induce antibody and cellular immune responses against a large variety of viral epitopes in order to neutralize extracellular viruses (59–61). Several types of vaccines are currently under development and have shown promise. For example, a recombinant vaccine composed of HCV glycoproteins E1 and E2 is capable of eliciting a cross-neutralizing antibody response against different HCV genotypes in animal studies and human volunteers (62–65). Inactivated cell culture derived HCV inoculated into mice generates a protective humoral response (66,67). Another approach is to use DNA vaccines. DNA vaccines are composed of plasmids that encode part of the HCV genome. The plasmid directs expression of HCV proteins to stimulate a cellular immune response (68). Other vaccination strategies

include the use of synthetic HCV peptides, viral vectors expressing HCV proteins and HCV-like particles (61).

While some HCV vaccines have entered clinical trials (69) the quest to develop a HCV vaccine remains difficult due to a variety of host and viral factors. For example, the high genetic variation of HCV and resulting diversity of HCV proteins leads to difficulty in inducing a broad and long lived host immune response (70–72).

1.2 Hepatitis C Virus Molecular Biology

1.2.1 Virion Structure

The HCV virion is approximately 60nm in diameter and is composed of a lipid envelope and a nucleocapsid encapsulating the HCV genome (73). Embedded in the lipid envelope are dimers of two major glycoproteins E1 and E2. Beneath the lipid envelope is the nucleocapsid composed of core protein enclosing a positive single strand RNA.

HCV particles produced *in vivo* are complexed with cellular components such as apolipoprotein (apo) B and E and lipids to form lipo-viral particles (LVP). LVPs resemble very low density lipoproteins (VLDL) and low density lipoproteins (LDL) with densities ranging from 1.06 to 1.25g/mL (74–76). Evidence suggests that there is a direct interaction between ApoE and viral E1/E2 heterodimers. This interaction with lipoproteins may play a role in HCV binding and entry (75,77–79).

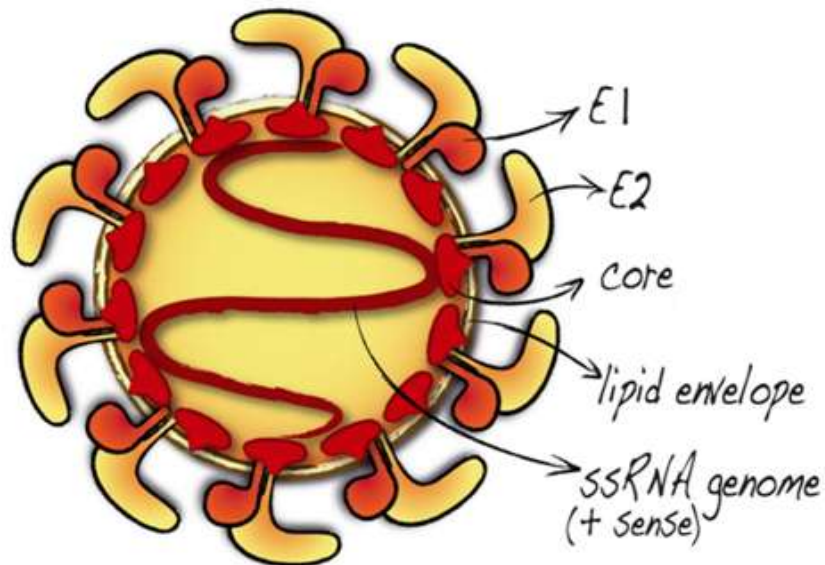


Figure 1.3 - The HCV Virion: The HCV particle is composed of E1 and E2 heterodimers found on the lipid envelope. Within the envelope is the nucleocapsid that is composed of core proteins. The nucleocapsid houses the positive sense single stranded RNA genome of HCV. Adapted from Thime *et al.* 2015 (80).

1.2.2 Genome Characteristics

HCV is a single stranded RNA virus belonging to the Flaviviridae family and the Hepacivirus genus (81). HCV has a 9.5 kilobase (kb) positive sense RNA genome with a single open reading frame (ORF) flanked by non translated regions (NTRs) at the 5' and 3' ends of the RNA strand. The 5' NTR contains an internal ribosomal entry site (IRES) which recruits the 40S ribosomal subunit and eukaryotic initiation factor 3 (eIF3) to initiate translation of the ORF and produce a single polyprotein (82). The ORF codes for structural proteins and non-structural (NS) proteins. Structural proteins include core and glycoproteins E1 and E2 which form the virus

particle. NS proteins include p7 protein, NS2 protease, NS3-4a complex with protease and helicase activity, NS4b, NS5a, and NS5b RNA dependent RNA polymerase (52).

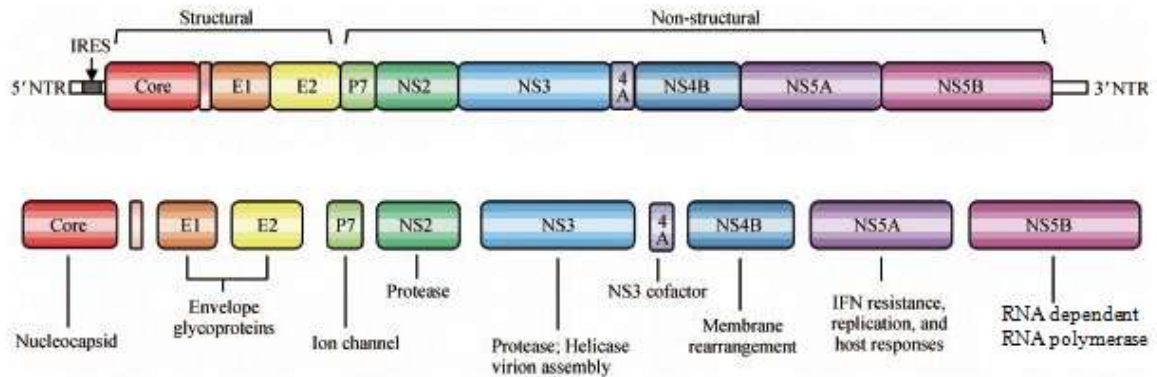


Figure 1.4 – HCV Genome: HCV uses a single strand positive RNA genome. The 5' and 3' end do not code for proteins and are referred to as NTR. The HCV proteins are translated as a polyprotein that is composed of structural proteins and nonstructural proteins. Structural proteins include core, E1 and E2 whereas non structural proteins include p7 ion channel, NS2 protease, N3-4a protease/ helicase, NS4b, NS5a and NS5b. IRES present at the 5' end of the genome initiates the translation of the HCV polyprotein. Adapted from Kao *et al.* 2012 (83).

1.2.3 Protein Overview

The HCV RNA is translated in the cytoplasm to produce the first member of the polyprotein, core. Immediately after the core is the signal sequence which causes the translocation of the polyprotein into the ER lumen. There, the host signal peptide peptidase (SPP) cleaves core to yield a 191 amino acid (aa) immature core protein which undergoes additional cleavage by SPP at its C terminal end to produce a

mature 177aa core protein (84–86). Signalase then cleaves the polyprotein in the lumen of the ER to produce the mature proteins E1, E2 and p7 (87,88). Next, NS2 cleaves in cis the NS2/NS3 junction to release NS3 from the remainder of the polyprotein. NS3 then proteolytically cleaves the junction between NS5a and NS5b to yield NS5b and the polyprotein composed of NS4a to NS5a in trans. This intermediate is then cleaved between NS4a and NS4b to produce NS4b/NS5a polyprotein. Finally, the NS4b/NS5a polyprotein is cleaved by the NS3-4a protease to produce the individual proteins NS4b and NS5a (52,89). Each HCV protein plays a role in the lifecycle of HCV. A summary of each protein's function is listed below.

Core – the mature core protein is 21kDa in size is found as a membrane bound protein as a dimer (52). Core oligomerises with the HCV RNA to form the nucleocapsid of the HCV virion. It is composed of two domains, domain 1 (D1) and domain 2 (D2) which have exclusive functions. D1 has RNA chaperone activity which is needed to remodel and package RNA into the virion (90). Additionally, D1 interacts with a variety of host factors to alter cellular function (91). For example, it interacts with cellular proteins such as microsomal transfer protein (MTP) and diacylglycerol acyltransferase 1 (DGAT-1) leading to the development of steatosis (as discussed in section 1.3.6) (92–97). D2, on the other hand, interacts with the phospholipids present on the membrane of lipid droplets (98,99).

E1 and E2 – the envelope glycoproteins, E1 and E2 are 35 and 72 kDa respectively in size. They play a role in the assembly of infectious particle, entry and fusion with the endosome to release the HCV particle into the cytoplasm (52). Both E1 and E2 contain a single transmembrane domain (TMD) after signalase cleavage (52), the TMD functions to retain E1 and E2 at the membrane and aids in E1-E2 heterodimer

formation through formation of disulfide bonds (100). The formation of heterodimers has been implicated to play an active role in the budding of HCV. E2 is composed of 3 domains, D1, D2, and D3. D1 and D3 are associated with CD81 receptor binding while D2 is the loop associated with endosomal fusion (101). Truncated forms of E2 have also been implicated in the binding to surface receptors such as CD81, scavenger receptor B-1 (SRB-1), high density lipoprotein (HDL) receptor LDL receptor, claudin-1 and occludin (52).

P7 – p7 forms hexamers or heptamers which have cation channel activity and is associated with virus production (102–104). The function of p7 remains to be elucidated. One possibility is that it prevents acidification of cellular organelles and prevents premature conformational changes of HCV proteins (105).

NS2 – NS2 is a 20-22kDa protease that functions to auto-catalytically cleave the polyprotein using the NS3 N terminal to release NS3 from the rest of the polyprotein (103, 104). NS2 also plays a role in HCV assembly through interactions with other structural and non-structural proteins such as E1, E2, p7, NS3 and NS5a (79, 104–108).

NS3-4a Complex – NS3 is a multifunctional protein that possesses a serine protease at its N terminus that requires NS4a as a cofactor while the C terminus possesses NTPase/RNA helicase activity (109, 110). NS3-4a protein is found on membranes associated with the ER such as mitochondrial associated membranes (MAMs) (111, 112). The serine protease recognizes the cleavage sequences D/E-X-X-X-X-C/T and S/A-X-X-X which are found on a variety of cellular proteins. However, very few cellular proteins are cleaved by NS3-4a, suggesting additional mechanisms to control

specificity (113). The C terminus of NS3 couples ATP hydrolysis to the unwinding of double stranded RNA in an inchworm or ratchet-like fashion (116).

NS4b – NS4b is a 27kDa protein that induces the formation of the membranous web complex, the site for the HCV replication in the cytoplasm (117–119). In order to induce membranous web formation, NS4b must form trimers by C-terminal palmitoylation. NS4b also interacts with other viral proteins and possibly possesses NTPase activity (117, 118).

NS5a – NS5a is a 56-58kDa membrane associated phosphoprotein that is involved in a variety of processes that include HCV RNA replication, HCV particle formation, modulation of cell signaling pathways and modulation of the interferon response (79, 119). NS5a is composed of 3 domains, D1 and D2 are involved in RNA replication while D3 is essential in assembly through interactions with core protein (103, 120–122). Additionally, D1 is associated with binding to lipid droplets (126).

NS5b – NS5b is a 68 kDa RNA dependent RNA polymerase with a “right hand” shape. Its finger, palm, and thumb domains completely enclose the active site. NS5b binds single stranded RNA in a groove between finger and thumb domains while NTPs are taken up into the active site (52). NS5b synthesizes the complimentary negative sense RNA using the positive sense RNA as a template. Subsequently, NS5b also synthesizes the positive sense RNA strand from the negative sense RNA after NS3 NTPase/helicase activity unwinds the double stranded RNA complex (52).

1.2.4 Life Cycle

The lifecycle of HCV is summarized in Figure 1.5. Each step of the lifecycle will be discussed in further detail below.

1.2.4.1 Entry

It has been proposed that HCV infection is initiated when binding occurs between heparan sulfate proteoglycan syndecan 1 and LDL receptors present on the surface of hepatocytes, binds to ApoE present on the envelope of the HCV particle. Next, cellular receptors SRB1 and CD81 mediate high affinity attachment of the HCV particle. HCV interacts with SRB1 either directly through interaction with the hypervariable region (HVR) of E2 or through ApoB present in the LVP to unmask the binding site for CD81 (127–134). Following CD81 interaction with E2, activation of the epidermal growth factor receptor (EGFR) leads to activation of Ras (135). Activated Ras associates with CD81 and induces the lateral diffusion of CD81 in the membrane along with the HCV particle, to claudin 1 (CLDN1) (136). Additionally, CD81 may use Rho GTPase to move towards CLDN1 via actin cytoskeleton rearrangements (137). Receptors such as Niemann-Pick C1-like 1 (NPC1L1), occludin (OCLN) and transferrin receptor 1 have roles in HCV entry but their precise function remains unclear (130, 135, 136). Once the HCV particle reaches the tight junction where CLDN1 is located, it is taken up via clathrin and dynamin-dependent endocytosis (140).

1.2.4.2 Uncoating and Fusion

The HCV particle, along with CD81 and CDLN1, is taken into the cell by a retrograde actin transport mechanism and transferred to Rab5a positive early endosomes (141). During endosomal acidification, it has been proposed that the low pH causes viral protein E1 to interact with host cell receptors and undergo a rearrangement creating a fusion pore and releasing the HCV nucleocapsid into the cytosol (142–148). It was proposed that NPC1L1 may facilitate HCV fusion by interacting with the cholesterol present within the HCV envelope (149). Despite the extensive work done to elucidate the precise mechanism of fusion, uncoating and release of HCV RNA into the cytoplasm, it still remains unclear.

1.2.4.3 Replication

After uncoating translation of the HCV genome begins with the recruitment of ribosomes to the IRES present at the 5' end of the RNA genome. The cellular factor miR-122 promotes the translation of HCV RNA by binding to the 5' end of the HCV RNA (150). Additionally, miR-122 can also protect the HCV RNA from 5'-3' degradation by exonuclease and prevents the recognition of HCV RNA by PRR such as RIG-I to avoid immune recognition (148, 149). After processing of the polyprotein, both structural and non-structural proteins become associated with the ER. In order to replicate the RNA genome, NS4b along with other non-structural proteins induces membranous web formation (52). Additionally, core and NS5a recruit nuclear pore proteins to the membranous web to prevent proteins lacking nuclear localization sequences (NLS) from entering the membranous web. For

example, proteins such as pattern recognition receptors (PRR) that lack a NLS cannot enter the membranous web. The exclusion of PRRs from the membranous web prevents the detection of HCV RNA, thus, preventing the activation of an innate immune response (153–155). HCV RNA, core and replicase components have been found surrounding lipid droplets. NS5a interaction with Rab19 and Tail-Interacting Protein 47 (TIP47) are responsible for this interaction between HCV RNA and lipid droplets (156–159).

1.2.4.2 Assembly and Egress

Core protein homodimerizes and is loaded onto to lipid droplets by MAPK regulated cytosolic phospholipase A2 (PLA2G4) where it interacts with DGAT-1 at the lipid droplet surface (81, 96, 157, 158). The lipid droplet surface is considered to be the site of HCV assembly since inhibition of lipid droplet synthesis blocks HCV assembly (162). NS2 interacts with E1, E2 and p7 in order to move these proteins towards the virus assembly site at the surface of lipid droplets (104, 106–108). Other HCV nonstructural proteins such as NS3/4a, NS4b and NS5b also play a role in assembly of the HCV particle but their exact roles remain unclear (163–165). Overall, the mechanism of HCV assembly into a virus particle remains unclear (133).

The VLDL secretion pathway has been implicated in the egress of HCV since patient derived HCV virions contain ApoB, ApoC1 and ApoE (166–168). MTP, found at in the ER, lipidates ApoB within the lumen of the ER by adding triglyceride and phospholipids to ApoB (164, 166). Nucleocapsids present on lipid droplets then fuse with lipid-enriched ApoB, ApoC and ApoE complexes (163, 164). These then exit through the endosomal-sorting complex required for transport (ESC-RT) pathway to

release LVPs from the cell. However, it remains unclear how HCV buds from the ER to use the ESC-RT pathway (170)

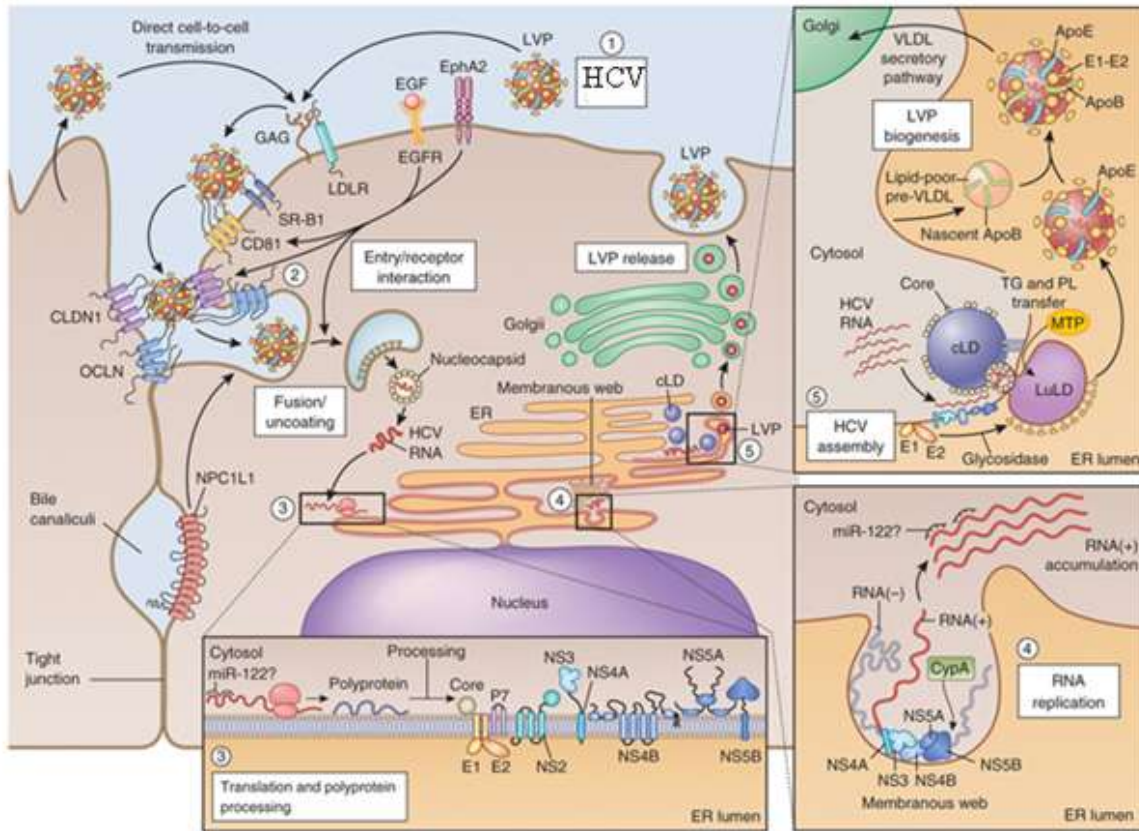


Figure 1.5 – HCV Lifecycle The HCV particle initiates infection by binding to glycosaminoglycans (GAGs) present on the surface of hepatocytes such as heparan sulfate proteoglycan syndecan 1. By binding GAGs, HCV E2 then binds to CD81 and SRB-1 which causes internalization of the HCV particle using CLDN1, OCLN with the help of other surface receptors such as EGFR and NPC1L1. The HCV particle uncoats within the endosomes, releasing the HCV RNA into the cytoplasm. Next, HCV RNA docks onto the ER where the polyprotein is produced, miR-122 has been implicated in this process. The polyprotein is cleaved to produce single proteins which create a membranous web structure where HCV RNA can be replicated. The HCV particle is then assembled on the surface of lipid droplets and released via the VLDL secretory pathway along with apoB and apoE. Adapted from Scheel & Rice 2013 (171).

1.3 Metabolism and the Effects of HCV Infection

Chronic infection with HCV causes metabolic changes leading to diseases such as metabolic syndrome, insulin resistance and steatosis (172). This is supported by studies that show the increased risk of these metabolic diseases in HCV infected individuals compared to individuals who are not infected with HCV. For example, there is a 2.5 fold increase in developing steatosis, characterized by the accumulation of lipids within the liver, in chronically infected patients compared to uninfected individuals (173,174). Several pieces of evidence suggest that HCV induces metabolic changes within the cells. First, HCV proteins increase oxidative stress of the cell, leading to changes in overall cellular metabolism (175). Second, microarray studies show that during HCV infection in chimpanzees, there are changes in expression of genes associated with lipid metabolism (176–178). The development of metabolic diseases such as insulin resistance and steatosis during infection is not surprising since both these diseases and the HCV lifecycle are closely linked with lipid metabolism (179).

1.3.1 Metabolism of Glucose through Glycolysis

Extracellular glucose is taken into the cytoplasm of hepatocytes by glucose transporter 2 (GLUT) (180). The glucose within the cell is metabolized through the glycolysis pathway where it is eventually converted into pyruvate. Each molecule of glucose entering this pathway yields 2 ATP, 2 NADH and 2 molecules of pyruvate (181). Glycolytic intermediates can also be shuttled to pathways associated with synthesis of macromolecules such as nucleotides, lipids and non essential amino acids

(NEAA). For example, glucose-6-phosphate (G6P) can enter the pentose phosphate pathway (PPP) to produce the pentose group in nucleic acids or glycogenesis to synthesize glycogen. Glyceraldehydes-3-phosphate (G3P) can be used to produce phospholipids and triglycerides while 3-phosphoglyceric acid (3PG) can be used to produce some NEAAs (178, Figure 1.5).

There are two possible fates for pyruvate in mammalian cells, either conversion to lactate or conversion to acetyl-CoA. If oxygen is limited, pyruvate is converted to lactate by anaerobic glycolysis. If oxygen is present, the mitochondrial pyruvate dehydrogenase complex (PDC) converts one molecule of pyruvate to one molecule of acetyl-CoA and one molecule of CO₂ (Figure 1.5). The acetyl-CoA can be further catabolized through the TCA cycle and oxidative phosphorylation (OXPHOS). Overall, glycolysis only generates 2 molecules of ATP while complete oxidation of glucose can generate up to 36 ATP molecules (181).

The amount of glycolysis that occurs within a hepatocyte is controlled by hormones such as insulin and glucagon. Insulin promotes glycogenesis and decreases the amount of glucose that is catabolized through glycolysis. Conversely, the hormone glucagon promotes formation of glucose via gluconeogenesis and increases its degradation through glycolysis (181).

Glycolysis

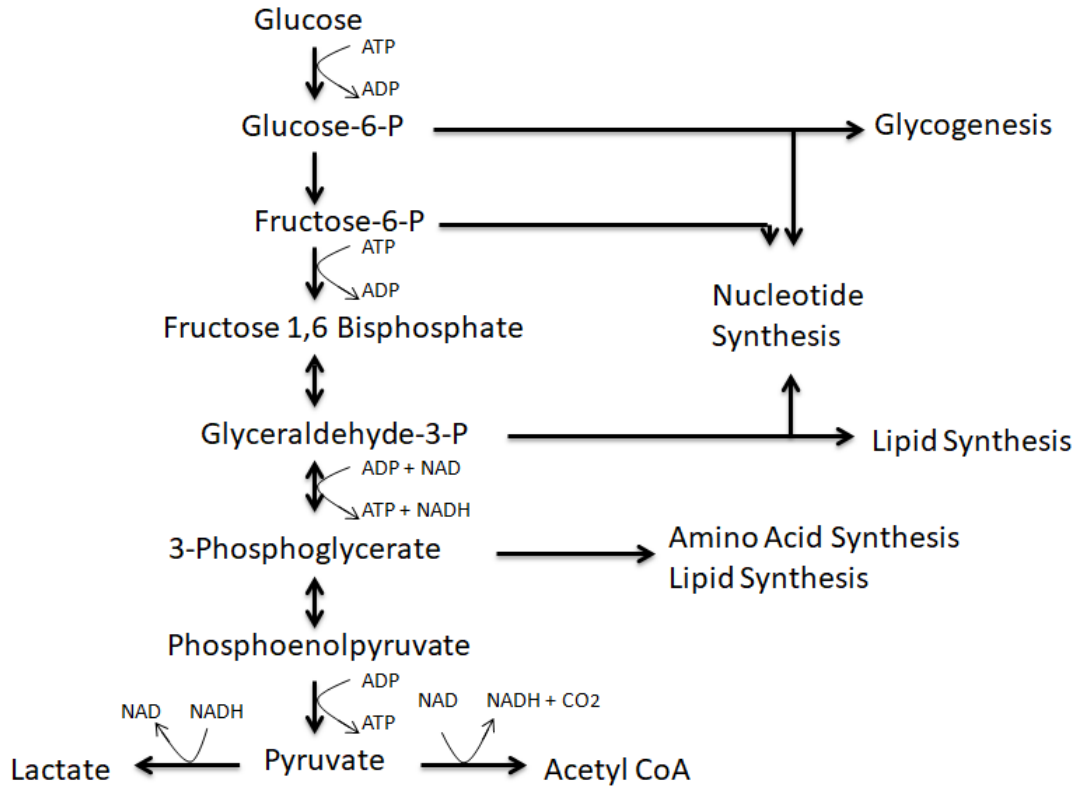


Figure 1.6 – The Glycolysis Pathway: In glycolysis, glucose is first converted to glucose-6 phosphate (G6P) using a single molecule of ATP. Next, G6P is converted to fructose-6-phosphate (F6P) at the expense of another molecule of ATP and rearranged to yield fructose 1, 6 bisphosphate (F16P). Next F16P is cleaved to produce 2 molecules of glyceraldehydes-3-phosphate (G3P). G3P is converted to 3-phosphoglycerate (3PG) while producing a molecule of ATP and NADH per molecule of G3P. Next, 3PG is used to generate phosphoenolpyruvate (PEP) which is then converted to yield pyruvate and a single molecule of ATP. There are two possible outcomes of pyruvate, either conversion to lactate to maintain a pool of NAD^+ or acetyl-CoA for oxidative phosphorylation (OXPHOS) in the mitochondria by the pyruvate dehydrogenase complex (PDC). The glycolysis pathway produces intermediates that are precursors for the synthesis of other molecules involved in cell division. For example, G6P, F6P and F16P are precursors for nucleotides. G3P and 3PG are precursors for lipids such as triglycerides.

1.3.2 Disturbances of Glucose Metabolism during Hepatitis C Virus Infection

There is evidence that infection with HCV causes the development of insulin resistance (IR) and type 2 diabetes in chronically infected patients. A study found the odds risk of developing type 2 diabetes in patients chronically infected with HCV compared to uninfected individuals is 3.77 (183). Additionally, it has been hypothesized that HCV-induced insulin resistance plays a role in the development of steatosis and increases the rate of fibrosis in chronically infected individuals (180, 181). The proposed mechanisms of insulin resistance in chronic HCV are summarized in Figure 1.7.

One mechanism involves HCV core mediated inhibition of insulin signaling by upregulating the phosphorylation of serine (SER) on insulin receptor substrate 1 (IRS1). SER phosphorylated IRS1 cannot interact with insulin receptor 1 (IR1) and is targeted for proteosomal degradation (182, 183). IRS1 is targeted for degradation by the inhibition of tuberous sclerosis 1 and 2 (TSC1/2) by HCV core protein (187). TSC1/2 negatively regulates mammalian target of rapamycin (mTOR). The inhibition of TSC1/2 leads to activation of mTOR and degradation of SER phosphorylated IRS1 (188). Lastly, HCV has also been found to degrade IR1 through a core mediated increase in expression of the suppressor of cytokine signaling (SOCS) family and TNF α production (189).

Overall, the reduction in IR signaling leads to a reduction in activity of phosphatidylinositol-4,5-bisphosphate 3-kinase - protein kinase B (PI3-AKT) signaling pathway (190). A reduction in PI3-AKT signaling ultimately results in impaired cellular response to insulin such as an increase in gluconeogenesis via

increase forkhead box protein (FOXO1) activity and a reduction in glucose uptake by downregulation of GLUT2 and GLUT4 (188).

Ultimately, by inducing insulin resistance in the infected hepatocytes, less glucose is taken up by the cell forcing it to rely on other means to compensate for the reduced glycolysis.

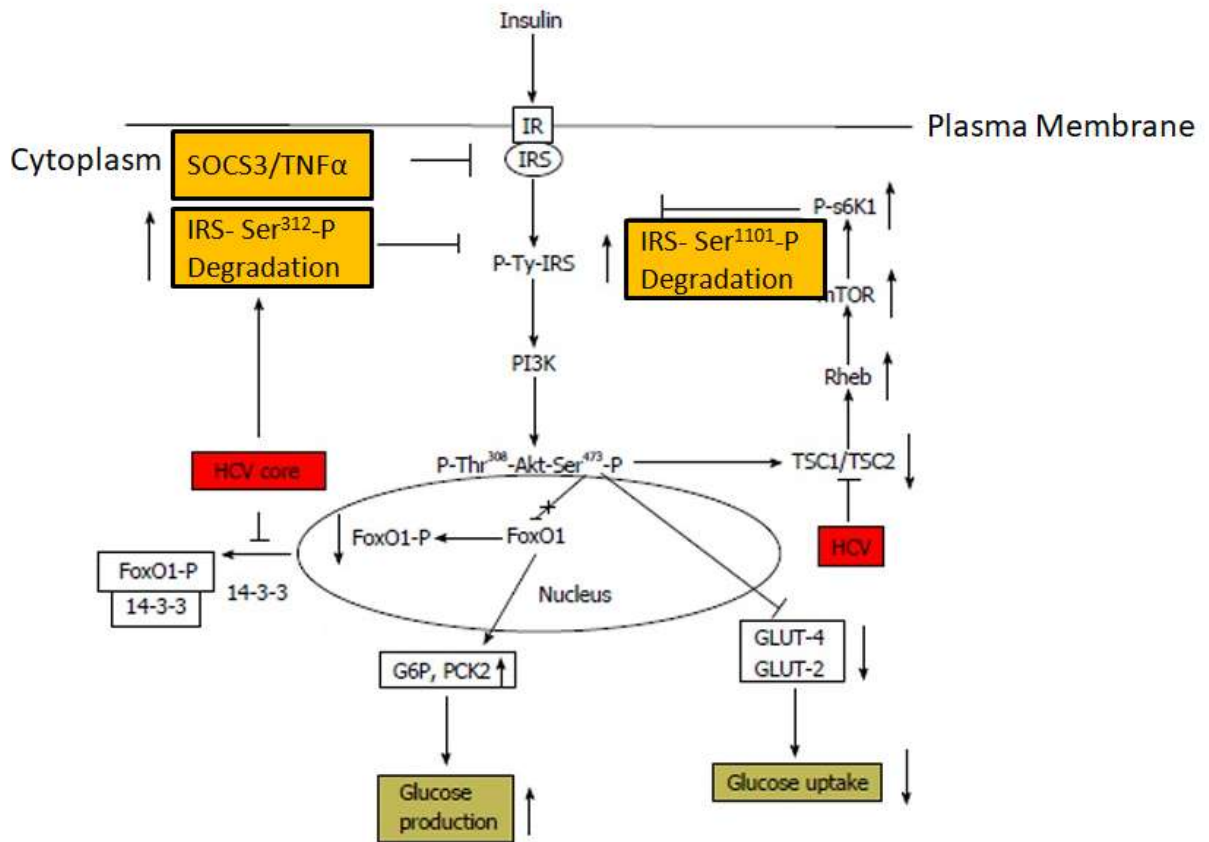


Figure 1.7 – Mechanism of Insulin Resistance due to HCV Infection: HCV can cause insulin resistance through a variety of mechanisms. HCV core increases the degradation of insulin receptor 1 (IRS) by increasing the phosphorylation of the serine residue rather than the tyrosine residue. Additionally, HCV induces suppressor of cytokine signaling (SOCS) and TNF α production which can lead to further degradation of IRS. Lastly, IRS can be degraded due to the inhibition of tuberous sclerosis (TSC) by HCV. The reduction in IRS signaling leads to a decrease in glucose uptake and increase in gluconeogenesis. Adapted from Bose & Ray 2014 (188).

1.3.3 Lipid Metabolism

The metabolism of lipid droplets is summarized in Figure 1.8. Lipid droplets can be considered an organelle composed primarily of triglyceride and sterol esters enclosed in a monolayer of phospholipids and cholesterol (187, 188). There are also proteins of the perilipin family that provide the lipid droplets with structural integrity, lipid synthesis enzymes, lipases and trafficking proteins (193–196). The metabolic pathways associated with lipid metabolism are regulated by the hormones insulin and glucagon. The presence of insulin stimulates synthesis of lipids while preventing lipolysis in the liver (197). Conversely, glucagon stimulates lipolysis by increasing expression of genes associated with lipolysis pathways in the liver (198).

1.3.4 Formation of Lipid Droplets

There are two ways cells acquire fatty acids in the liver, *de novo* synthesis or uptake of extracellular lipids. The triglycerides of extracellular lipoproteins are broken down by lipoprotein lipase found on the surface of cells. This releases fatty acids which are taken up by the fatty acid translocase (FAT) (195, 196).

Fatty acid can also be obtained via *de novo* synthesis consuming citrate from the TCA cycle. The citrate generated in the mitochondria is transported into the cytoplasm where it is converted to malonyl-CoA by fatty acid synthase enzymes. Through multiple reactions, malonyl-CoA units are joined to produce a fatty acid. The end product of the reaction is a fatty acid conjugated to a molecule of CoA which can be incorporated into triglyceride using enzymes of the glycerol-3-phosphate acyltransferase family to produce diacylglyceride (DG), the final step to produce

triglyceride is catalyzed by the enzyme DGAT-1. The newly synthesized triglyceride is then shuttled into the ER (201).

Sterols, another component of lipid droplets, are synthesized from mevalonate and deposited into the ER as a sterol ester using acyl-CoA cholesterol acyltransferase or obtained from the degradation of lipoproteins. Lastly, phospholipids are produced through glycerolipid synthesis pathways. The sterol esters, triglyceride and phospholipids present in the ER membrane bud from the ER to form the lipid droplet, the exact mechanism of this budding process remains elusive (201).

1.3.5 Consumption of Lipid Droplets through Lipolysis

The triglycerides present within lipid droplets are broken down by multiple enzymes to provide cells with energy. The first steps in degradation of triglyceride, catalyzed by adipose triglyceride lipase hydrolyze (ATGL), yields DG and a fatty acid. Next, hormone sensitive lipase (HSL), the rate limiting step of this pathway, converts DG to monoacylglycerol (MG) and another fatty acid. The last step, which yields a fatty acid and a glycerol, is catalyzed by monoacylglycerol lipase (201).

The fatty acid released by hydrolysis of triglyceride is shuttled into the mitochondria using the transporter carnitine palmitoyltransferase 1a (CPT-1). CPT-1, the rate limiting step of β -oxidation, is a protein found on the outer membrane of mitochondria. Each cycle of β -oxidation releases two carbons from the fatty acid in the form of acetyl-CoA. This process continues until the fatty acid is completely oxidized to form acetyl-CoA (202).

The acetyl Co-A produced by β -oxidation can enter either the TCA cycle or the ketogenesis pathway. The choice of pathways is determined by the concentration of acetyl-CoA in the mitochondria. At low concentrations, acetyl-CoA enters the TCA cycle where it reduces NAD^+ and FAD into NADH and FADH_2 . NADH and FADH_2 is oxidized at the electron transport chain to produce ATP by OXPHOS. However, when fatty acids are broken down by β -oxidation, excess acetyl-CoA is generated which enters the ketogenesis pathway to produce acetoacetate. The acetoacetate is spontaneously degraded to produce acetone or be converted into 3-hydroxybutyrate. Collectively, these compounds are referred to as ketone bodies and can be oxidized to provide cells with ATP (202). *In vivo*, the ketogenesis pathway is highly active within hepatocytes to produce ketone bodies that are used as an energy source in other organs such as the brain (203).

The metabolism of fatty acid is regulated by the transcription factor peroxisome proliferator-activated receptors α ($\text{PPAR}\alpha$) in hepatocytes. $\text{PPAR}\alpha$ is activated by the binding of ligands such as fatty acids. Activated $\text{PPAR}\alpha$ binds to promoter sequences upstream of multiple target genes to promote expression of proteins associated with uptake of fatty acids, intracellular fatty acid trafficking, β -oxidation, ketogenesis, triglyceride storage and lipolysis (200, 201).

1.3.6 Disturbances of Lipid Metabolism during Hepatitis C Virus Infection

Insulin resistance has been suggested to be one of the factors leading up to the development of steatosis otherwise known as fatty liver disease (see Section 1.3.2) which is characterized by the accumulation of triglyceride, in the form of lipid

droplets, in the cytoplasm of hepatocytes (206). Several mechanisms have been proposed to explain how HCV infection induces steatosis; they are summarized below (Figure 1.8).

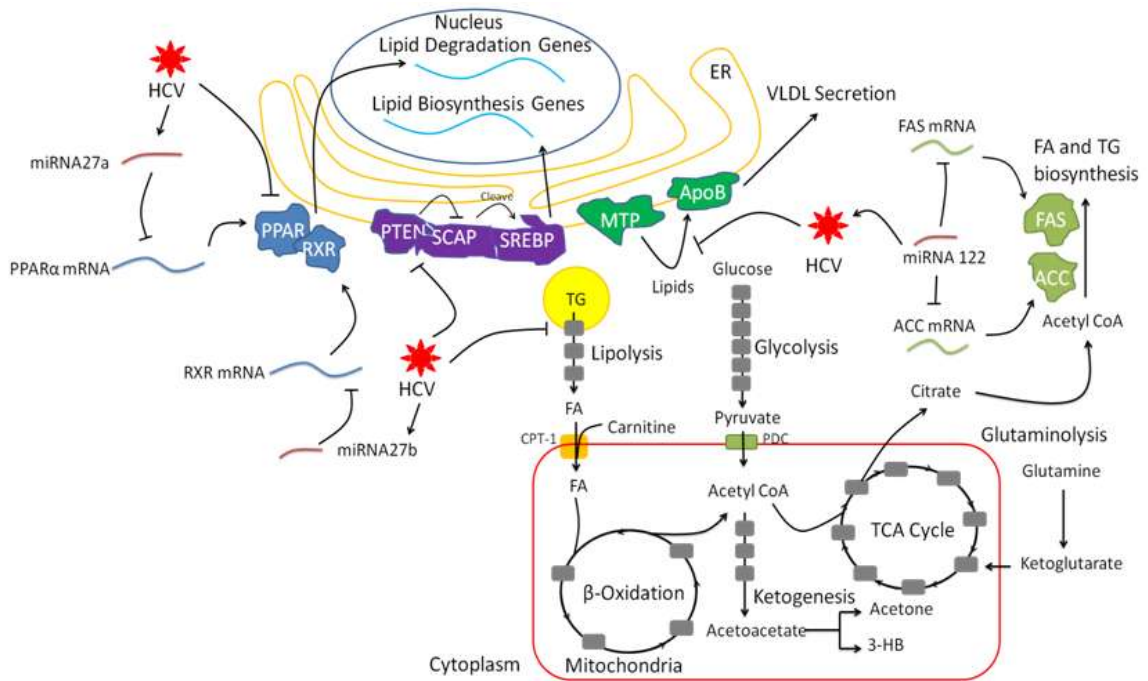


Figure 1.8 – The Mechanism of HCV Induced Steatosis: Phosphate and tensin homolog (PTEN) retains sterol regulatory element binding protein (SREBP) and SREBP cleavage activating protein (SCAP) in the endoplasmic reticulum (ER). Inhibition of PTEN and subsequent activation of SCAP leads to cleavage of SREBP to produce its active form. The active SREBP enters the nucleus to promote expression of genes associated with lipid synthesis. Peroxisome proliferate activated receptor α (PPAR α) interacts with retinoid X receptor (RXR) to promote expression of genes associated with lipid degradation. Both PPAR α and RXR mRNA are degraded by miR-27a and miR-27b. Microsomal transfer protein (MTP) lipidates apolipoprotein B (ApoB), leading to secretion of VLDL. Triglycerides (TG) found in lipid droplets undergo lipolysis to produce fatty acids (FA). FA is transported into the mitochondria by the mitochondria membrane bound protein, carnitine palmitoyl transferase 1a (CPT-1). These FA is oxidized by β -oxidation to yield one molecule of acetyl-CoA per cycle until it is completely oxidized. Another source of acetyl-CoA is glycolysis and the subsequent oxidation of

pyruvate by the pyruvate dehydrogenase complex (PDC). Acetyl-CoA can enter the TCA cycle where it is completely oxidized or the ketogenesis pathway to yield the ketone bodies acetoacetate, acetone and 3-hydroxybutyrate (3HB). Intermediates such as citrate in the TCA cycle are precursor of FA and TG. Another pathway that feeds into the TCA cycle is glutaminolysis. The citrate produced from the TCA cycle is exported into the cytoplasm where it can be converted to a fatty acid using acetyl-CoA carboxylase (ACC) and fatty acid synthase (FAS). Translation of FAS and ACC mRNA is inhibited by miR-122. HCV causes lipid accumulation by inhibiting PPAR, PTEN and MTP leading to decreased lipid degradation, increased lipid synthesis and decreased export of lipids. Additionally, increased miR-27 and preventing miR-122 from interacting with transcripts encoding for FAS and ACC leads to decreased lipid degradation and increased lipid synthesis. Each grey block indicates an enzymatic step within the respective pathway.

1.3.6.1 Increased Lipogenesis

One mechanism by which HCV induces steatosis is by increasing the synthesis of fatty acids which are deposited into lipid droplets as triglycerides. One way to increase fatty acid synthesis is by the activation of the transcription factor sterol regulatory element binding protein (SREBP) which is associated with lipogenesis and cholesterologenesis (178). There are three SREBP isoforms expressed in the liver, SREBP-1a, SREBP-1c and SREBP-2 (207). Usually SREBPs are retained in the ER along with SREBP cleavage activating protein (SCAP) by phosphatase and tensin homologue (PTEN) and insulin response proteins (Insig) 1 and 2 (204, 205). SCAP is a sensor for the levels of intracellular sterols and an escort for SREBP. When sterol levels are low, the active SREBP binds to SREBP response element (SRE) and increases expression of genes for cholesterol and lipid synthesis (210). HCV can activate SREBP through several mechanisms. First, HCV infection can induce oxidative stress which activates the PI3-AKT pathway. This leads to inactivation of PTEN, activation of SCAP, and leads to nuclear translocation of SREBP (211).

Second, the induction of NLRP3 inflammasome degrades Insig-1 and Insig-2 through caspase 1 cleavage leading to the activation of SREBP (210). Finally, HCV can increase transcription of SREBP itself by the activation of liver X receptor (LXR) by HCV NS2 protein. LXR then binds an element found in the SREBP promoter, leading to increased expression of cholesterol and lipid synthesis genes (212).

The second mechanism that HCV uses to increase fatty acid synthesis is to sequester miR-122. The HCV RNA acts as a “sponge” for miR-122 due to the need for miRNA to increase the stability and promote translation of the HCV RNA. By interacting with the HCV RNA, miR-122 cannot target transcripts encoding acetyl-CoA carboxylase (ACC) for degradation. ACC is the enzyme required to convert acetyl-CoA to malonyl-CoA, the building block for fatty acids. Additionally, miR-122 also targets transcripts that encode for fatty acid synthase (FAS) for degradation. By sequestering miR-122, the transcripts associated with fatty acid synthesis are no longer repressed and they are translated to produce proteins associated with fatty acid synthesis. Thus, leading to an increase in fatty acid synthesis (71, 209–211).

Finally, the last mechanism leading to increased triglyceride accumulation within HCV infected hepatocytes originates extracellularly. HCV infection leads to increased expression of miR-27b which targets the transcript coding angiopoietin-like 3 (ANGPTL3), an inhibitor of extracellular lipoprotein lipases, for degradation. By removing the inhibition of the extracellular lipases, more triglyceride is degraded to yield fatty acids which can be taken up by cells and converted back into triglyceride (212, 213).

1.3.6.2 Decreased Lipid Catabolism

Another mechanism to induce steatosis is to decrease β -oxidation of fatty acids. For example, during HCV infection, there is a downregulation of PPAR α . PPAR α is a nuclear receptor that is highly expressed in hepatocytes and induces expression of genes involved in the catabolism of fatty acid by β -oxidation and ketogenesis. The exact mechanism HCV uses to inhibit PPAR α function remains unclear. Expression of HCV core protein significantly reduces transcription of PPAR α transcripts and CPT-1 (212, 214–217). Additionally, there is evidence that miR-27a and miR-27b play a role in further decreasing PPAR α activity. MiR-27a targets transcripts for retinoid X receptor (RXR) leading to decrease activation of PPAR α . MiR-27b targets transcripts coding for PPAR α for degradation, reducing its expression. Both miR-27a and miR-27b are upregulated during HCV infection, decreasing expression of genes involved in lipolysis and β -oxidation and leading to lipid accumulation (212, 213, 218).

Additionally, core can interact with lipid droplets through DGAT-1, this can slow down the turnover of lipid droplets by preventing HSL from degrading triglyceride. Consequently this leads to a reduction in triglyceride degradation (97).

1.3.6.3 Decreased Lipoprotein Secretion

HCV infection can also lead to the accumulation of lipid droplets by reducing the amount of VLDL secreted by hepatocytes. MTP is found in the ER lumen stabilizing ApoB by lipidating ApoB. Lipidated ApoB can bind triglycerides to form VLDL which is exported from the cell. During HCV infection, a combination of core and

nonstructural proteins reduces MTP activity. This leads to an accumulation of intracellular lipids since less triglyceride is secreted from the cell in the form of VLDL (93, 95, 219).

1.3.7 The Warburg Effect: The relationship between Glycolysis and Synthetic Pathways

In 1924, Otto Warburg observed that cancer cells, unlike healthy cells, convert large amounts of glucose to pyruvate by glycolysis and subsequent conversion of pyruvate into lactate in the presence of oxygen. This process is termed aerobic glycolysis, the phenomenon where cells preferentially undergo glycolysis and fermentation despite having sufficient oxygen readily available for cells to utilize the TCA cycle and oxidative phosphorylation (OXPHOS) (224). This phenomenon is not limited to cancer cells as it is also seen in highly proliferative cells suggesting that aerobic glycolysis plays an important role in cell division (225,226).

It has been proposed that aerobic glycolysis is due to dysfunctional mitochondria but this hypothesis does not take into account that mitochondria found within cancer cells and rapidly proliferating cells are highly active (227–229). Contemporary theories suggest that aerobic glycolysis occurs to balance two needs of rapidly dividing cells: ATP production and production of intermediates needed for the synthesis of cell components (182). During aerobic glycolysis, 93% of glucose is converted to either lactate or alanine and secreted from the cell (230). By directing large amounts of pyruvate to lactate and alanine, rapidly proliferating cells can maintain a pool of glycolytic intermediates needed as substrate for the synthesis of amino acids,

nucleotides and lipids (231,232). For example, G6P can be used to produce nucleotides, G3P can be used to produce NEAA such as serine, glycine and cystine or it can be converted to phospholipids or triglyceride. Although most of the pyruvate is converted to lactate, some pyruvate enters the TCA cycle producing further substrates such as citrate needed to produce fatty acids and cholesterol (182).

It has been proposed that another function of increased lactate production stems from the regeneration of NAD^+ from NADH that is coupled to the reduction of pyruvate to lactate. The NAD^+ produced is needed for the conversion of G3P to 3PG. Thus, by maintaining a pool of NAD^+ , cells are able to maintain the flux of glycolysis needed to supply intermediates needed for the production of lipids, proteins and cholesterol required for the formation of a new cell (182).

Another characteristic of some cancer cells and other highly proliferative cells is the uptake of large amounts of glutamine needed to maintain a constant supply of NADPH. NADPH is generated by two methods, either through metabolism of glutamine through malate dehydrogenase enzyme or during the conversion of glutamine to lactate. NADPH is a cofactor required in large quantities in nucleotide, amino acid and lipid biosynthesis (230). Another function of glutamine is to replenish intermediates within the TCA cycle. This process is termed anaplerosis (230,233). Glutamine can enter the TCA cycle by the glutaminase pathway which converts glutamine into glutamate which then enters the TCA cycle as α -ketoglutarate (182).

1.4. Huh7.5 Cells as an *in vitro* Model to Study HCV

The Japanese fulminant hepatitis 1 (JFH) strain of HCV is often used as a model to study HCV infection in cell culture as it shows high rates of infection and replication efficiency without requiring any tissue adaptive mutations. Furthermore, it can infect and undergo its full replication cycle in a variety of cell lines such as HepG2, Huh7 and IMY-N9. JFH belongs to the genotype 2a cluster and was initially isolated from a fulminant hepatitis patient in 1999. The sequence analysis of the JFH-1 strain shows some variation within the 5'NTR, core, NS3 and NS5a compared to the sequences found in most genotype 2a viruses (234).

One cell line that is highly permissive to JFH infection relative to other cell lines is the human hepatoma Huh7 cells derived from the liver tumor from a Japanese patient in 1982 (235). Despite these cells supporting the full HCV lifecycle, infection of these cells with HCV was inefficient, averaging about 1 infected cell per 1 million cells (236). As a consequence, a cell line that was more permissive to HCV infection was needed. By transfecting Huh7 cells with HCV plasmids and isolating HCV positive cell, cells were subjected to prolonged IFN α treatment to eliminate the sub-genomic HCV. The Huh7.5 cell line was established when these cells were cleared of the sub-genomic HCV. It was shown that these cells were highly permissive to HCV infection compared to the parental Huh7 cell line (237).

The Huh7.5 cell line are usually cultured in fetal bovine serum (FBS) but culturing Huh7.5 cells in the presence of human serum (HS), results in the restoration of many hepatocyte specific characteristics, functions and processes (238). Restored hepatocyte characteristics include contact inhibition, morphology similar to primary hepatocytes, secretion of VLDL and increased secretion of albumin compared to cells

grown in FBS media. Other restored hepatocyte characteristics include production of transcripts associated with regulation of lipid metabolism such as LXR, PPAR α and PPAR γ (238). LXR is associated with cholesterol processing and secretion while both PPAR proteins are involved in mitochondrial function, fatty acid uptake, β -oxidation, triglyceride metabolism and overall lipid metabolism. Finally, when cultured in HS media, the cells produce more lipids compared to cells grown in FBS media (238,239).

Not only is there higher HCV production in cells grown in HS media, the virus produced also has different physical characteristics compared to virus produced in cells grown in FBS media. Notably, it has lower density compared to virus produced in cells grown in FBS media (238). The lower density is similar that observed in HCV isolated from patients which can be explained by the association of HCV particles with ApoB (77). A limitation of using hepatoma cells cultured in FBS to grow HCV is that VLDL secretion is absent in these cells. Thus, these cell culture systems cannot fully support a natural HCV replication cycle. The restored VLDL secretion in cells growing in HS media, this may allow the cells to better support HCV replication (240). Lastly, the virus produced in cells grown in HS have a specific infectivity of 1 in 236 particles compared to 1 in 2513 particles seen in virus produced by cells grown in FBS (238). Overall, the restoration of hepatocyte-specific characteristics, functions and processes in cells grown in HS suggest that it may be a better model to study HCV infection *in vitro* than cells cultured in the presence of FBS.

1.5 Objectives and Hypothesis

1.5.1 Objective

The objective of this project is to use Huh7.5 cells cultured in HS media as a model to study HCV-induced changes in host lipid catabolism.

1.5.2 Hypothesis

When Huh7.5 cells cultured in HS media are infected with HCV, the breakdown of fatty acid from triglyceride and subsequent degradation of fatty acid through β -oxidation will be reduced. This reduction in lipid catabolism in HCV infected cells may be one of the factors leading to lipid accumulation. To determine if there is a reduction in fatty acid oxidation in HCV infected cells, levels of the relevant metabolites and proteins and the rates of lipid catabolic pathways will be examined. By studying the reduction in fatty acid oxidation, we will provide direct evidence that there is a reduction in lipid catabolism during HCV infection.

CHAPTER 2: Materials and Methods

Chapter 2: Material and Methods

2.1 Huh7.5 Standard Cell Culture Conditions

The Huh7.5 cell line was derived from human hepatoma cells (235,237). These cells were cultured using Dulbecco's Modified Eagle's Medium 5796 (DMEM5796) (Sigma-Aldrich, Cat.# D5796-500ML) supplemented with either 10% FBS (Sigma-Aldrich, F1051-500ML) or 2% HS (Valley Biomedical, Cat.# HP1022) and 50 IU/mL penicillin and 10ug/mL streptomycin. These cells were maintained in a 5% CO₂ incubator at 37 °C (238).

2.1.1 Huh7.5 FBS Cultured Cells

The traditional method of culturing Huh7.5 cells uses DMEM5796 that was supplemented with 10% FBS. Cells were propagated twice a week at 25% seeding density. To propagate these cells when they were confluent, the monolayer was washed once with filter sterilized phosphate buffered saline (PBS) (136.9mM NaCl, 2.68mM KCl, 6.48mM Na₂HPO₄ and 0.866mM KH₂(PO₄)₂, pH 7.4). Next, cells were removed from the flask using trypsin digestion (107.3mM KCl, 6.84mM NaCl, 11.9mM NaHCO₃, 3.2mM Dextrose, 0.5g/L Trypsin and 0.5mM Disodium EDTA) incubated at 37 °C for several minutes. The flask was percussed and the trypsin reaction was inactivated using DMEM5796 supplemented with 10% FBS. Enough DMEM5796 was added to suspend the cells at 1 million cells/mL, in the case of T-75cm² flask, 2.5 million cells were added to the new flask. Cells were normally confluent 3-4 days after propagation (238).

2.1.2 Huh7.5 HS Cultured Cells

Huh7.5 cells were grown for a minimum for 21 days in the presence of 2% HS supplemented DMEM5796 to restore hepatocyte-specific functions and processes. When split, the trypsin was inactivated using DMEM5796 supplemented with 2% HS and seeding at 33% density into the new flask. After 4 days of growth, cells were removed from the plastic as described previously and seeded into a new flask at 50% density and the cells were maintained for a minimum of 17 additional days with media changes twice a week (238). Cells were cultured on Primaria tissue culture flasks (Corning, Cat.# 353810).

2.1.3 Infection of Huh7.5 Cells

Huh7.5 cells in either HS or FBS supplemented DMEM5796 were prepared as described above. However, to inactivate the trypsin reaction, HS and FBS supplemented media was replaced with 2% delipidated HS (dHS) or 5% delipidated FBS (dFBS) supplemented DMEM5796. The cells were grown overnight in delipidated serum supplemented DMEM5796. In a T-75cm² flask, cells cultured in HS supplemented media were 60-70% confluent while cells in FBS supplemented with FBS was 50-60% confluent the next day. One genome equivalent (GE) of HCV RNA per cell was used to infect cells for 4 hours at 37 °C. After 4 hours, the supernatant was removed and replaced with either DMEM5796 supplemented with 2% HS or 10% FBS (238).

2.1.4 Treatment of HCV Infected Cells with Sofosbuvir to Determine Dose

Response

Huh7.5 cells were grown for a minimum of 21 days with or without HCV infection. After 21 days, the media was removed and replaced with DMEM5796 supplemented with 2% HS, 50 IU/mL penicillin, 10ug/mL streptomycin and Sofosbuvir. Cells were treated with a Sofosbuvir concentration of 0.001µg/mL, 0.01µg/mL, 0.03µg/mL, 0.1µg/mL, 0.3µg/mL, 1µg/mL, 3µg/mL or 10µg/mL. The media was replaced every 4 days with new media containing the same concentration of Sofosbuvir as the media previously removed. Samples of the supernatant were taken prior to every media change to determine HCV production.

2.1.5 Lipoprotein Depletion of Human Serum and Fetal Bovine Serum

A 5mL HiTrap Heparin Hp column (GE Healthcare, 50005Cat.# 48) was connected to a 60mL syringe driven by a Harvard Apparatus PHD 2000 syringe pump. First, the heparin column was rinsed with 50mL of elution buffer composed of 0.05M NaP and 2M NaCl at 5mL/min. Next, the column was rinsed with 50mL binding buffer (39mL of 0.2M NaH₂PO₄, 61mL 0.2M Na₂HPO₄, and 300mL MilliQ water) at 5mL/min. Next, 50mL of either FBS or HS was run through the column at 2mL/ minute. To completely remove the lipoprotein from HS, the serum must be run through the column twice while a single run was sufficient to remove most lipoprotein in FBS. The first 5mL was discarded as it was composed primarily of the binding buffer. Once the serum had been collected, 50mL of elution buffer (0.05M NaP and 2M NaCl) was run through the column at 5mL/min to dissociate lipoproteins from the

column. The delipidated serum obtained from the column was sterile filtered with a 0.22µm filter (Millex, Cat.# SLG033RS) and stored at -20 °C before use.

2.2 Testing for Differentiation

2.2.1 Determining VLDL Secretion with Fast Protein Liquid Chromatography (FPLC)

The cell monolayer was washed three times with serum free DMEM5796 then placed in Opti-MEM media (Gibco, Cat.# 31985070) and the media collected 24 hours later. The media was concentrated using 15mL 100k MWCO ultracentrifugal filters (EMD Millipore, Cat.# UFC910024) by centrifuging the sample at 3000G for 15 minutes at 15°C. Samples were stored at 4°C until analysis by the Lipidomics Core Facility (in the Faculty of Medicine and Dentistry, University of Alberta in Edmonton). Briefly, the concentrated media (200µl) was injected into an Agilent 1200 HPLC instrument equipped with a Superose 6 10/300 FPLC column. Assays for triglycerides were performed at 37 °C using a post-column reaction. The reaction products were measured using Agilent Chemstation software at 500 nm (238,241).

2.2.2 Quantifying Albumin Concentration

Cell monolayers were washed three times with serum free DMEM5796 then incubated with Opti-MEM media. Samples of media were collected during the last wash and after 6 hours of incubation with Opti-MEM (238).

Albumin concentration was determined by a sandwich ELISA. First, ELISA plates were coated with 100 μ l of 0.625 μ g/mL goat anti- human albumin antibody (Bethyl, Cat.# A80229A) diluted in coating buffer (50mM NaHCO₃, 51.9mM Na₂CO₃) overnight at 4°C. The next day, wells were washed three times with Tris-buffered saline + 0.1% Tween-20 (TBST) (10mM Tris-HCl, 150mM NaCl and 0.1% Tween-20) and incubated in the blocking buffer (TBST and 1% gelatin; Bio-Rad, Cat.# 1706537) for 30 minutes at room temperature. Meanwhile, samples were prepared by diluting them 1:40 in the blocking buffer. A working stock of human serum (already diluted at 1:100) served as a positive control, the positive control was further diluted at 1:100, for a total dilution of 1:10,000. The negative control consists of mouse serum stock already diluted at 1:150, the control was further diluted 1:133 for a final dilution of 1:20,000.

After 30 minutes of incubation, the blocking buffer was removed and 133 μ l of the blocking buffer was added to wells that will contain the unknown samples and controls. Next, 100 μ l of the blocking buffer was added into wells used for serial dilution of the samples. A volume of 1 μ l taken from the unknown sample, positive control, and albumin stock needed to generate the standard curve was added to each well. Lastly, 100 μ l of the negative control was used. The samples in the wells were mix thoroughly by pipetting up and down 10 times then 33 μ l was transferred to the next well containing 100 μ l of blocking buffer to serially dilute the samples at 1:4. The extra 33 μ l for the well with the highest dilution was discarded to provide a consistent 100 μ l in each well. The samples were then incubated in the plate coated with primary antibody for 1 hour at room temperature. After the incubation, the wells were washed three times with TBST and incubated with 100 μ l of 6.25ng/mL goat anti-human HRP conjugated antibody (Bethyl, Cat.# A80229P) for 1 hour at room

temperature . Following the 1 hour incubation, wells were washed three times with TBST, and incubated with 100µl of TMB substrate for 15 minutes (238). Lastly, 100µl of 1M phosphoric acid was added. Plates were then read using the SpectraMax Plus 384 plate reader from Molecular Devices at 450nm.

2.3 HCV Quantification

2.3.1 Production of HCV

JFH-1 HCV obtained from T. Wakita was used to infect severe combined immunodeficient/Albumin- urokinase-type plasminogen activator (SCID/Alb-uPA) mice transplanted with human hepatocytes. Serum from infected mice was collected and subsequently used to infect Huh7.5 cells cultured in DMEM5796 supplemented with 10% FBS. The infected cells were propagated twice a week for 6 months to select for virus with reduced cytopathic effects. The selected viral stocks were sequenced and the mutations listed in Table 2.1 were found.

The JFH strains used in the experiments have been propagated an additional 4 times since it was last sequenced. In the 4 passages, new mutations may have arisen or previous mutations may have reverted.

	Mutation	Codon Change	AA Change	Gene
1	T391Y	CGT to CGY	Arg to Arg	Core
2	T429C	ATC to ACC	Ile to Ile	Core
3	C754T	CCC to CCT	Pro to Pro	Core

4	G1138A	GTG to GTA	Val to Val	E1
5	T1142G	TCC to GCC	Ser to Ala	E1
6	C11180T	CTC to CTT	Leu to Leu	E1
7	A1568G	AAC to GAC	Asn to Asp	E2
8	A1575G	CAG to CGG	Gln to Arg	E2
9	T1637C	TTG to CTG	Leu to Leu	E2
10	T2967T	GTG to GYG	Val to Val or Ala	p7
11	C2979T	GCC to GTC	Ala to Val	NS2
12	A3185T	ACT to TCT	Thr to Ser	NS2
13	T3735Y	GTC to GYC	Val to Val or Ala	NS3
14	A3830R	ACC to RCC	Thr to Thr or Ala	NS3
15	T6770C	TTT to CTT	Phe to Leu	NS5A
16	A7163G	ATG to GTG	Met to Val	NS5A
17	A7195G	TTA to TTG	Leu to Leu	NS5A
18	C7653T	ACC to ATC	Thr to Ile	NS5B
19	A7655T	ACC to TCC	Thr to Ser	NS5B
20	T8149A	GTT to GTA	Val to Val	NS5B
21	G8222A	GTA to ATA	Val to Ile	NS5B
22	A9113G	ACG to GCG	Thr to Ala	NS5B

Table 2.1 – JFH-1 Tissue Culture Adapted Virus Mutations. JFH-1 was used to infect SCID/Alb-uPA mice transplanted with human hepatocytes. Serum from infected mice was collected and used to infect Huh7.5 cells cultured in DMEM5796 supplemented with 10% FBS. The cells were propagated twice a week for 6 months and viral stocks were obtained and sequenced. The specific locations of the mutations within the JFH-1 genome are listed along with the specific amino acid change. Y indicates T or C.

2.3.2 HCV RNA Isolation

A sample of 200µl of media from cells was taken to determine the amount of HCV RNA present. HCV RNA was isolated using the High Pure Viral Nucleic Acid Kit (Roche, Cat.# 11858874001) according to manufacturer's instructions. This kit uses a guanidine purification method in order to isolate RNA. The positive controls were pre existing HCV stocks with known titres. Ultra pure water (Invitrogen, Cat.# 10977015) was used as negative control along with media taken from uninfected cells. The HCV RNA isolated from the supernatant was eluted from the columns provided by the kits using 50µl of the provided elution buffer.

2.3.3 HCV RNA Quantification by qRT-PCR

The first strand complimentary DNA (cDNA) synthesis reaction was prepared by combining 11µl of the elution buffer containing HCV RNA, 1µl of 10mM dNTP mix (Invitrogen, Cat.# 10297018) and 1µl of 2µM HCV-specific reverse primer. The reverse primer was complementary to nucleotide sequence 315-293 within the 5'NTR of the HCV genome (5'- GTG TTT CTT TTG GTT TTT CTT TGA GGT TTA GG – 3'). Hybridization of the reverse primer to the HCV genome was performed for 5 minutes at 65°C then a minimum of 1 minute at 4 °C in the TProfessional Basic Thermocycle from Biometra. Next, 4µl of 5x First Strand Synthesis buffer, 1µl of 0.1M DTT, 1µl of RNaseOut (Invitrogen, Cat.# 10777019), and 1µl of Superscript III RT 200 units (Invitrogen, Cat.# 1808093) were added to the HCV genome and reverse primer hybrid. The cDNA synthesis was formed by incubating the mixture for

1 hour at 55 °C followed by the inactivation of the reverse transcription reaction at 70 °C for 15 minutes in the TProfessional Basic Thermocycle (238).

To determine the HCV RNA present through quantitative polymerase chain reaction (qPCR), 2.5µl of the cDNA mixture was combined with 12.5µl of the TaqMan Universal PCR Master Mix (Applied Biosystems, Cat.# 4324018), 2.25µl of the 10µM forward primer, 2.25µl of the 10µM reverse primer, 2.5µl of the 2.5µM HCV specific probe, and 3µl of ultra pure water for a total volume of 25µl. Each sample was tested in duplicate. The forward primer was complementary to the nucleotide sequence at 150-168 found at the 5' NTR of the HCV genome. The sequence of the forward primer was as follows: TCT GCG GAA CCG GTG AGT A. The 6-carboxyfluorescein (FAM) probe was complementary at the position 315-331 found within the 5'NTR of the genome and has the sequence CAC GGT CTA CGA GAC CTC CCG GGG CAC. The standard curve was generated using known amounts (10^1 to 10^6 copies/mL) of a cloned HCV genomic cDNA plasmid. The PCR conditions were 50 °C for 2 minutes to optimize UNG activity in the TaqMan Universal PCR Master Mix, 95 °C for 10 minutes to activate the DNA polymerase in the TaqMan Universal PCR Master Mix, 95 °C for 15 seconds to denature the DNA and 60 °C for 1 minute to allow for replication. The third and fourth steps were repeated 44 more times for a total of 45 cycles (238). The reaction was carried out on 96 well plates (Axygen, Cat.# 32168051) and the Bio-Rad CFX96™ Optics Module. Using the software Bio-Rad CFX manager v3.1, the qPCR threshold was manually changed to the middle of the geometric phase of the amplification curve for the standard curves. The calculated values of samples were adjusted for dilutions and represented as HCV RNA copies/mL.

2.3.4 Titering by Limiting Dilutions (50% Tissue Culture Infective Dose)

Huh7.5 cells were plated onto flat-bottom 96 well plates coated with poly L lysine (PLL) at 25% density (12,500cells/ well) in dFBS. Cells were left overnight and infected the next day with 10 fold serial dilutions of samples containing virus in DMEM5796 supplemented with 10% FBS and 0.1mM non essential amino acid (NEAA) (Gibo, Cat.# 03438). From each dilution of HCV, 50µl was added to each well within a single column. Negative control contained media without virus and the positive control was a sample of virus of known concentration. Cells were incubated with virus for 4 hours at 37°C then media was aspirated and replaced with 100µl of DMEM5796 supplemented with 10% FBS and 0.1mM NEAA. After 72 hours, the confluent monolayer was washed twice with PBS then fixed and permeabilized with ice cold methanol for a minimum of 30 minutes at -20°C. After fixation, cells were washed twice with PBS and twice with PBS 0.1% Tween (PBST) and blocked for 30mins using blocking buffer containing 1% BSA in 0.2% skim milk in PBST. The block was removed and 3% H₂O₂ in PBS was added to the cells for 5 minutes to inactivate any endogenous peroxidase activity. Cells were washed again and incubated with 50µL of anti-NS5a antibody 9E10 (supplied by Charlie Rice from the Rockefeller University) at 0.1µg/mL for 1 hour. The primary antibody was removed and cells were washed twice with PBS and twice with PBST. Next, cells were incubated with goat anti-mouse secondary antibody conjugated to HRP (US Biological, Cat.# I1904-06C) for 30 minutes then cells were washed twice with PBS and twice with PBST. DAB substrate (Dako, Cat.# K3468) diluted at 1 drop/mL, as per manufacturer's instructions, was added and incubated for 5 minutes. Cells were washed with PBS twice and left in PBS for viewing. Cells were viewed using the CTL- Immunospot S6 Micro Analyzer. The tissue culture infectious dose 50/mL

(TCID₅₀) was defined as the dose at which 50% of the wells showing positive staining for HCV infection. The TCID₅₀ was calculated using Reed & Muench Calculator (242).

2.3.5 Immunofluorescence Staining of HCV Core Protein

Cells were plated onto 12 well plates containing PLL coated coverslips at the appropriate density and cultured accordingly (21 days for cells grown in HS and 1 week in cells grown in FBS). Once the cells were ready, they were first washed twice with 4°C PBS and fixed using a 1:1 v/v of methanol and acetone for a minimum of 20 minutes at -20 °C. After fixation, cells were washed twice with PBST with 5 minutes per wash. Next, the cells were blocked for 1 hour using 1% BSA and 2.5mM EDTA in PBS at room temperature. To incubate with anti-HCV core antibody (Thermofisher, Cat.# mAB8691), a humidification chamber was created by taping the edge of a piece of parafilm to the bench and adding 50µl of the antibody solution composed of 0.1µg/mL anti- HCV core antibody in blocking buffer. Coverslips were then placed with the cells faced down onto the antibody droplets. To complete the humidification chamber, a wet paper towel was placed around the coverslips, covered with the 12 well plate cover and an additional wet paper towels were placed on top. The primary antibody incubation was 1.5 hour at room temperature then the coverslips were moved back into the plate and washed twice with PBST. The coverslips were then incubated for 1 hour with 100µl of 1µg/mL goat anti-rabbit antibody conjugated to Alexa488 (Abcam, Cat.# ab97050) in blocking buffer by recreating the humidifying chamber. The coverslips were returned to the plates and washed twice with PBST.

In order to view the nuclei of each cell, coverslips were incubated for 5 minutes with 500 μ l of 1:5000 dilution of Hoescht 33342 (Invitrogen, Cat.# H3570) in PBS. After incubation, cells were washed twice with PBST and mounted onto microscope slides (Fisherbrand, Cat.# 1250015) using a drop of glycerol mounting media (Thermofisher, Cat.# 484985).

The cells were viewed using Zeiss fluorescence microscope and version 4.6 of Axiovision software.

2.4 Coating Plates

2.4.1 Coating Plates and Coverslips with Poly L Lysine

PLL (Sigma-Alrich, Cat.# P8920) diluted to 0.01% w/v in water was added to each well, the volume added was dependent on the surface area of each well. Normally, a volume of 0.1, 1 or 2mL was added to 96, 12 and 6 well plates respectively for at minimum of 1 minute. Next, the PLL was removed and the plates were allowed to dry. Once dried, 70% ethanol was used to wash the plates. After a minimum of 1 minute, the ethanol was removed and plates were left for minimum of 30 minutes under UV exposure, with a 90 degree rotation of the plates after 15 minutes. Coverslips (Fisherbrand, Cat.# 1254584) were normally coated in 12 well plates.

2.4.2 Coating Plates with Collagen

A solution containing 1mg/mL collagen in 0.013M HCl was sterilized using a 0.22 μ m syringe filter. Next, enough of the collagen solution was placed onto each well to

cover the bottom and plates were incubated at room temperature for 30 minutes. After, the collagen solution was removed and the plates were washed once with PBS. The PBS was removed and fresh PBS was added into the wells, the plates were wrapped in parafilm and stored at 4°C until use.

2.5 Testing for Lipid Content

2.5.1 Bicinchoninic Acid Protein Assay

Cell monolayers were first washed twice with PBS to remove any residual proteins present in the media. Next, the cells were lysed at 4 °C using radioimmunoprecipitation assay (RIPA) buffer (50mM Tris-HCl pH, 150mM NaCl, 0.1% SDS, 1% NP40 and 0.5% deoxcholalic acid in MilliQ water) supplemented with the EDTA free protease inhibitor (Roche, Cat.# 11873580001) for 15 minutes. The protein lysate was spun at 17000 x g for 15 minutes to pellet any cellular debris. The protein concentration was determined using the micro bicinchoninic acid (BCA) protein assay according to manufacturer's specifications (Pierce, Cat.# 23235). In brief, solutions A (alkaline tartrate-carbonate buffer), B (BCA) and C (CuSO₄) were mixed at a 25:24:1 ratio, 150µl of the resulting mixture was pipetted into each well on a 96 well enzyme-linked immunosorbent assay (ELISA) plate (Costar, Cat.# 0720035). Protein samples were serially diluted at 1:10 to obtain a value on the standard curve produced from albumin standards provided with the micro BCA kit. A volume of 150µl from the protein sample was added to the BCA mixture in each well, samples were assayed in duplicate. The plate was sealed using polyethylene sealing tape (Costar, Cat.# 6524) and incubated at 37°C for 2 hours (243). After incubation,

the plate was analyzed at 562nm using the SpectraMax Plus 384 plate reader from Molecular Devices.

2.5.2 Total Lipid Classes Analysis by HPLC

Huh7.5 cells were removed from the tissue culture plates using Accutase (Gibco, Cat.# A1110501), the reaction was inactivated using serum free DMEM5796 and transferred to a 15mL conical tube to pellet cells at 1000 x g for 5 minutes at room temperature. The pellet was washed once with PBS then resuspended in PBS. The equivalent of 1mg of total cellular protein was used for the total lipid class analysis by High Performance Liquid Chromatography (HPLC).

Lipids were extracted from cells suspended in PBS by combining the protein sample with 3.75mL of 1:1 chloroform:methanol, 1.25mL of chloroform and 1.25mL of mildly acidified NaCl (0.9g NaCl, three drops acetic acid in 100mL MilliQ water) in glass vials (Pyrex, Cat.# 982616X) using 5mL glass pipettes (Fisherbrand, Cat.# 1367827E). The internal standards, 200µl of 4.5mg/mL Batyl alcohol and 50µl dipalmitoyl-phosphatidyl-dimethylethanolamine (PDME) supplied from the Lipids Core Facility were included to quantify lipids present in each sample. The aqueous and organic layers within the tube were vortexed thoroughly and separated by spinning the samples at 1200 x g for 10 minutes at 4°C. The organic phase was removed from the bottom of the glass vial using the two pipette method and transferred to a new glass vial that had been washed with isopropanol then chloroform to remove any protein and lipid contaminants. The chloroform was evaporated using a nitrogen stream to prevent oxidation of lipids present within

samples. The lipids were resuspended in 100µl of 1:1 chloroform: octane then samples were analyzed by the Lipidomics Core Facility in Edmonton using an Agilent 1100 instrument equipped with a quaternary pump and Alltech ELSD2000 Evaporative Light-Scattering Detector. The lipids present in the samples were separated using a three-solvent gradient on an Onyx monolithic silica normal-phase column.

2.5.3 Oil Red O Staining

Cells grown on coverslips were washed once with PBS, fixed with 10% buffered formal phosphate and incubated at room temperature for 10 minutes on a shaker. The cells were washed with 60% triethyl phosphate (TEP) (Sigma, Cat.# 538728) diluted in distilled water for a minimum of one minute. Coverslips were incubated in Oil Red O (24.5mM in 60% TEP) for 15 minutes at room temperature on a shaker. After staining, coverslips were washed twice with 60% TEP for a minimum of 1 minute per wash. Next, coverslips were washed once with distilled water and incubated with alum haematoxylin (1.5g haematoxylin, 50ml 1% iodine in 95% absolute alcohol, 700mL saturated aqueous ammonium and 250mL distilled water) for 5 minutes at room temperature. Subsequently, coverslips were washed twice with distilled water, once with Scott Tap water (14.5mM K₂CO₃ and 16.5mM MgSO₄) and twice with distilled water. Coverslips were mounted using Vectashield hard set (Vector Laboratories, Cat.# H-1400) onto microscope slides (244). Slides were viewed using Carl Zeiss Axio Imager M1 and photos were taken using Axiovision version 4.7.1.

2.5.4 Flow Cytometry

The cell monolayer was removed from the flasks using Accutase to reduce the amount of cell aggregates and resuspended in serum free DMEM5796. The cells were pelleted at 1000 x g for 5 minutes in 15mL conical tube. Next, cells were washed once with 2mL PBS each and fixed using 2mL of 4% PFA for 15 minutes at room temperature. The cells were washed twice by resuspending in PBS then pelleting the cells at 1000 x g. To permeabilize cells, 2mL of permeabilization buffer (Biolegend, Cat.# 421002) was added to the cells and cells were incubated for 5 minutes at room temperature. The permeabilization step was repeated again.

The cells were counted using the Bio-Rad TC20 automated cell counter and 2 million cells were incubated with 500µl of 1ug/mL of anti-NS5a 9E10 antibody diluted in permeabilization buffer for 25 minutes at room temperature and washed twice with permeabilization buffer. Next, cells were incubated with 500µl of 1ug/mL anti-mouse Alexa647 antibody (Invitrogen, Cat.# A21236) for 20 minutes at room temperature and washed twice with permeabilization buffer.

To stain neutral lipids, cells were incubated for 15 minutes at 37°C in 2mL of 2µg/ml of Bodipy 493/503 (Thermofisher, Cat.# D3922) diluted in FACS buffer (2mM EDTA and 2% FBS in PBS). Next, cells were washed twice using FACS buffer to remove any extracellular Bodipy493/503. The cells were resuspended in FACS buffer for analysis. Controls used in this experiment include unstained cells, NS5a stained cells, isotype control, and Bodipy 493/503 stained cells.

The samples were run on the BD LSR Fortessa X-20 machine and BD FACSDIVA version 8.0.1 software.

2.6 Assessment of Metabolism

2.6.1 NMR Analysis of End Product Metabolites

Approximately 24 hours before sample collection, the cell monolayer was washed 3 times using serum free DMEM5796 and incubated in serum free DMEM5796. After 24 hours, the supernatant collected and filtered with a 0.22um filter to remove any large debris. Nanosep 3k Omega centrifuge tubes (Millipore, Cat.# UFC500396) were rinsed three times with MilliQ water to remove lipid complexes and large proteins that would obscure the NMR results from these sample. The filters were spun at 13,000 x g for 10 minutes, 630µl of the flow through was combined with 70µl internal standard 1 (WAS-1) in NMR tubes. WAS-1 was supplied by Chenomx Inc, Edmonton, Canada.

The NMR data was acquired in a Varian two-channel VNMRS 600 MHz NMR spectrometer with a HX 5mm probe and metabolites were identified and quantified using a target profiling technique developed by Chenomx Inc. The analysis was conducted by Chenomx Inc.

2.6.2 Testing for the Dependency on Glycolysis, β -oxidation and Glutaminolysis

Cells were prepared for analysis using instructions provided by the Seahorse XF Mito Fuel Flex Test Kit. Briefly, cell monolayers were grown on 24 well plates (Agilent, Cat.#102342-100) and washed once with 500ul PBS then 150ul assay medium (Agilent, Cat.#102353-100, pH 7.4). Cells were left in a non CO₂, 37°C incubator for a minimum of 30 minutes to allow cells to adjust to the assay medium. The assay medium was supplemented with 1mM pyruvate (Gibco, Cat.#11360070), 2mM

glutamine (Gibco, Cat.#25030081) and 10mM glucose (Gibco, Cat.#A2494001) to test cell's dependency on fatty acid oxidation, glutaminolysis and glycolysis respectively. The drug BPTES was used to inhibit glutaminolysis through inhibition of glutaminase (GLS1) to prevent incorporation of α -ketoglutarate in the TCA cycle. Etomoxir was used to inhibit CPT-1 to prevent transport of fatty acid into the mitochondria to undergo β -oxidation. UK5099 was used to inhibit mitochondrial pyruvate carrier (MPC) to prevent metabolism of pyruvate by the pyruvate dehydrogenase complex (PDC) within the mitochondria. The respective concentration and volumes used is summarized in Table 2.2. The drugs were dissolved in the assay medium and loaded onto sensor cartridges according to manufacturer's instructions (Agilent, Cat.# 102340-100). The analysis was conducted using the XFe24 analyzer (generously allowed by Michelakis Evangelos, HMRC 424) and the program Wave v1.2. The instrument run protocol is summarized in Table 2.3.

The XFe24 analyzer creates transient microchamber by moving the probes within the sensor cartridge 200 μ m above the cells. The probes contain a flourophore that is quenched by oxygen. Based on the amount of quenching, the analyzer can determine the oxygen consumption rate (OCR).

Pathway	Port	Drug	Injection Port Concentration (μM)	Well Concentration (μM)	Volume (μL)
Glutamine Dependency	A	BPTES	30	3	56
Fatty Acid Dependency	A	Etomoxir	40	4	56
Glucose Dependency	A	UK5099	20	2	56

Table 2.2 – Concentration of Drugs Loaded onto Sensor Cartridges to Measure the Dependency on Glycolysis, β -oxidation and Glutaminolysis. In order to test the dependency on glycolysis, β -oxidation and glutaminolysis, a specific inhibitor was required. The concentration of the inhibitor added to the sensors was 10 times the well concentration.

Command	Number of Cycles	Time per Command (min)
Mix, Wait and Measure	3	3, 2, 3
Inject Port A	-	-
Mix, Wait and Measure	5	3, 2, 3

Table 2.3 – The Instrument Run Protocol for Measuring the Dependency on Glycolysis, β -oxidation and Glutaminolysis. The injections of all ports are followed by the next cycle of mix, wait and measure with minimal delay.

2.6.3 Measuring Oxidation of Endogenous Fatty Acids

Cells were prepared for analysis using instructions provided by the technical brief titled “Simultaneously measuring oxidation of exogenous and endogenous fatty acids using the XF Palmitate-BSA FAO substrate with the XF Cell Mito Stress Test” provided by Agilent. Briefly, cell monolayers were grown on 24 well plates from Agilent and placed in substrate limited DMEM (Agilent, Cat.#102353-100 supplemented with 0.5mM glucose, 1mM glutamine, 0.5mM carnitine and either 1%

HS or FBS) for 24 hours prior to the day of the assay. On the day of the assay, cells were washed three times with 500µl PBS and once with 500µl of fatty acid oxidation (FAO) medium (111mM NaCl, 4.7mM KCL, 1.25CaCl₂, 2mM MgSO₄, 1.2mM NaH₂PO₄, 2.5 mM glucose, 0.5mM carnitine and 5mM HEPES at pH 7.4) per well. Cells were then incubated with 450µl of FAO medium in a non CO₂, 37°C incubator for a minimum of 30 minutes to allow cells to adjust to the assay medium. A volume of 50µl of 400µM etomoxir was added to half the wells 15 minutes prior to the assay. The other half received 50µl of a drug vehicle control. The cells are incubated in a non CO₂, 37°C incubator for 15 minutes.

The sensors were loaded with inhibitors from the Mito Stress Test Kit according to instructions provided. The concentration and volumes of each drug are summarized in Table 2.4. The inhibitor oligomycin was used to inhibit ATP synthase to determine ATP production. FCCP is an uncoupling agent that interrupts ATP synthesis by disrupting the proton gradient of the mitochondria. A combination of rotenone and antimycin A were used to measure non-mitochondrial respiration by shutting down mitochondrial respiration by inhibiting complex I and III of the electron transfer chain.

The plate and sensors are loaded into the XFe24 analyzer (generously allowed by Michelakis Evangelos, HMRC 424) and the analysis was conducted using the software Wave v1.2. The instrument run protocol is summarized in Table 2.4.

Inhibitor	Port	Port Concentration (μM)	Volume Added to Port (μl)	Well Concentration (μM)	Final Well Volume (μL)
Oligomycin	A	10	56	1	556
FCCP	B	10	62	1	618
Rotenone/ Antimycin A	C	5	69	0.5	687

Table 2.4 – Concentration and Volume of Inhibitors used in Measuring Endogenous Fatty Acid Oxidation using the XF Analyzer. The inhibitors were added to the ports on the sensors at a concentration 10 times of the final concentration. Each inhibitor was added at different times.

Command	Number of Cycles	Time per Command (min)
Mix, Wait and Measure	4	3, 2, 3
Inject Port A	-	-
Mix, Wait and Measure	3	3, 2, 3
Inject Port B	-	-
Mix, Wait and Measure	3	3, 2, 3
Inject Port C	-	-
Mix, Wait and Measure	3	3, 2, 3

Table 2.5 – The Instrument Run Protocol for Measuring Endogenous Oxidation of Fatty Acids using the XFe24 Analyzer. The injections of all ports are followed by the next cycle of mix, wait and measure with minimal delay.

Parameter	Definition
Nonmitochondrial Respiration	Rate after rotenone and antimycin A injection
Basal Respiration	(Rate prior to oligomycin injection) – (Nonmitochondrial Respiration)
Endogenous β -oxidation	(Basal Respiration in etomoxir untreated cells) – (Basal Respiration in etomoxir treated cells)
Maximum β -oxidation	(Rate after FCCP injection) – (Nonmitochondrial Respiration)
Spare Capacity for β -oxidation	(Maximum β -oxidation) – (Endogenous β -oxidation)

Table 2.6 – Calculating the different aspects of β -oxidation. The calculations for the different aspects of β -oxidation are listed.

2.7 Western Blot Analysis

The sodium dodecyl sulfate polyacrylamide gel electrophoresis (SDS-PAGE) gel was composed of a separating gel and a stacking gel. A 10% separating gel was prepared first using 10.83mL dH₂O, 3.75mL 2M Tris pH 8.8, 5mL Bis/Acrylamide 29:1 (40%), 200 μ l 10% SDS, 200 μ l 10% APS and 20 μ l TEMED. The solution was loaded between glass plates with 1.5mm spacers. Isopropanol was added to the separating gel in order to prevent any bubble formation and allow for levelling of the separating gel. The separating gel was allowed to polymerize for 30 minutes at room temperature. Next, the stacking gel was prepared using 2.66mL H₂O, 1.25mL 0.5M Tris pH 6.8, 987 μ l bis/Acrylamide 29:1 (40%), 50 μ l 10% SDS, 50 μ l 10% APS and 5 μ l TEMED and loaded over top the separating gel. The stacking gel was allowed to polymerize for 20 minutes at room temperature. Samples were prepared by boiling 20 μ g of protein and 15 μ l loading buffer (125mM Tris-HCl pH 6.8, 5% SDS, 10% 2ME, 15% glycerol and 0.1% bromophenol blue) for 13 minutes.

The SDS-polyacrylamide was loaded onto the gel apparatus and chambers were filled with SDS-PAGE running buffer (247.6mM Tris, 191.8mM glycine and 3.47mM SDS) and samples loaded into each wells using a Hamilton syringe to directly deposit samples into the bottom of the well. The samples were run at 80V for 30 minutes to allow the SDS-PAGE standards (Bio-Rad, Cat.# 1610373) and proteins to separate from the stacking gel using the FB300 from Fisher Biotech. The voltage was increased to 120V for 1 hour.

After electrophoresis, the gel apparatus was disassembled and gels were incubated in semi dry transfer buffer (39mM glycine, 48mM Tris base, 0.037% SDS and 20% methanol in water, pH was 8.8) for a minimum of 5 minutes at room temperature after removing the stacking gel. The gel was then moved onto a stack of two filter papers on the semi-dry transfer apparatus from Tyler Research. Next, a nitrocellulose membrane (GE Healthcare Life Sciences, Cat.# 10600003) was placed on top of the gel and another piece of filter paper was placed on the stack. The semi dry transfer was conducted with Model 200/2.0 from Bio-Rad using the settings 0.5mA and 26V for 1.5 hours.

After transfer the membrane was stained using Ponceau (3mM Ponceau S, 13.7mM 5-sulfosalicylic acid, 142mM 100% TCA) for 1 minute then washed 3 times with water to visualize the proteins transferred on the membrane. The membrane was then blocked for a minimum of 1 hour using PBST + 1% BSA. After the blocking step, the membrane was incubated with primary antibody directed against the protein of interest and an antibody directed to a loading control overnight at room temperature. The membrane was washed three times with PBST the next morning and incubated with goat anti-rabbit or mouse secondary antibody conjugated with IR dye (Licor,

Cat.# 92632221 and Cat.# 92632210) diluted to 0.1ug/mL in block for 1 hour. The membrane was washed 3 times with PBST and left in PBS for viewing. The membrane was scanned using Odyssey CLx from Licor under the settings: 84um for resolution and high for quality.

The resulting scan was analyzed by normalizing the k counts (fluorescent intensity) of the protein of interest divided the loading control using the program Odyssey v1.2.

2.8 Statistical Analysis

Statistical analysis was performed using Prism software for PC version 7. The data represented in the results section were expressed as mean \pm the standard deviation (SD). Unpaired Student's t test was used to calculate the significance in experiments with two groups. One way ANOVA analysis was used to calculate significance in experiments with more than two groups. P values less than $p < 0.05$ was considered significant.

***CHAPTER 3: Huh7.5 Cells
Cultured in HS as a Model to
Study HCV Infection***

Chapter 3: Huh7.5 Cells Cultured in HS as a Model to Study HCV Infection

3.1 Culturing Huh7.5 cells in HS leads to differentiation

The secretion of VLDL and increased albumin secretion were chosen as markers to confirm that Huh7.5 cells grown in DMEM5796 supplemented with 2% HS for a minimum of 21 days leads to differentiation (238). After 21 days of growth in HS media, cells were washed three times with serum free DMEM 5796 then placed in Opti-MEM media. Samples were taken after 6 hour incubation with Opti-MEM media to determine the concentration of albumin secreted using a quantitative ELISA analysis (Section 2.2.2). Similarly, cells grown in 10% FBS were subjected to the same method of preparation. The results showed that HS cultured cells secreted on average 5.6ug/mL albumin compared to 1.1ug/mL from cells grown in the presence of FBS. The 5.1 fold increase in the production of albumin in cells grown in HS compared to cells grown in FBS media (Figure 3.1) was consistent with previous findings (238).

After 24 hour incubation in Opti-MEM, the supernatant was collected, concentrated and subjected to FPLC lipoprotein analysis to determine the lipoprotein profile secreted from these cells. As expected, cells cultured in the presence of HS for 21 days secreted VLDL indicated by the peak at 20 minutes (Figure 3.2A), in line with previous results (238). The other peaks found at 30, 40, and 55 minutes are LDL, HDL, and glycerol respectively. The glycerol comes from the filters. The peaks corresponding to VLDL, LDL and HDL are absent from the last wash (Figure 3.2E). The secreted lipoprotein profile of HS cultured cells is similar to the lipoprotein profile found in normal human sera (238). When comparing the lipoprotein profile of HS and FBS cultured cells, the peak for VLDL at 20 minutes is absent for cells grown

in FBS (Figure 3.3B). When examining the lipoprotein profile of fetal bovine sera, there is very little VLDL present (Figure 3.2D). Overall, these results showed that cells cultured in the presence of HS secrete VLDL and have a lipoprotein profile similar to human sera. Whereas, cells cultured in FBS media lacked VLDL secretion and have a lipoprotein profile that was different from human serum.

In summary, cells grown in HS for 21 days have higher secretion of albumin compared to cells in FBS and display a lipoprotein profile similar to normal human sera. These results confirm that Huh7.5 cells are differentiated after 21 days and are consistent with data previously reported (238).

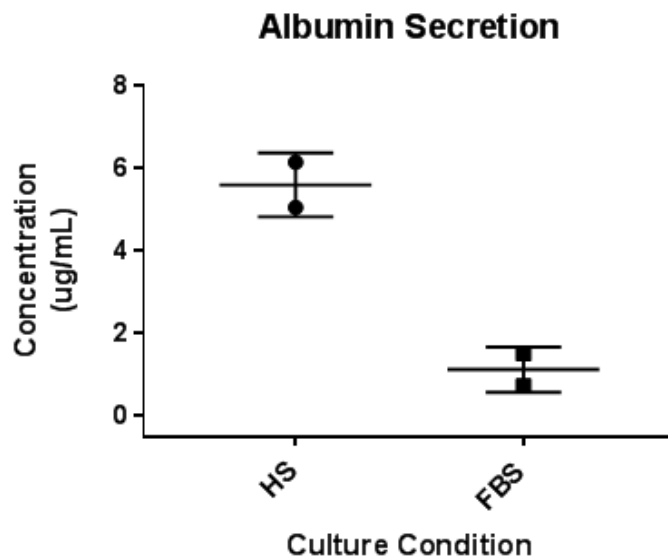


Figure 3.1 – Albumin Secretion in Cells Grown in 2% HS and 10% FBS Supplemented Media. Cells were differentiated in HS for 21 days, washed then placed in Opti-MEM media for 6 hours. Samples for albumin production are collected at 6 hours and quantified using an ELISA analysis. There was a 5.1 fold increase in albumin secreted when cells were cultured with HS media compared to cells cultured in FBS media. This experiment was conducted in duplicate and repeated twice. Each dot represents the average for the duplicate within a single experiment.

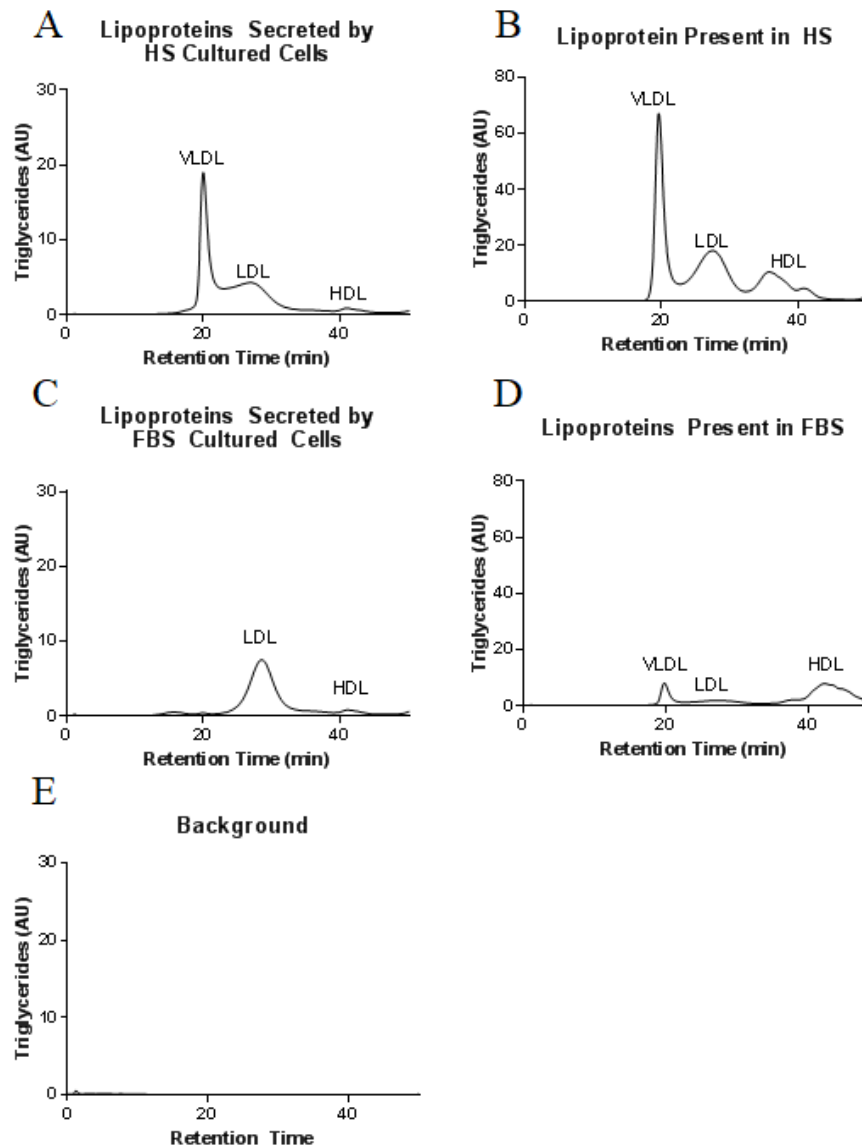


Figure 3.2 – Lipoprotein Profile of Huh7.5 Cells Cultured in 2% HS or 10% FBS Supplemented Media. Huh7.5 cells were differentiated in HS for 21 days. Cells are washed with Opti-MEM media three times. The last wash was collected as background. The cells were then incubated with Opti-MEM media for 24 hours. The supernatant was collected, concentrated and lipoproteins were separated using a size exclusion column. The sharp peak at 20 minutes indicates the presence of VLDL, the broad peaks are 30 and 40 minutes are LDL and HDL respectively. The peak between 50 to 60 minutes is glycerol from the filters. The TG lipoprotein profile of secreted lipoprotein from (A) cells cultured in the presence of 2% HS (B) human sera (C) cells cultured in 10% FBS (D) FBS (E) the last wash taken from cells. This experiment was conducted in duplicates and repeated twice, the lipoprotein profile shown here are the results from one experiment.

3.2 Assessment of Metabolism

Huh7.5 cells grown for 21 days in media supplemented with 2% HS have increased albumin and VLDL secretion compared to cells cultured in the presence of FBS (Section 3.1). Additionally, previous data has shown that cells grown in HS media have increased expression of the transcription factors LXR and PPAR α compared to cells cultured in FBS media. The increased expression of LXR and PPAR α suggests that HS cultured cells have increased lipid synthesis and β -oxidation compared to cells grown in FBS media (238). To determine if there are changes in these and other pathways when culturing Huh7.5 cells in media containing 2% HS compared to 10% FBS, additional studies were completed.

3.2.1 Assessment of Metabolomic Profile of Huh7.5 Cultured in HS or FBS Media

To determine the metabolomic profile of cells cultured in HS media and FBS media, NMR analysis was used to determine the concentration of metabolites secreted in the supernatant (Section 2.6.1). A total of 33 metabolites were detected with 10 compounds showing significant differences in concentration between the two culture conditions. The results are summarized in Table A.1 in the Appendix. Metabolites that were significantly different in concentration between the two culture conditions are presented in detail below.

3.2.1.1 Arginine Glycine and Proline Metabolism

The amino acids glycine, arginine and proline were detected at significant differences between cells grown in HS media and FBS media using NMR analysis. Arginine is an amino acid and is a component of DMEM5796 media. Arginine can be used to synthesize proteins or it can be metabolized by the urea cycle and creatine synthesis pathway. Both the urea cycle and creatine synthesis pathway are highly active in the liver (245,246) . Glycine is a nonessential amino acid that is also a component of the DMEM5796 media. Glycine can be used to synthesize proteins or it can be metabolized in a variety of pathways. For example, glycine is an intermediate in the creatine synthesis pathway while proline which is absent from the DMEM5796 media is the product of arginine and glycine metabolism (245,247). Ornithine is the first metabolite generated when arginine is metabolized in the urea cycle and creatine synthesis pathway. Ornithine is converted to glutamate 5-semialdehyde (G5S) by ornithine aminotransferase (OAT) then OAT converts G5S into 1-pyrroline-5-carboxylate (P5C). Finally, P5C is converted to proline using P5C reductase (Figure 3.3D) (245,247).

The amino acids glycine and arginine were utilized to a greater extent in HS relative to FBS cultured cells. Specifically, the concentration of glycine and arginine were 50% and 30% respectively lower in media taken from cells cultured in HS media relative to cells cultured in FBS media (Figure 3.3A – 3.3B). On the other hand, proline, which is not a component of DMEM5796 media, was 4 fold higher in cells grown in HS media relative to FBS media (Figure 3.3C). The increased synthesis of proline is likely related to the increased utilization of arginine and glycine in cells cultured in HS media as both amino acids are precursors of proline. Proline can be

found in many proteins, in particular, collagen which also contains large amounts of glycine, hydroxyproline, and arginine (248). The increased utilization of arginine, glycine to produce proline may be related to collagen synthesis. However, more experiments are needed confirm this hypothesis.

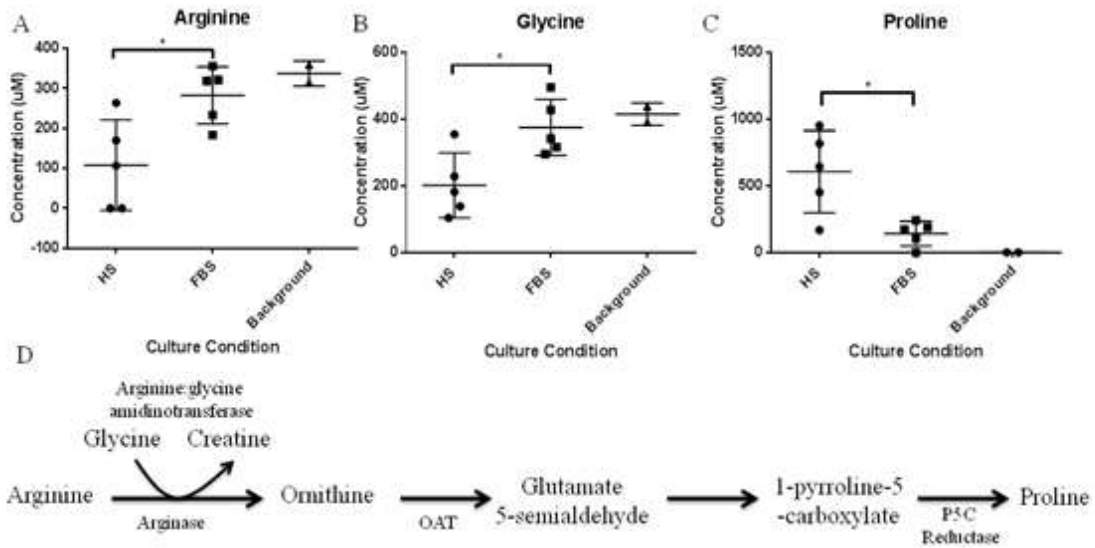


Figure 3.3 – Arginine, Glycine and Proline Metabolism in Cells Cultured in Huh7.5 Cells Cultured Using 2% HS Supplemented or 10% FBS Media. Huh7.5 cells were differentiated in media containing HS for 21 days then placed in serum free media. The supernatant was collected after 24 hours and analyzed using NMR. The concentration of (A) arginine and (B) glycine were significantly lower in supernatant taken from cells grown in media supplemented with HS compared to FBS. (C) There was significantly more proline detected in media taken from cells cultured in HS media compared to FBS media. (D) The pathway to synthesize proline using arginine and glycine as precursors. This experiment was conducted in duplicate and repeated 5 times. Each point represents the average value for each experiment. *P<0.05

3.2.1.2 Branched Carbon Amino Acids Metabolism

Two metabolites from the branched carbon amino acid (BCAA) degradation pathway were detected at significant differences between cells grown in HS media and FBS media using NMR analysis. They were 3-methyl-2-oxovalerate, the first intermediate of the isoleucine degradation pathway and 3-hydroxyisovalerate, one of the intermediates of the leucine degradation pathway (249). The differences are summarized in Section 3.2.1.2.1 and Section 3.2.1.2.2.

3.2.1.2.1 Isoleucine Degradation

In the isoleucine degradation pathway, isoleucine is first degraded to 3-methyl-2-oxovalerate by BCAA transferase (BCAT). Next, the rate limiting step of the isoleucine degradation pathway, the branched-chain alpha-keto acid dehydrogenase (BCKDH) complex converts 3-methyl-2-oxovalerate into 2-methylbutyryl-CoA (250). Through additional steps, the end products of the isoleucine degradation pathway are acetyl-CoA and propanoyl-CoA. The acetyl-CoA can either be further degraded by the TCA cycle or the ketogenesis pathway to provide ketone bodies for energy production (1.3.5) or it can be exported from mitochondria after the synthesis of citrate for the synthesis of fatty acids (251). The propanoyl-CoA can be converted to methylmalonyl CoA and finally succinate CoA, one of the intermediates of the TCA cycle using the enzyme methylmalonyl-CoA mutase (MCM) (249).

When cells were grown in HS media, there was no significant difference in the utilization of isoleucine when compared to cells grown in FBS media (Figure 3.4A). However, there was 50% less 3-methyl-2-oxovalerate detected in media taken from

cells cultured in HS media compared to cells cultured in FBS media (Figure 3.4B). Overall, these results suggest that the degradation of isoleucine into 3-methyl-2-oxovalerate was higher in cells cultured in FBS media compared to cells cultured in HS media. The increased degradation of isoleucine to yield the end products acetyl-CoA and propionyl CoA suggests that there may be an increase in the utilization of the TCA cycle in cells grown in FBS.

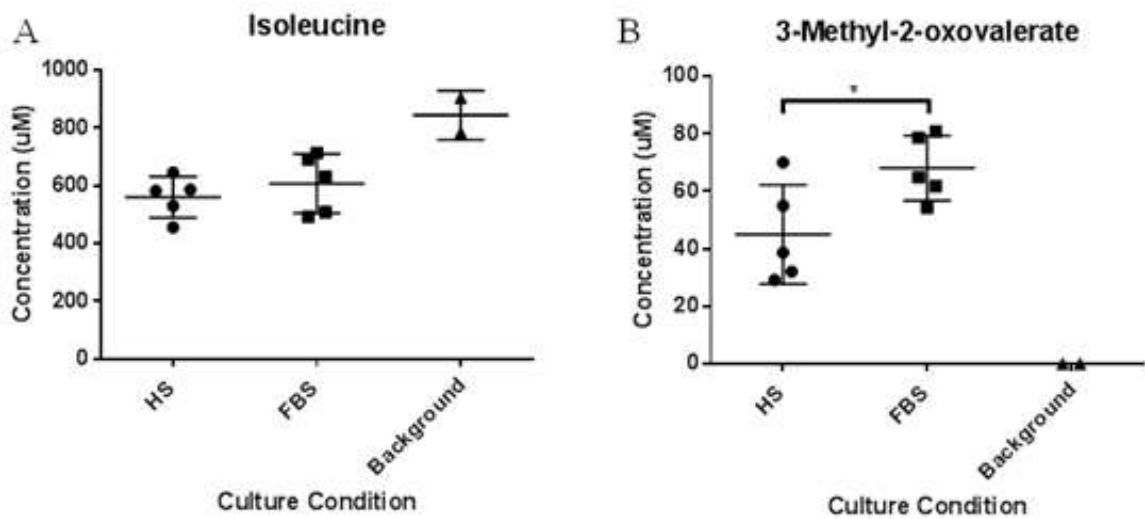


Figure 3.4 – Isoleucine Metabolism in Cells Cultured in Huh7.5 Cells Cultured Using 2% HS Supplemented or 10% FBS Media. Huh7.5 cells were differentiated in media containing HS for 21 days then placed in serum free media. The supernatant was collected after 24 hours and analyzed using NMR. The concentration of (A) isoleucine was similar in supernatant taken from cells grown in either culture conditions. (B) The concentration of 3-methyl-2-oxovalerate was significantly lower in supernatant taken from Huh7.5 cells cultured in HS media compared to FBS media. This experiment was conducted in duplicate and repeated 5 times. Each point represents the average value for each experiment. *P<0.05

3.2.1.2.2 Leucine Degradation

In the leucine degradation pathway, leucine is first converted to 4-methyl-2-oxopentanoate by BCAT. Next, 4-methyl-2-oxopentanoate is metabolized into 3-hydroxyisovalerate by BCAT. Further degradation of 3-hydroxyisovalerate yields β -hydroxy β -methylbutyrate (HMB), the precursor for 3-hydroxy-3-methylglutaryl-coenzyme A (HMG-CoA). HMG-CoA can be metabolized to produce acetoacetate in the ketogenesis pathway (Figure 3.9D) or it can be used to synthesize sterols (252–254).

The utilization of leucine in the two culture conditions was similar (Figure 3.5A). However, when cells were cultured in HS media, there was increased production of 3-hydroxyisovalerate compared to the absence of 3-hydroxyisovalerate found in cells grown in the presence of FBS media (Figure 3.5B). These results suggest that cells grown in using HS media utilize the leucine degradation pathway in order to generate 3-hydroxyisovalerate while cells grown FBS media did not degrade leucine.

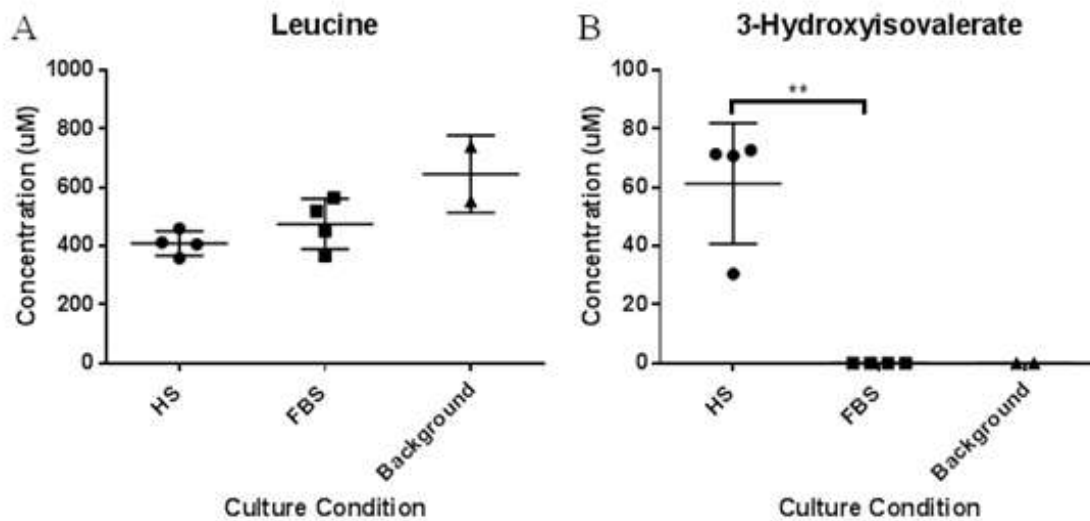


Figure 3.5 – Leucine Metabolism in Cells Cultured in Huh7.5 Cells Cultured Using 2% HS Supplemented or 10% FBS Media. Huh7.5 cells were differentiated in media containing HS for 21 days then placed in serum free media. The supernatant was collected after 24 hours and analyzed using NMR. The concentration of (A) leucine was similar in supernatant taken from cells grown in either culture conditions. (B) The concentration of 3-hydroxyisovalerate was significantly higher in supernatant taken from Huh7.5 cells cultured in HS media compared to FBS media. This experiment was conducted in duplicate and repeated 5 times. Each point represents the average value for each experiment. *P<0.05

3.2.1.3 Methionine Metabolism

Methionine metabolism was significantly different between Huh7.5 cells grown under the two culture conditions. Methionine is an essential amino acid that can be used to synthesize protein or enter two pathways, the methionine cycle which produces S-adenosyl methionine (SAM) and homocysteine. S-adenosylmethionine synthase is the rate limiting enzyme that catalyzes the conversion of methionine to SAM. SAM is

used to methylate phospholipids, proteins and metabolites. For example, SAM can be used to synthesize phosphatidylcholine (PC) from phosphatidylethanolamine (PE) through a series of enzymatic reactions. Moreover, SAM is required to synthesize carnitine, which is required by CPT-1 to transport fatty acids into the mitochondria. SAM can be converted to homocysteine by adenosylhomocysteinase. Homocysteine can either be converted back into methionine or converted to cysteine as part of the transsulfuration pathway. Cysteine can be converted to several different metabolites in the transsulfuration sequence. For instance, cysteine can be converted to either glutathione which is an antioxidant, taurine, a major component of bile acid, or pyruvate. Both the methionine cycle and transsulfuration pathway are highly active pathways within hepatocytes (255–257). The conversion of homocysteine into methionine requires tetrahydrofolate (THF). The production of THF is coupled to the production of formate. Formate is derived from metabolites found in the glycine and tryptophan degradation pathways (258).

The results from the NMR analysis showed that when cells were cultured in HS media, there was significantly higher utilization of methionine relative to cells cultured in FBS media. Specifically, there was a 35% increase in methionine utilization in cells cultured in HS media compared to FBS media (Figure 3.6A). However, there was no difference in the concentration of formate in cells grown in HS media and FBS media (Figure 3.6B). Taken together, these results suggest that the methionine cycle within Huh7.5 cells grown with HS media are more active compared to cells grown in FBS media.

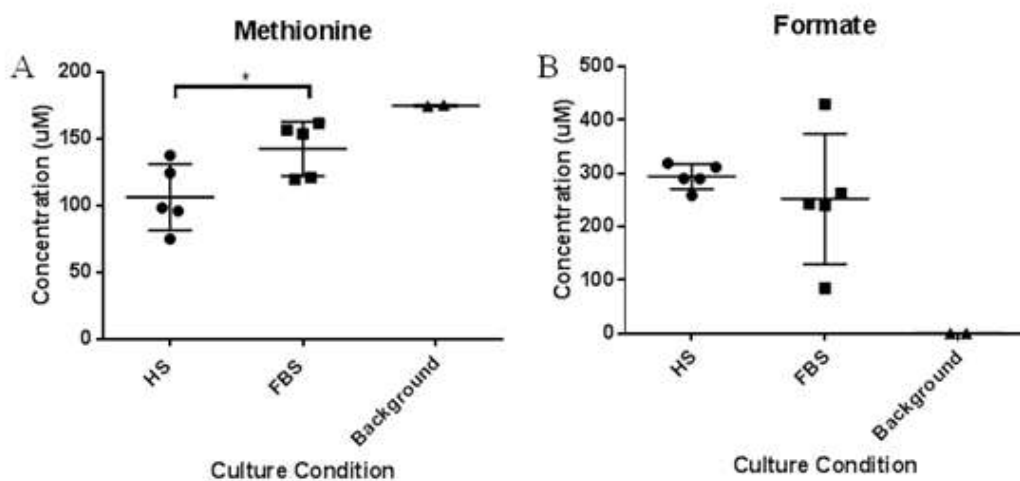


Figure 3.6 – Methionine Metabolism in Cells Cultured in Huh7.5 Cells Cultured Using 2% HS Supplemented or 10% FBS Media. Huh7.5 cells were differentiated in media containing HS for 21 days then placed in serum free media. The supernatant was collected after 24 hours and analyzed using NMR. The concentration of (A) methionine was significantly lower in supernatant taken from Huh7.5 cells cultured in HS compared to FBS while (B) there was no difference in formate in HS or FBS media cultured cells. This experiment was conducted in duplicate and repeated 5 times. Each point represents the average value for each experiment. *P<0.05

3.2.1.4 Phospholipid Metabolism

The metabolite O-phosphocholine was detected at significant differences between cells grown in HS media and FBS media using NMR analysis. O-phosphocholine is normally an intracellular metabolite that is an intermediate of the CDP-choline pathway that generates phosphatidylcholine (PC), the end product of the CDP-choline pathway (Figure 3.7C). PC, the most common phospholipid, is involved in the synthesis of membranes and secretion of lipoproteins (259). It has also been shown that synthesis of PC is closely linked with secretion of VLDL (260,261).

The choline present within the media was utilized similarly in cells were cultured in HS and FBS media (Figure 3.7A). However, there was 7 fold less O-phosphocholine present in media taken from cells grown in HS media compared to cells grown in FBS media (Figure 3.7B). Since O-phosphocholine is normally an intracellular metabolite, the presence of O-phosphocholine in the media may be related cell lysis. If this is true, the increase in O-phosphocholine detected in the media in cells grown in FBS media may be related to an increase in cell death.

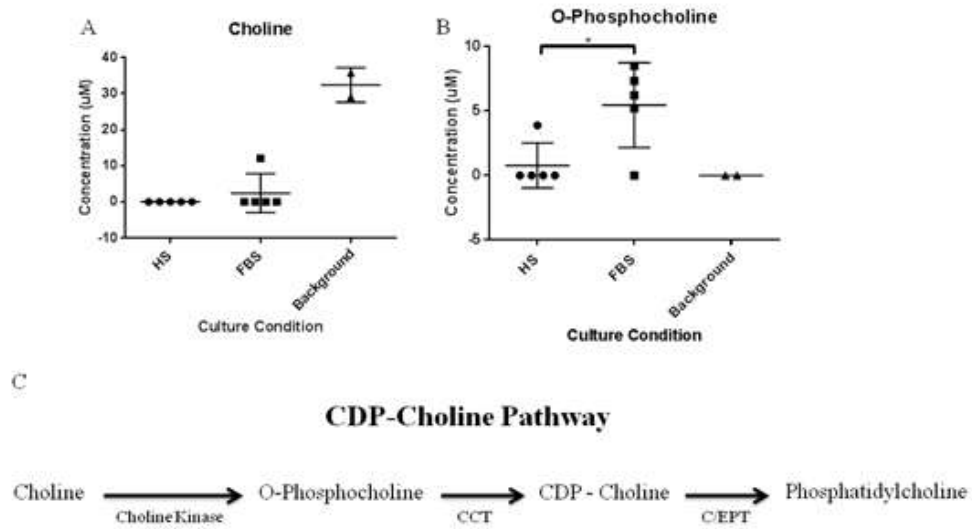


Figure 3.7 –Phospholipid Metabolism in Cells Cultured in Huh7.5 Cells Cultured Using 2% HS Supplemented or 10% FBS Media. Huh7.5 cells were differentiated in media containing HS for 21 days then placed in serum free media. The supernatant was collected after 24 hours and analyzed using NMR. The concentration of (A) choline was similar in supernatant taken from cells cultured using HS and FBS media. (B) The concentration of O-phosphocholine in supernatant taken from Huh7.5 cells cultured in HS was significantly lower compared to FBS. (C) The CDP-choline pathway produces O-phosphocholine as a precursor to synthesize phosphatidylcholine. CTP-phosphocholine cytidyltransferase (CCT) Choline/ ethanolamine phosphotransferase (C/EPT). This experiment was conducted in duplicate and repeated 5 times. Each point represents the average value for each experiment. *P<0.05

3.2.1.5 Glycolysis

The metabolites associated with glycolysis such as glucose, pyruvate and lactate were detected at significant differences between cells grown in HS media and FBS media using NMR analysis (Figure 1.6). The concentration of glucose detected in media taken from Huh7.5 cells cultured in HS and FBS media were similar (Figure 3.8A). However, the concentration of pyruvate was 10 times lower in media taken from cells cultured using HS media compared to FBS media (Figure 3.8B). The levels of lactate secreted by cells grown in HS and FBS media were similar (Figure 3.8C). Overall, these results suggest that glycolysis in cells grown using HS media convert minimal levels of glucose to pyruvate. The glucose entering glycolysis is most likely converted to intermediates that could be utilized to synthesize amino acids, lipids and glycogen (Figure 1.6). In cells cultured in FBS, a large concentration of glucose is converted into pyruvate which is then utilized in the TCA cycle. These results suggest that HS cultured cells do not utilize glycolysis to synthesize pyruvate whereas cells cultured in FBS utilize glycolysis to generate high concentrations of pyruvate. This glycolytic flux in FBS cultured cells is reminiscent of the Warburg effect while cells cultured in HS do not display the Warburg effect (182).

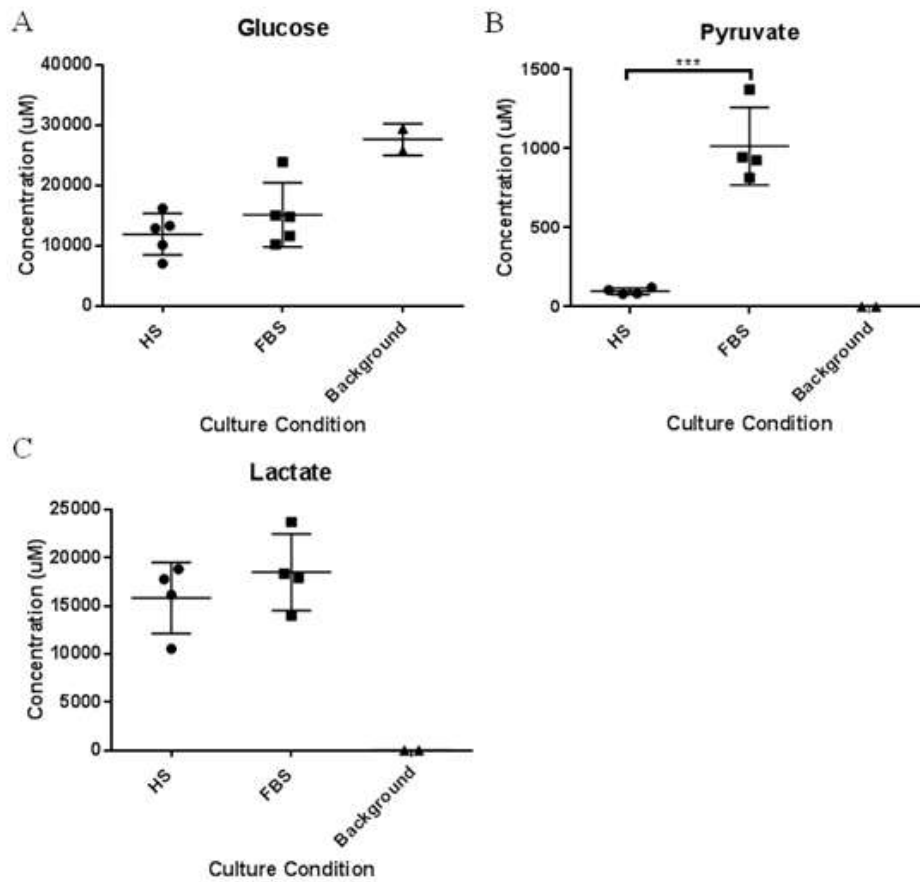


Figure 3.8 – Glycolysis in Cells Cultured in Huh7.5 Cells Cultured Using 2% HS Supplemented or 10% FBS Media. Huh7.5 cells were differentiated in media containing HS for 21 days then placed in serum free media. The supernatant was collected after 24 hours and analyzed using NMR. The concentration of (A) glucose was similar in supernatant taken from cells cultured with either HS or FBS media. (B) The concentration of pyruvate was significantly lower in supernatant taken from Huh7.5 cells cultured in HS media compared to FBS media. (C) There was no difference in lactate in cells cultured using HS media or FBS media. This experiment was conducted in duplicate and repeated 5 times. Each point signifies the average value for each experiment. ***P<0.001

3.2.1.6 Ketogenesis

The ketone bodies, acetone, acetoacetate and 3-hydroxybutyrate were detected at significant differences between cells grown in HS media and FBS media using NMR analysis. These ketone bodies are products of the ketogenesis pathway (Figure 3.9D). The ketogenesis pathway is highly active within hepatocytes where there is an abundance of acetyl-CoA due to the breakdown of fatty acids through β -oxidation (Section 1.3.5). The results from the NMR analysis show that there was a 21 fold increase in acetoacetate and 8 fold increase in 3-hydroxybutyrate present in media taken from cells cultured in HS media compared to FBS media (Figure 9A – 9B). Overall, these results imply that the ketogenesis pathway is utilized more within differentiated cells cultured in HS media relative to cells cultured in the FBS media. The increased production of ketone bodies may be directly related to the increase in β -oxidation. Sections 3.2.2 to Section 3.3 will examine the levels of β -oxidation in Huh7.5 cells grown in HS and FBS media.

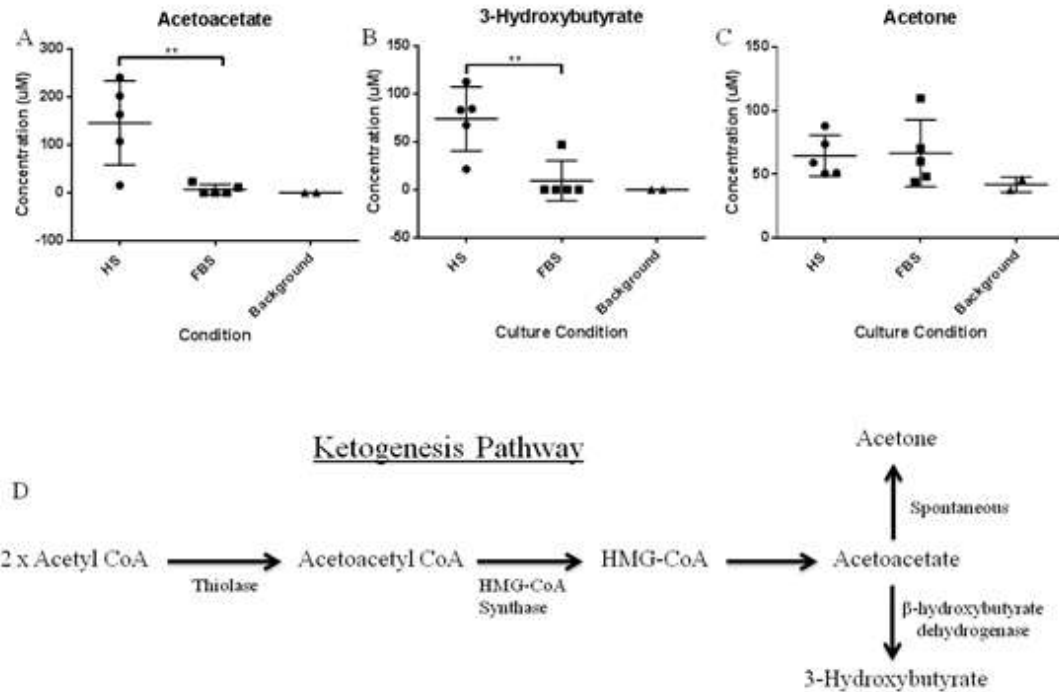


Figure 3.9 –Ketogenesis in Cells Cultured in Huh7.5 Cells Cultured Using 2% HS Supplemented or 10% FBS Media. Huh7.5 cells were differentiated in media containing HS for 21 days then placed in serum free media. The supernatant was collected after 24 hours and analyzed using NMR. The concentration of (A) acetoacetate (B) 3-hydroxybutyrate was higher in supernatant taken from Huh7.5 cells cultured in HS media compared to FBS media while (C) the concentration of acetone did not change. (D) The end products of ketogenesis are acetoacetate, 3-hydroxybutyrate and acetone. Hydroxymethylglutaryl-CoA (HMG-CoA). This experiment was conducted in duplicate and repeated five times. Each point represents the average value for each experiment. **P<0.01

3.2.2 Assessment of Metabolic Flux

The results from the NMR analysis show that there was a reduction in glycolysis as a source of pyruvate in Huh7.5 cells cultured in 2% HS media (Section 3.2.1.5). The results from Section 3.2.1.6 show that there was an increase in β -oxidation through the increase in ketone bodies when cells were grown in HS media compared to FBS media. To confirm that there is a change in the utilization of glycolysis and β -

oxidation, the Seahorse XFe24 analyzer was used. This analyzer measures the oxygen consumption rate (OCR) as a marker for the TCA cycle activity. The TCA cycle leads to the reduction of NAD^+ and FAD to yield NADH and FADH_2 . NADH and FADH_2 are oxidized by OXPHOS while consuming oxygen. The utilization of oxygen is detected by the analyzer. Using the XFe24 analyzer, the cell's dependency for utilizing the glutaminolysis pathway was also examined. The dependency refers to the ability for the cell's mitochondria to utilize a particular pathway.

In order to differentiate between the various pathways that feed into the TCA cycle, inhibitors such as etomoxir, BPTES, UK5099 were injected into the cell culture wells after the third basal measurement to determine the dependency the cells have on each pathway. Etomoxir inhibits β -oxidation through CPT-1 inhibition, BPTES inhibits glutaminolysis by GLS1 inhibition and UK5099 inhibits the oxidation of pyruvate by PDC. When a cell is highly dependent on a particular pathway, the OCR will decrease significantly once that pathway is inhibited (Section 2.6.2).

To determine the metabolic flux through each pathway, the analysis was conducted on Huh7.5 cells differentiated in HS media for at least 21 days and cells cultured in FBS media. The values of each measurement in treated cells were normalized to the value of untreated cells. The steady decline in oxygen consumption was a consequence of a reduced supply of oxygen since no new oxygen was introduced into the wells during this assay. When UK-5099 was used to inhibit PDC after the third OCR measurement (approximately 10 minutes), there was no change in the OCR in cells grown in HS while there was a 25% reduction in OCR for cells cultured in FBS (Figure 3.10A). This result showed that cells cultured in FBS media were significantly more dependent on the glycolysis pathway to provide pyruvate for the

TCA cycle compared to cells grown in HS media. When β -oxidation was inhibited with etomoxir, there was a reduction in OCR in both HS and FBS cultured cells. However, the cells cultured in HS media showed a 30% reduction in OCR compared to a 15% reduction in cells cultured in FBS media (Figure 3.10B), suggesting that there was a larger dependency on β -oxidation in cells grown in HS. When investigating the dependency both HS and FBS media cultured cells have for the glutaminolysis pathway, GLS1 was inhibited using BPTES. The result showed that there was a similar reduction in OCR in cells grown in HS media and FBS media suggesting a similar dependency on glutaminolysis (Figure 3.10C). These results suggest that the mitochondria in cells cultured in HS media preferentially utilize β -oxidation instead of glycolysis compared to cells cultured in FBS media.

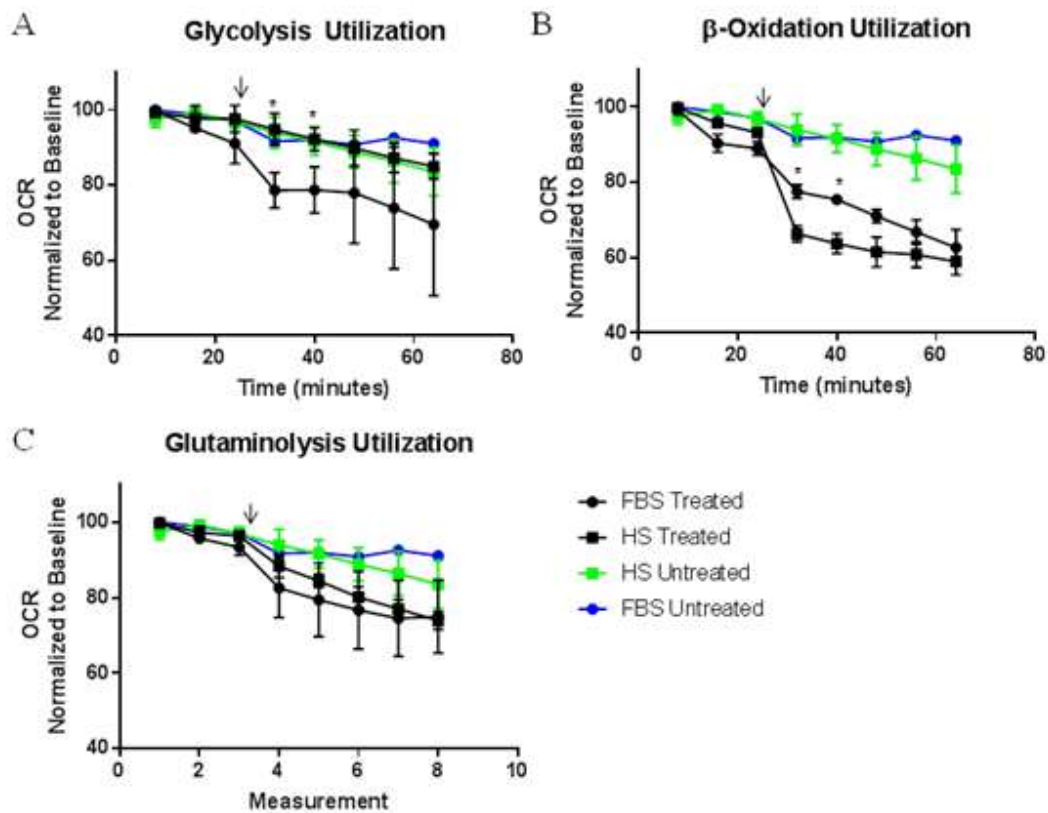


Figure 3.10 – Dependency of β -oxidation, Glycolysis and Glutaminolysis in Cells Cultured in Huh7.5 Cells Cultured Using 2% HS Supplemented or 10% FBS Media. Huh7.5 cells were differentiated in 2% HS supplemented media for 28 days grown cells and FBS cultured cells were analyzed using the XFe24 analyzer. The first three points were basal measurements. The inhibitor was added after the third timepoint. (A) The inhibitor of MPC, UK5099 was added after the third time point to measure dependency on glycolysis to provide pyruvate for the TCA cycle (B) The inhibitor of CPT-1, etomoxir was added after the third time point to measure dependency on β -oxidation to provide acetyl-CoA for the TCA cycle (C) The inhibitor BPTES was added after the third time point to measure dependency on glutaminolysis to provide α ketoglutarate for the TCA cycle. This experiment was conducted in duplicate and repeated three times. Each point represents the average measurement for all three experiments. *P<0.05. Arrows indicate the addition of inhibitors.

3.2.3 Assessment of the Rate of β -oxidation

The results from Section 3.2.2 suggests a greater dependency of β -oxidation in cells that are cultured using HS media compared to FBS media. To determine the exact rate of β -oxidation that occurs in cells grown in HS or FBS media, the OCR of cells were analyzed using the XFe24 analyzer from Seahorse Bioscience. The inhibitors oligomycin (ATPase inhibitor), FCCP (proton gradient uncoupler) and a combination of rotenone and antimycin A (inhibitors of the electron transport chain) were injected into cell culture wells to measure endogenous, maximum and spare capacity for β -oxidation (Section 2.6.3). The endogenous β -oxidation is defined as the level of β -oxidation to meet the energetic demand of the cell under baseline conditions. The maximum β -oxidation is defined as the maximum rate of β -oxidation that a cell can achieve. The spare capacity of β -oxidation is defined as the cells ability to respond to energetic demands by increasing the rate of β -oxidation. There was a 10 fold increase in the endogenous β -oxidation in cells grown in HS media compared to cells grown in FBS media. Additionally, the maximum β -oxidation and spare capacity for β -oxidation was 3.5 and 6.5 fold higher in cells grown in HS media relative to FBS media (Figure 3.11). These results show that in HS differentiated cells, β -oxidation is highly active compared to cells that are grown using FBS media.

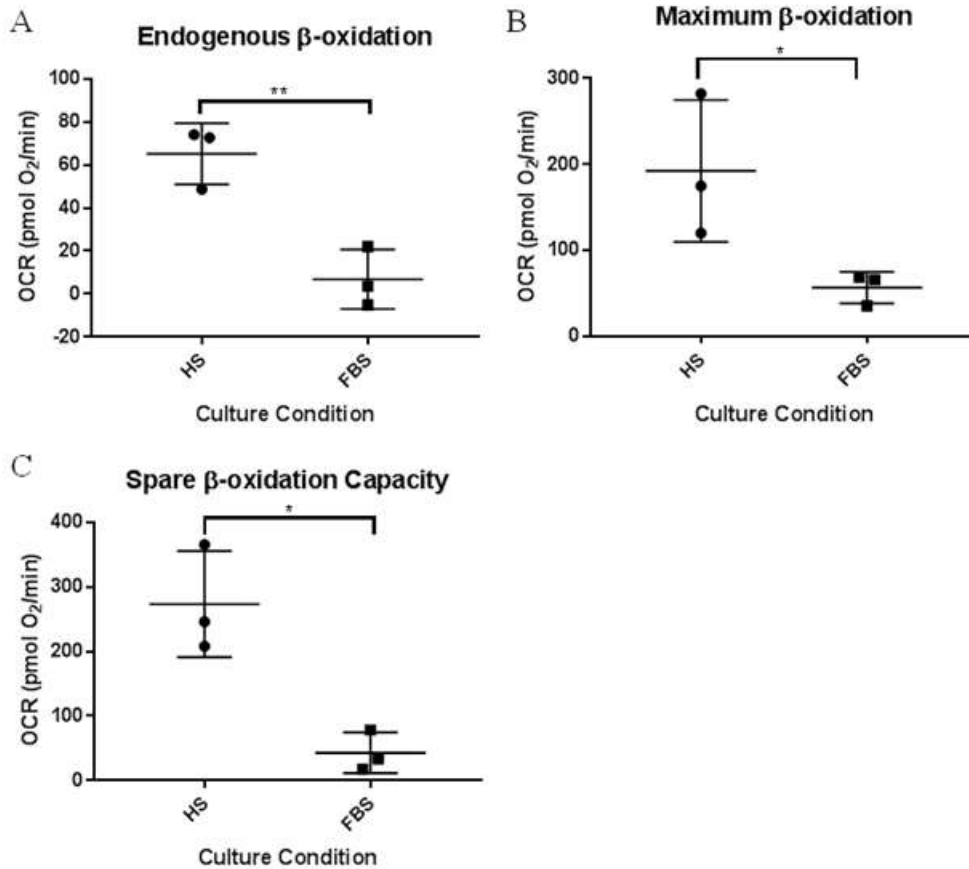


Figure 3.11 – Endogenous β -oxidation, Maximum β -oxidation and Spare Capacity for β oxidation in Huh7.5 Cells Cultured using 2% HS Supplemented or 10% FBS Media. Huh7.5 cells were differentiated in 2% HS supplemented media for 28 days grown cells and FBS cultured cells were analyzed using the XFe24 analyzer. The endogenous β -oxidation was calculated by taking the basal OCR and subtracting the nonmitochondrial respiration rate after rotenone and antimycin A were added. The maximum β -oxidation was calculated by taking the maximal OCR after the addition of FCCP and subtracting the nonmitochondrial respiration. The spare capacity for β -oxidation was calculated by taking the maximal β -oxidation and subtracting the basal respiration. (A) There was significantly higher endogenous β -oxidation (B) maximum β -oxidation and (C) spare capacity for β -oxidation in cells cultured using HS media compared to FBS media. This experiment was conducted in triplicates and repeated three times. Each point represents the average value for each experiment. * $P < 0.05$ ** $P < 0.01$

3.3 Assessment of the Rate Limiting Step of β -oxidation

The previous findings show an increase in β -oxidation and ketogenesis in cells cultured in HS media relative to cells grown in FBS media. To provide additional evidence that β -oxidation is increased in cells cultured with HS, levels of CPT-1, the enzyme catalyzing the rate limiting step of β -oxidation, were examined using a quantitative western blot (Section 2.7). The ratio of the fluorescence intensity between the loading control β -tubulin and CPT-1 was determined for each sample and normalized to FBS which was set at a value of 1. When comparing the CPT-1 protein levels in the two different culture systems, there was approximately 7 times more CPT-1 present in cells cultured in HS media compared to FBS media (Figure 3.12). The levels of CPT-1 in primary hepatocytes (PHH) are much higher still, at 100 fold greater than in Huh7.5 cells cultured in FBS media.

These results show an increase in CPT-1 in cells grown in the HS media compared to cells cultured in FBS media. The increase in CPT-1 found in cells grown in HS media was more reflective of a PHH compared to cells grown using FBS media. This suggests that that Huh7.5 cells grown with HS may be a better model to study β -oxidation compared to cells grown in FBS.

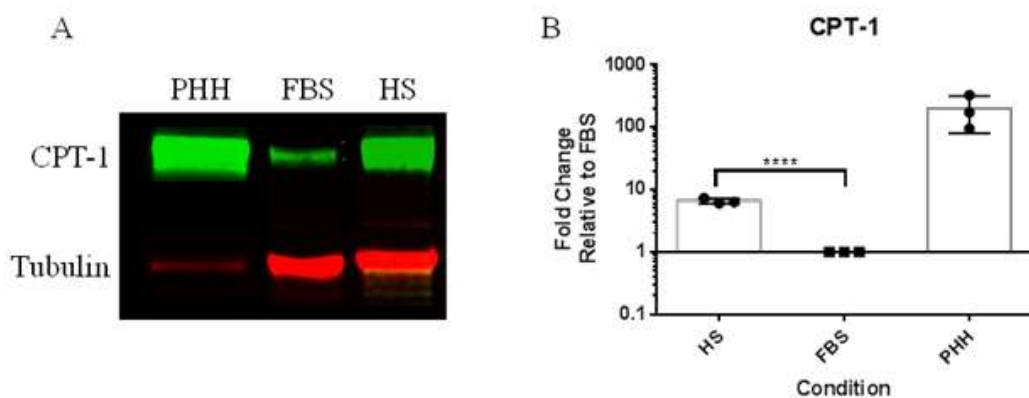


Figure 3.12 – CPT-1 Production in Huh7.5 Cells. Cell lysates were subjected to SDS-PAGE and Western blot analysis using a Licor approach. (A) 5 μ g of protein was loaded into the lane containing lysates from primary hepatocytes (PHH) while 20 μ g of protein was loaded in lanes containing lysates from HS and FBS cultured cells. CPT-1 is shown in green (82kDa). The loading control, β -tubulin is shown in red (51kDa). (B) The ratio of signal intensity was obtained from CPT-1 and tubulin and normalized to FBS to control for the varying fluorescent intensity between each experiment. This experiment was repeated three times. Each point represents the average value for each experiment. **** $P < 0.0001$

3.4 Assessment of Lipids

The experiments from Section 3.2.1.6 to 3.3 showed that there are higher levels of β -oxidation within cells cultured in HS media relative to FBS media. To determine if there are more substrates such as triglycerides and fatty acids available for β -oxidation, two approaches were used to determine lipid content in Huh7.5 cells cultured in 2% HS media for 21 days.

3.4.1. Assessment of Lipid Droplets

The lipid droplets in cells cultured in FBS or HS media for 21 days were stained with Oil Red O (Section 2.5.3). The results showed that cells that are grown in HS media have much larger lipid droplets compared to cells cultured in FBS media through the red staining (Figure 3.13). Overall, the increase in lipid droplet formation in cells cultured in HS was consistent with data reported previously (238).

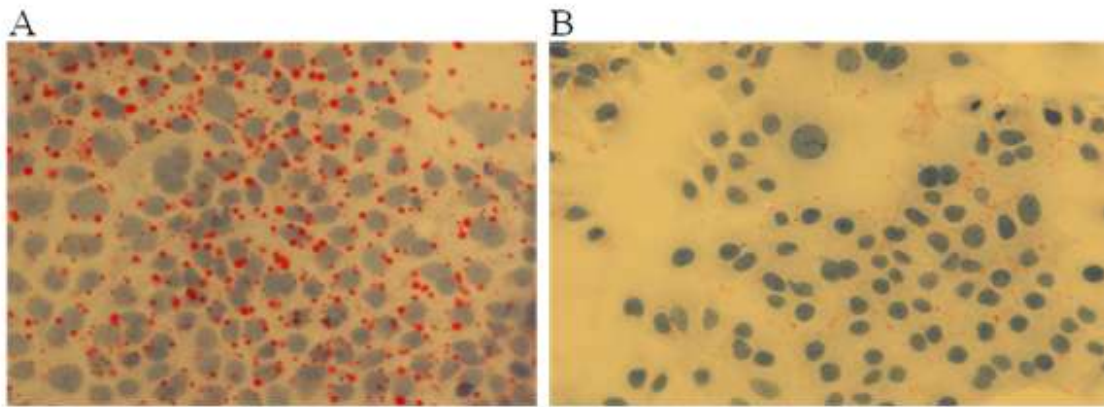


Figure 3.13 – Lipid Droplets in Cells Cultured in Huh7.5 Cells Cultured Using 2% HS Supplemented or 10% FBS Media. Huh7.5 Cells were differentiated in media containing HS for 21 days. Cells were fixed and stained using Oil Red O. Lipid droplets are shown in red and nucleus in blue. (A) There are larger lipid droplets in cells cultured in HS (B) than cells cultured in FBS.

3.4.2 Assessment of Total Lipid Content

In order for cells to utilize β -oxidation, cells need to have triglyceride available as a substrate. Triglycerides are broken down to yield fatty acids which are degraded through β -oxidation. To determine the amount of lipids present in Huh7.5 cells under

both culture conditions, lipids were extracted using chloroform: methanol. The lipids were then separated using a three solvent gradient in an Onyx monolithic silica normal phase column (Section 2.5.2). This analysis was conducted in the Lipidomics Core Facility in Edmonton. The lipids detected include triglycerides, phospholipids and cholesterol (Section 3.3.1.2.1 and Section 3.3.1.2.2).

3.4.2.1 Triglycerides and Fatty Acid Content

The previous experiment using Oil Red O to stain lipid droplets in Huh7.5 cells showed that cells grown in the presence of HS have larger and more lipid droplets. In order to quantify the triglyceride present in cells cultured in HS and FBS, extracted lipids were analyzed using HPLC total lipid class analysis. The results from the analysis show that when cells were grown in HS media there is a 3.7 fold increase in triglyceride compared to FBS media. Fatty acids were also detected using this method of analysis. There was a significant increase in the mass of fatty acids present in cells grown in HS media compared to FBS media (Figure 3.14).

Overall, this set of results is consistent with our hypothesis that Huh7.5 cells grown in HS have increased triglyceride present within each cell. Additionally, this result is consistent with data reported previously (238).

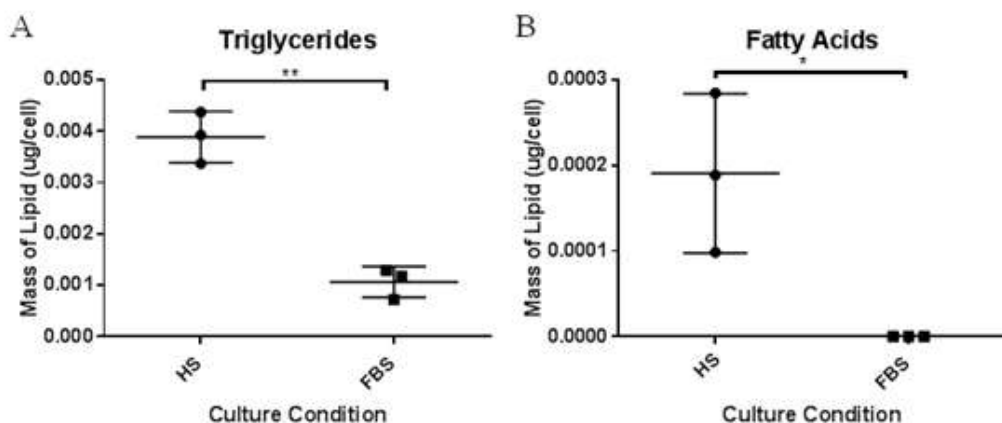


Figure 3.14 –Triglyceride and Fatty Acid Content in Cells Cultured in 2% HS Media or 10% FBS Media. Lipids were extracted from Huh7.5 cells grown HS media for 21 days or FBS media. The lipids were analyzed using HPLC total lipid class analysis (Lipidomics Core Facility in Edmonton). The mass of lipids were normalized to cell number. (A) The mass of triglycerides and (B) fatty acid was higher in cells cultured in HS media compared to FBS media. This experiment was conducted in duplicate and repeated 3 times. Each point represents the average value for each experiment. * P<0.05
** P<0.01

3.4.2.2 Phospholipid and Cholesterol Content

Phospholipids and cholesterol were detected in the HPLC total lipid class analysis. The precursor to phospholipids, DG was detected, along with phospholipids such as PC, PE and sphingomyelin. PC and PE are the most common phospholipids present within plasma membranes. Sphingomyelin, also a phospholipid is involved in cellular signaling and cholesterol clustering in the plasma membrane (262–264). The main purpose of cholesterol in the cell is to modulate the fluidity of the plasma membrane (264).

When cells were cultured in HS media, there was no significant difference in the mass of DG detected when normalized to cell number. However, the phospholipids PE, PC and sphingomyelin were respectively 13, 7 and 4 fold greater in cells grown with HS (Figure 3.15). Additionally, there was 6 fold more free cholesterol and 9 fold more cholesterol esters (16:0 and 18:0) in cells cultured in the presence of HS. However, the cholesterol ester (20:4) was absent in cells grown with HS media or FBS media (Figure 3.16). Overall, these results suggest that there are much more phospholipids and cholesterol per HS media grown cell compared to FBS media grown cells.

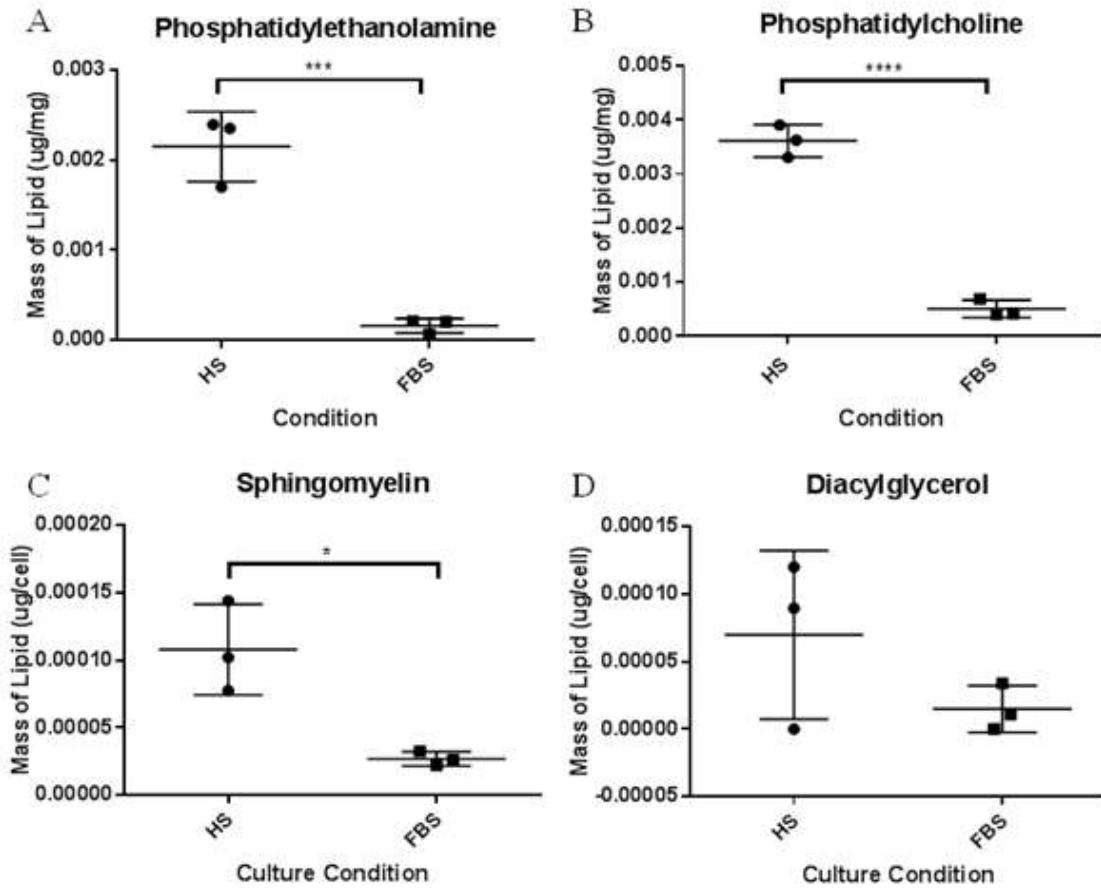


Figure 3.15 – Phospholipid Content in Cells Cultured in 2% HS Media or 10% FBS Media. Lipids were extracted from Huh7.5 cells grown in FBS and differentiated cells grown in media containing HS for 21 days. The lipids were analyzed using HPLC total lipid class analysis (Lipidomics Core Facility in Edmonton). The mass of lipids were normalized to cell number. (A) The mass of phosphatidylethanolamine (B) phosphatidylcholine (C) sphingomyelin was significantly higher in cells cultured in HS media compared to FBS media (D) there was no difference in diacylglycerol in HS cultured and FBS cultured cells. This experiment was conducted in duplicate and repeated 3 times. Each point represents the average value for each experiment. *P<0.05 *** P<0.001 **** P<0.0001

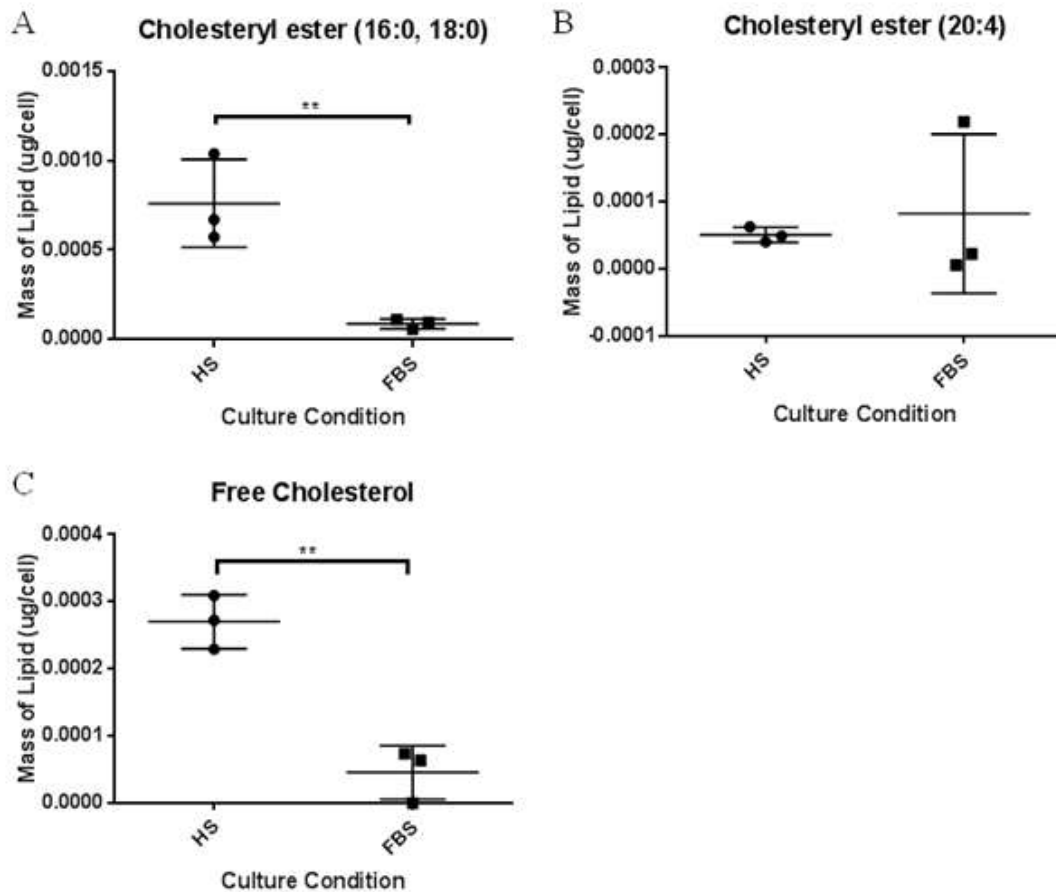


Figure 3.16 –Cholesterol Content in Cells Cultured in 2% HS Media or 10% FBS Media. Lipids were extracted from Huh7.5 cells grown in FBS and differentiated cells grown in media containing HS for 21 days. The lipids were analyzed using HPLC total lipid class analysis (Lipidomics Core Facility in Edmonton). The mass of lipids were normalized to cell number. (A) The mass of cholesterol esters 16:0 and 18:0 was significantly higher in cells cultured in HS media compared to FBS media (B) There is no difference in cholesterol esters 20:4 (C) There was higher free cholesterol cells grown in HS compared to FBS media. This experiment was conducted in duplicate and repeated 3 times. Each point signifies the average value for each experiment. ** P<0.01

3.5 HS Differentiated Cells as a Model to Study HCV

The results from Section 3.2 to Section 3.3 show increased lipid metabolism in cells grown in HS media. Prior to using Huh7.5 cells cultured in HS to study the effects of HCV infection on lipid metabolism, these cells were infected with HCV to examine the characteristics of the infection and the proportion of cells infected with HCV.

3.5.1 Assessment of HCV Production

To determine virus production in Huh7.5 cells grown in the presence of HS and FBS, cells were infected at a GE of 1. Supernatant was collected at different time points post infection for quantification of HCV RNA through qPCR (Section 2.3.2 to Section 2.3.3). Virus released by HS media cultured cells reached 1.5×10^7 HCV RNA copies per mL 13 days post infection. At 21 days post infection, the virus production remained relatively stable at 2.1×10^7 HCV RNA copies per mL (Figure 3.17).

In cells grown in FBS media, virus production reached a maximum at days 10 post infection (1×10^6 HCV RNA copies per mL). The virus production decreased sharply 13 days post infection (Figure 3.17). By microscopy, the reduction of HCV RNA at day 13 was a result of massive cell lysis due to HCV infection. The reduction in virus production continued to 17 days post infection when the experiment was terminated due to the lack of adherent cells. This experiment showed that HS cultured cells produce more virus compared to cells grown in FBS without undergoing cell lysis as indicated by the stable production of HCV until the experiment was terminated.

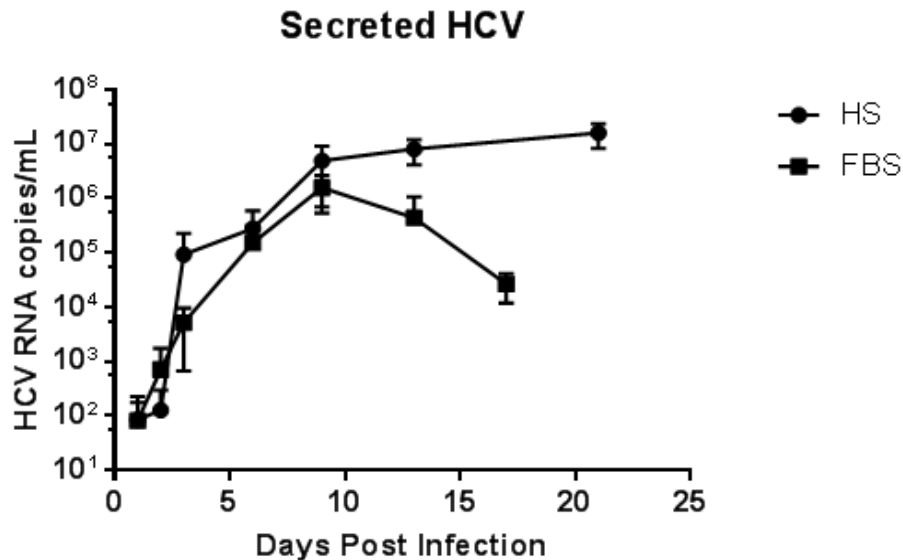


Figure 3.17 – HCV Production in Huh7.5 Cells in Two Different Culture Systems. Huh7.5 cells are infected for 4 hours at GE of 1 after an overnight incubation in delipidated serum. Samples were collected at different time points and HCV RNA was quantified using qPCR. This experiment was repeated twice. Each point represents the average value for both experiments.

3.5.2 Assessment of Specific Infectivity of HCV

Next, the specific infectivity of HCV produced under the two culture conditions was examined using a TCID₅₀ assay. It was previously reported that virus produced from cells grown in HS media have a 10 fold increase in specific infectivity compared to cells cultured in media supplemented with FBS (238). Huh7.5 cells grown in FBS media were infected with HCV produced from either HS or FBS cultured cells. An initial stock of 3×10^6 HCV RNA/ml was used to infect cells, the stock was serially diluted from 10^{-1} to 10^{-6} to determine the concentration where 50% of the wells had

positive staining for HCV infection. The TCID₅₀ was calculated using the Reed and Muench method (Section 2.3.4).

The specific infectivity of virus produced in cells cultured in HS was 1 per 247 copies of HCV RNA. This is similar to values reported previously (238). On the other hand, the specific infectivity of virus produced in cells cultured in FBS was 1 per 1241 copies of HCV RNA (Figure 3.18). HCV produced in cells cultured in HS was 5 fold more infectious than virus produced in cells cultured in FBS.

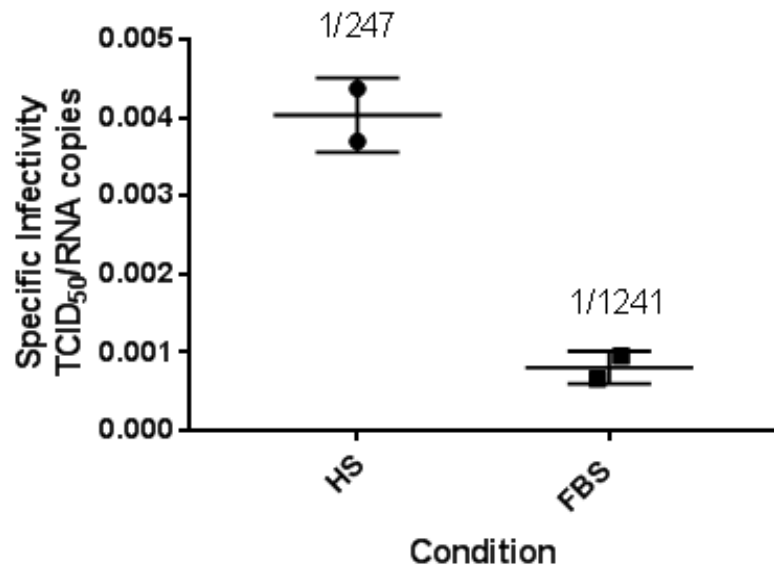


Figure 3.18 – Specific Infectivity of HCV Produced in Huh7.5 Cells. Cells were incubated overnight in DFBS then infected with serially diluted HCV produced from cells grown in HS media or FBS media for 4 hours. After 72 hours, cells were fixed and anti-NS5a antibody was used as a marker for HCV infection. The TCID₅₀ was defined as the concentration required to infect 50% of the wells. The TCID⁵⁰ was calculated using Reed and Muench method. This experiment was repeated twice. Each point represents the average value for each experiment.

3.5.3 Assessment of Proportion of HCV Infected Cells

To study metabolic differences between HCV infected and uninfected cells, we needed to determine the time at which all the cells were infected. To assess the proportions of cells that are infected with HCV in cells grown in HS and FBS, cells were infected with HCV during the differentiation process. The cells were grown on coverslips and subjected to fluorescence microscopy to view cells that stained positively for HCV core protein. Cells grown in HS media and infected with HCV infection for 7 days, approximately 90% of the cells were positive for HCV core (Figure 3.19A – 3.19C). At 21 days post infection, all cells stained positive for HCV core (Figure 3.20A – 3.30C). Conversely, when cells were grown in FBS in the presence of HCV infection for 7 days, 70-80% of the cells stained positive for HCV core with minimal cell lysis (Figure 3.20A – 3.20C). The high specificity of the anti-core antibody used in the assay is indicated by the lack of staining in uninfected cells (Figure 3.19D – 3.19E, Figure 3.20D – 3.20E and Figure 3.21D – 3.20E).

These results show that that the optimal time to study HCV infection of cells in HS media was 21 days post infection when cells are fully differentiated and are 100% infected.

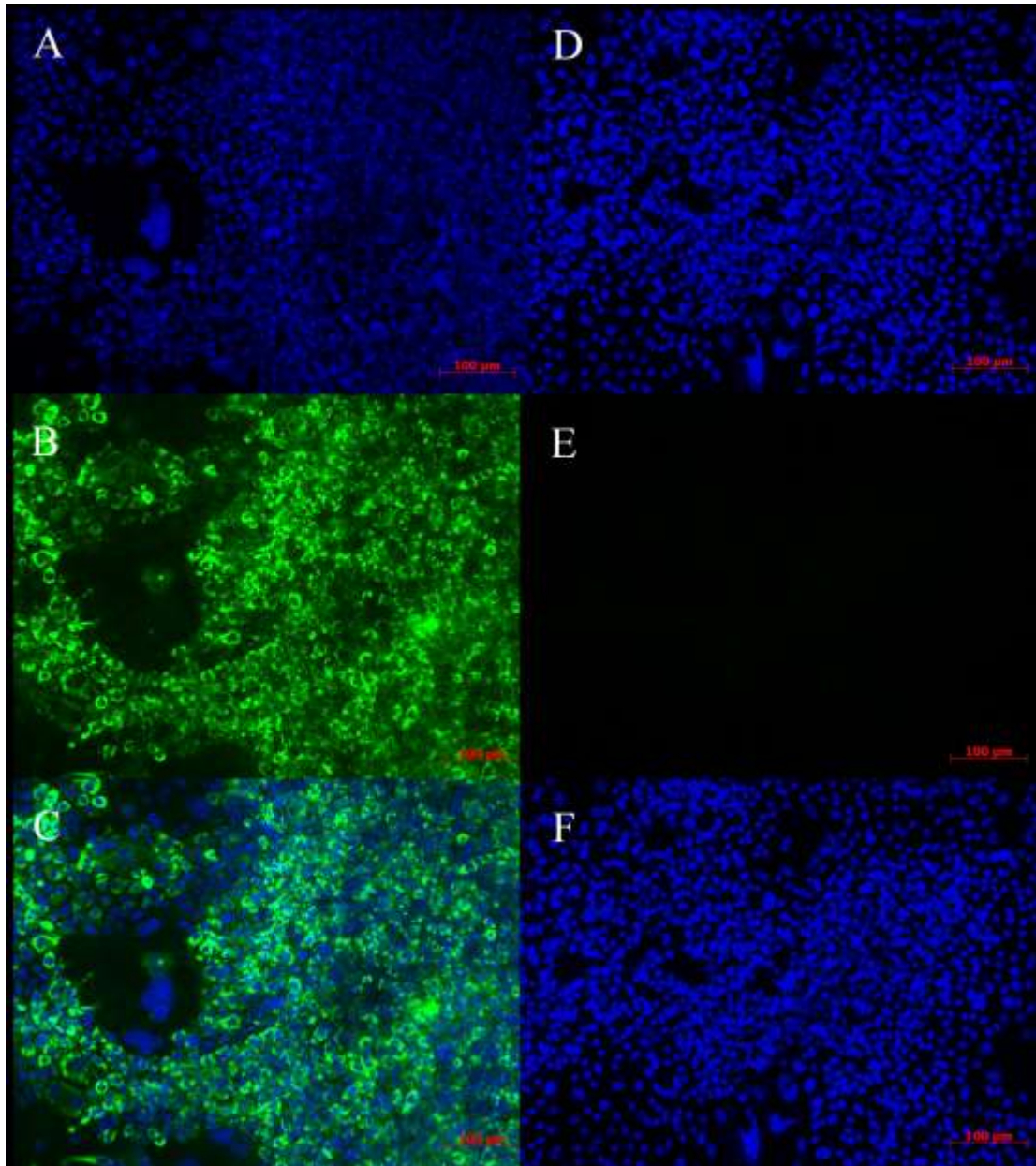


Figure 3.19 – Proportion of Huh7.5 Cells Cultured in 2% HS Media with HCV Infection for 7 Days. Huh7.5 cells were grown in HS media for 7 days with or without HCV infection then fixed. Anti-HCV core protein was used as a primary antibody. The secondary antibody is Alexafluor 488 which is fluorescent green. The nucleus of each cell is stained blue using Hoechst. (A) Nuclear staining in infected cells (B) Alexafluor488 staining in infected cells (C) Merge of the previous two channels. (D) Nuclear staining of uninfected cells (E) Alexafluor488 staining on uninfected cells (F) Merge of the previous two channels.

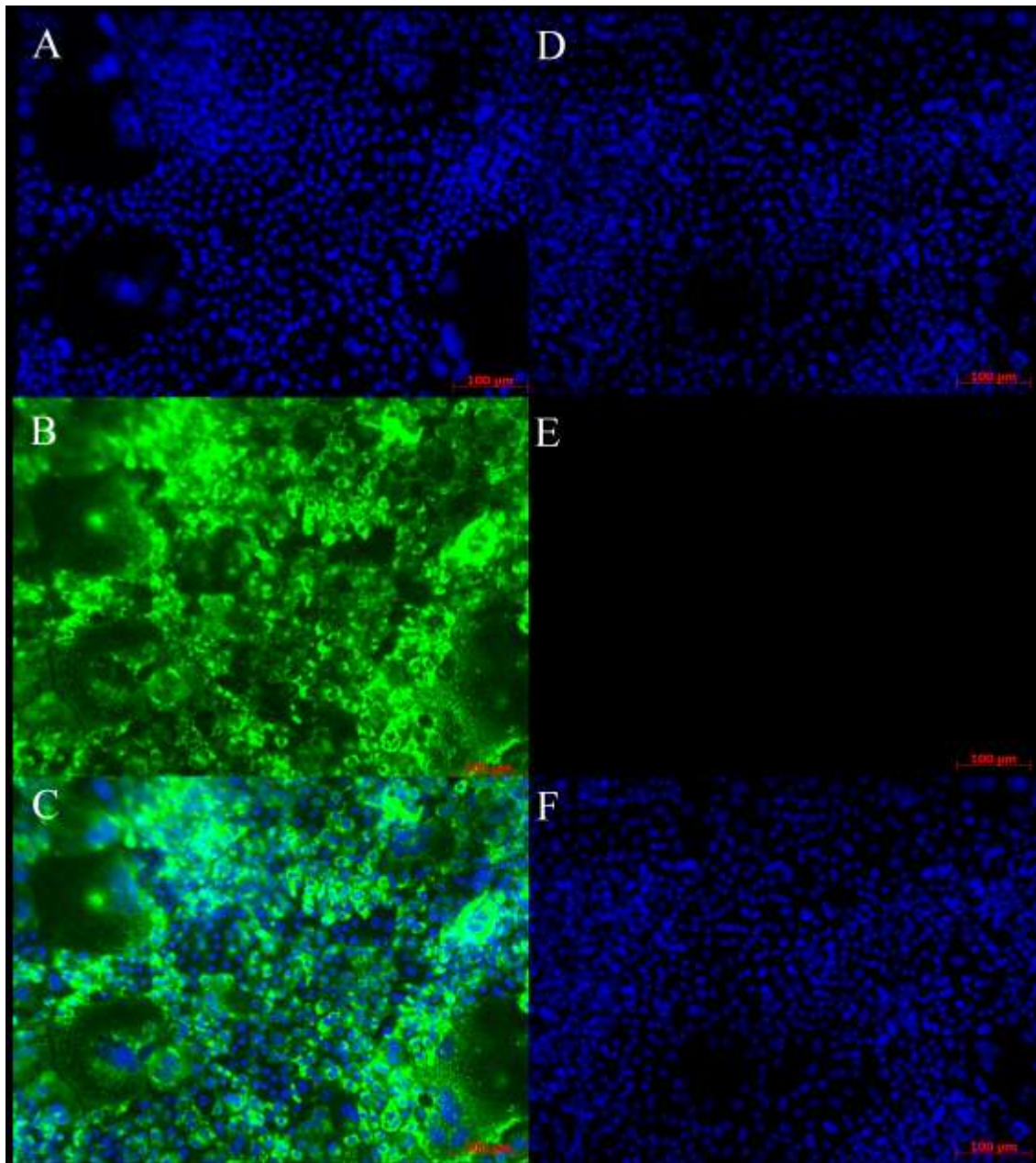


Figure 3.20 – Proportion of Huh7.5 Cells Cultured in 2% HS Media with HCV Infection for 21 Days. Huh7.5 cells were grown in HS media for 21 days with or without HCV infection then fixed. Anti-HCV core protein was used as a primary antibody. The secondary antibody is Alexafluor 488 which is fluorescent green. The nucleus of each cell is stained blue using Hoechst. (A) Nuclear staining in infected cells (B) Alexafluor488 staining in infected cells (C) Merge of the previous two channels. (D) Nuclear staining of uninfected cells (E) Alexafluor488 staining on uninfected cells (F) Merge of the previous two channels.

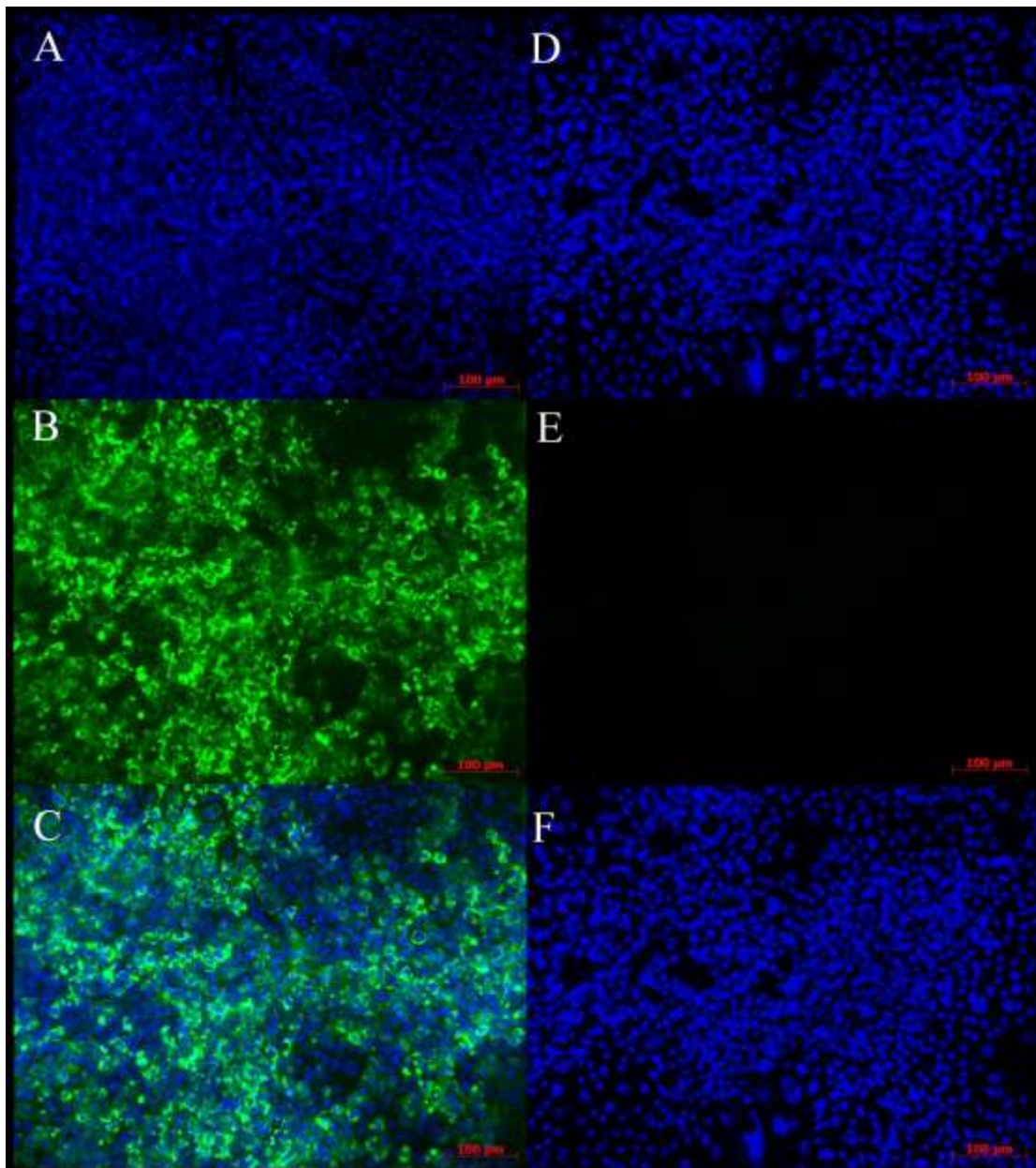


Figure 3.21 – Proportions of Huh7.5 Cells Grown in 10% FBS Media Infected with HCV in the two Culture Systems. Huh7.5 cells grown using FBS media were fixed after 7 days of HCV infection. Anti-HCV core protein was used as a primary antibody. The secondary antibody is Alexafluor 488 which is fluorescent green. The nucleus of each cell is stained blue using Hoechst. (A) Nuclear staining in infected cells (B) Alexafluor488 staining in infected cells (C) Merge of the previous two channels. (D) Nuclear staining of uninfected cells (E) Alexafluor488 staining on uninfected cells (F) Merge of the previous two channels.

3.6 Summary of Differences in Huh7.5 Cells Cultured in HS and FBS

The markers of differentiated cells grown in HS media and cells grown in FBS media cultured cells were studied. The key biomarkers for proper differentiation were VLDL secretion and increased albumin secretion. The results from Section 3.1 showed that HS media cultured cells produced VLDL and increased albumin production compared to cells grown in FBS media. These results were comparable to data reported in literature (238).

Next, the metabolism of these cells was studied using NMR. NMR was used to determine secreted metabolites while the XFe24 analyzer was used to determine whether there were any changes in pathways such as glycolysis and β -oxidation when cells cultured in HS media compared to FBS media. A variety of metabolites showed significant differences in Huh7.5 cells cultured in HS media compared to FBS media. However, only the metabolites acetoacetate and 3-hydroxybutyrate were further examined as these compounds are produced in the ketogenesis pathway that is downstream of β -oxidation. The concentration of acetoacetate and 3-hydroxybutyrate were 21 and 8 fold higher in media taken from HS cultured cells respectively (Section 3.2.1.6). The increase in ketogenesis was reflected by an increase dependency on β -oxidation and increased rate of β -oxidation (Section 3.2.2 – 3.2.3) and increased production of CPT-1 in cells cultured in HS media (Section 3.3). Finally, the amount of lipid droplets present in HS and FBS cultured cells were examined using an Oil Red O stain. The results from this analysis showed that there were larger lipid droplets when cells are grown in media containing HS (Section 3.4.1). Next, the main component of lipid droplets, triglycerides, was examined using the HPLC total lipid class analysis. The results showed that there was 3.7 fold more TG present within cell

when they are grown in the presence of HS compared to FBS, consistent with our expectation and previously reported data (Section 3.4.2.1) (238).

Finally, Huh7.5 cells cultured in HS media were infected with HCV to determine the optimal time to collect media samples and cell lysates for analysis. Cells grown in HS media were infected for 21 days during the differentiation process and the proportion of cells that were infected was visualized using immunofluorescence. The analysis showed that after 21 days post infection, nearly all cells stained positive for HCV core. Thus, for future experiments, cells were grown for 21 days in HS media in the presence of HCV infection before any samples were collected.

***CHAPTER 4: The Effects of
HCV Infection on Lipid
Metabolism***

Chapter 4: The Effects of HCV Infection on Lipid Metabolism

4.1 Assessment of Metabolism during HCV Infection

To examine whether HCV infection leads to metabolic changes relative to uninfected cells, the metabolism of HCV infected and uninfected cells were examined using NMR to study changes in secreted metabolites. We focused on the secreted metabolites rather than the intracellular metabolites since very few intracellular metabolites detected in the NMR analysis. The XFe24 analyzer was used to confirm some of the results from the NMR analysis.

4.1.1 Assessment of Metabolomic Profile

The metabolomic profile of Huh7.5 cells cultured with or without HCV infection was examined. Cells were grown for a minimum of 21 days in media supplemented with HS, with or without HCV infection. The day before sample collection, cells were washed three times then incubated for 24 hours in serum free DMEM5796. The supernatant was collected from these cells and metabolites were measured using NMR (Section 2.6.1). Using this approach, a total of 16 out of 34 detected metabolites were significantly different between HCV infected and uninfected cells cultured in HS media. The results from the analysis are summarized in Table A.2 in the Appendix. The metabolites that showed significant differences between each condition were grouped into 4 categories: metabolites associated with amino acid metabolism, phospholipid metabolism, glucose metabolism and lipid metabolism.

4.1.1.1 Amino Acid Metabolism

4.1.1.1.1 Arginine, Glycine and Proline Metabolism

The amino acids glycine, arginine and proline were significantly different in the media of HCV infected and uninfected cells (Section 3.2.1.1). The amino acids glycine and arginine present in DMEM5796 media, were utilized significantly more slowly by HCV infected cells relative to uninfected cells. Specifically, there was 2 fold more arginine, and 1.8 fold more glycine detected in media take from HCV infected cells relative to uninfected cells (Figure 4.1A – 4.1B). On the other hand, proline, which is not a component of DMEM5796 media, was 3 fold lower in HCV infected cells (Figure 4.1C).

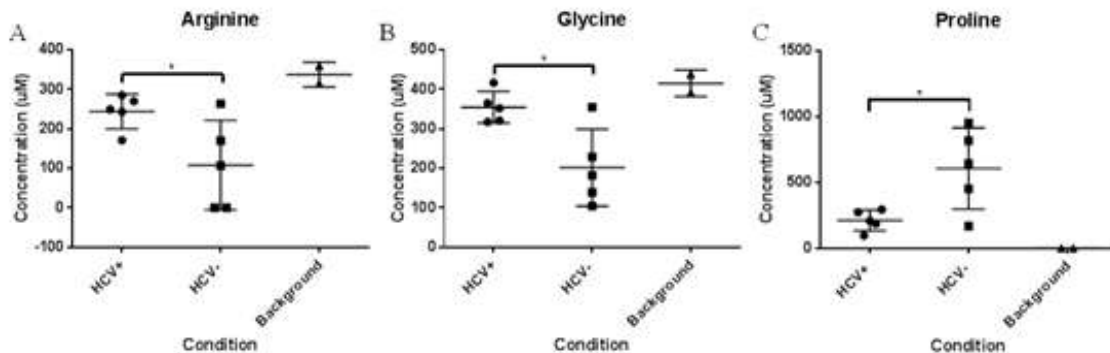


Figure 4.1 – Arginine, Glycine and Proline Metabolism in Huh7.5 Cells Cultured in 2% HS with or without HCV Infection. Huh7.5 cells were cultured in media containing HS for 21 days with or without HCV infection. Prior to collecting the supernatant for analysis, cells were placed in serum free media and incubated at 37°C. The supernatant was collected after 24 hours and analyzed using NMR. The concentration of (A) arginine, (B) glycine were significantly higher in HCV infected cells while (C) proline was lower in the supernatant taken from HCV infected cells compared to uninfected cells. This experiment was conducted in duplicate and repeated 5 times. Each point represents the average value for each experiment. *P<0.05

4.1.1.1.2 Tryptophan Metabolism

The amino acid tryptophan was significantly different in the supernatant of HCV infected and uninfected cells using NMR. Tryptophan is an essential amino acid that is involved in the synthesis of proteins, serotonin in the central nervous system and the kynurenine pathway in all tissues. In most tissues, including the liver, 95% of all tryptophan is metabolized in the kynurenine pathway. In this pathway, tryptophan is initially converted into kynurenine by tryptophan dioxygenase. Next, kynurenine is converted into 2-amino-3-carboxymuccinate semialdehyde through a series of multiple reactions involving the enzymes kynurenine hydroxylase, kynureninase and 3-hydroxyanthranilate 3, 4 dioxygenase. Finally, 2-amino-3-carboxymuccinate semialdehyde is metabolized to yield NAD^+ (265). NAD^+ can be reduced to yield NADH, NADH can be oxidized to synthesize ATP by OXPHOS. NAD^+ has also been implicated in the regulation of NAD-dependent deacetylase sirtuin 1 (SIRT1) (266–270). SIRT1 is known to deacetylate transcription factors that are major regulators of metabolism such as peroxisome proliferator-activated receptor gamma coactivator 1-alpha (PGC-1 α) and estrogen-related receptor alpha (ERR α). SIRT-1 regulation of PGC-1 leads to increase gluconeogenesis while SIRT-1 regulation of ERR α leads to increased expression of genes associated with gluconeogenesis, OXPHOS and fatty acid metabolism (267,271–273).

Tryptophan is one of the components of DMEM5796 media. When cells were cultured in the presence of HCV infection, there was a 3 fold increase in tryptophan detected relative to uninfected cells (Figure 4.2). The higher concentration of tryptophan detected in media taken from cells infected with HCV suggests that there is a reduced metabolism of tryptophan and possibly a reduction of NAD^+ synthesis.

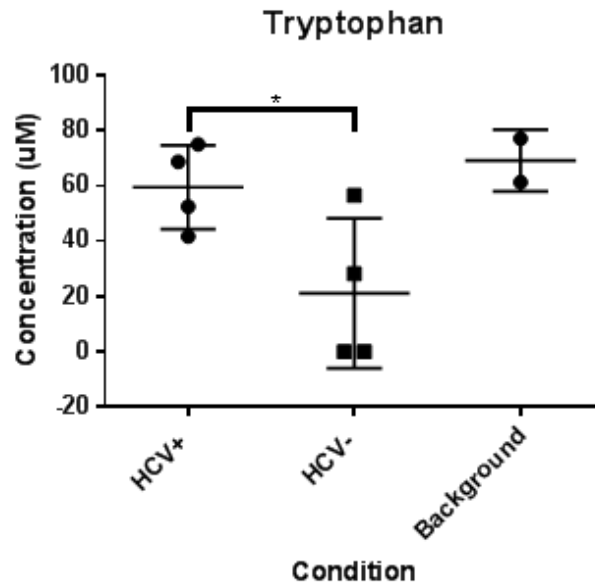


Figure 4.2 – Tryptophan Metabolism in Huh7.5 Cells Cultured in 2% HS with or without HCV Infection. Huh7.5 cells were cultured in media containing HS for 21 days with or without HCV infection. Prior to collecting the supernatant for analysis, cells are first placed in serum free media and incubated at 37°C. The supernatant was collected after 24 hours and analyzed using NMR. The concentration of tryptophan was lower in the supernatant taken from Huh7.5 cells cultured in HS in the presence of HCV compared to uninfected cells. This experiment was conducted in duplicate and repeated 4 times. Each point represents the average value for each experiment. *P<0.05

4.1.1.1.3 Methionine Metabolism

Methionine can be used to synthesize new proteins or it can be metabolized in two main pathways, the methionine cycle produces homocysteine which is an intermediate in the transsulfuration pathway. Formate is involved in the conversion of homocysteine into methionine (Section 3.2.1.3). The results from the NMR analysis show that during HCV infection, there was significantly lower utilization of

methionine compared to cells that were not infected with HCV. Specifically, there was approximately 50% more methionine detected in media taken from HCV infected cells compared to uninfected cells (Figure 4.3A). Formate, on the other hand, was 50% lower in media taken from HCV infected cells relative to uninfected cell (Figure 4.3B). These results suggest that the methionine cycle and transsulfuration pathways within HCV infected cells may be less active in producing metabolites such as glutathione, taurine and pyruvate. Additionally, there may be a reduction in the conversion of homocysteine into methionine in HCV infected cells.

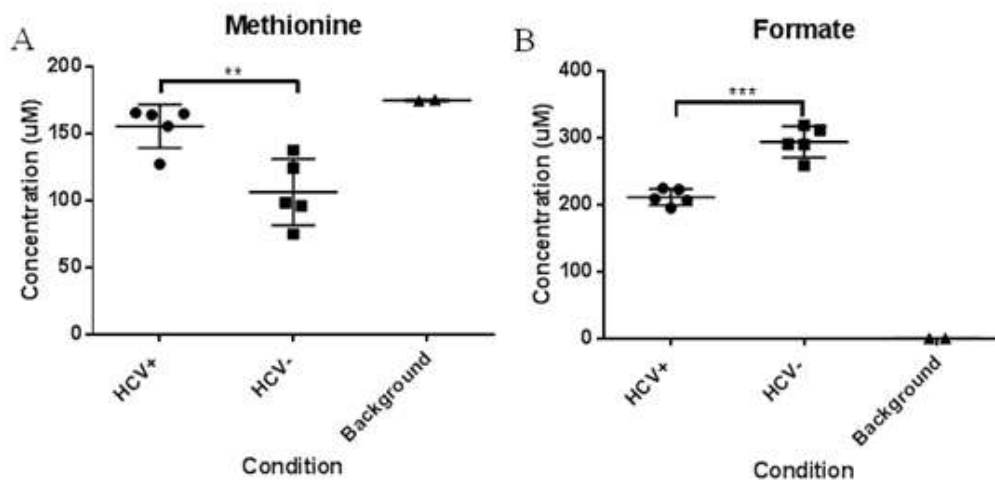


Figure 4.3 – Methionine Metabolism in Huh7.5 Cells Cultured in 2% HS with or without HCV Infection. Huh7.5 cells were cultured in media containing HS for 21 days with or without HCV infection. Prior to collecting the supernatant for analysis, cells are first placed in serum free media and incubated at 37°C. The supernatant was collected after 24 hours and analyzed using NMR. The concentration of (A) methionine was significantly higher in supernatant taken from cells that are infected with HCV while (B) the concentration of formate was significantly lower relative to uninfected cells. This experiment was conducted in duplicate and repeated 5 times. Each point signifies the average value for each experiment. **P<0.01 *** P<0.001

4.1.1.1.4 Alanine Metabolism

There was significant differences in alanine was detected in the supernatant of HCV infected compared to uninfected cells by using NMR. Alanine is a nonessential amino acid that is not a component of the DMEM5796 media. Alanine is used to synthesize new proteins or metabolized in the liver primarily through the actions of ALT. ALT catalyzes the reversible reaction between pyruvate and glutamate to produce alanine and α -ketoglutarate, an intermediate of the TCA cycle. *In vivo*, the liver is involved in

the uptake of alanine produced during protein degradation in the muscle and the conversion of the alanine to pyruvate as part of the alanine cycle (274). In cells infected with HCV, there was 50% less alanine detected in the media relative to uninfected cells suggesting a reduction in the conversion of pyruvate to alanine (Figure 4.4).

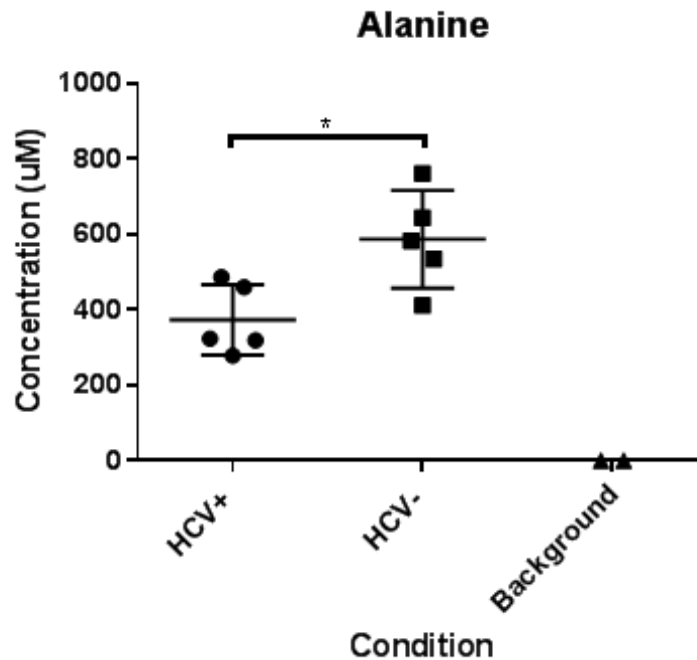


Figure 4.4 – Alanine Metabolism in Huh7.5 Cells Cultured in 2% HS with or without HCV Infection. Huh7.5 cells were cultured in media containing HS for 21 days with or without HCV infection. Prior to collecting the supernatant for analysis, cells are first placed in serum free media and incubated at 37°C. The supernatant was collected after 24 hours and analyzed using NMR. There was significantly less alanine detected in the supernatant take from HCV infected cells compared to uninfected cells. This experiment was conducted in duplicate and repeated 5 times. Each point represents the average value for each experiment. * P<0.05

4.1.1.1.5 Phenylalanine Metabolism

Phenylalanine, another component of the DMEM5796 media was detected at significantly difference concentrations in HCV infected and uninfected cells. This essential amino acid can be incorporated into protein or it can be metabolized to yield fumurate and acetoacetate that are part of the TCA cycle and ketogenesis pathway respectively (275). In cells cultured in the presence of HCV infection, there was a decrease in the utilization of phenylalanine relative to HCV uninfected cells (Figure 4.5). These results indicate that there may be increased phenylalanine metabolism in uninfected cells compared to infected cells.

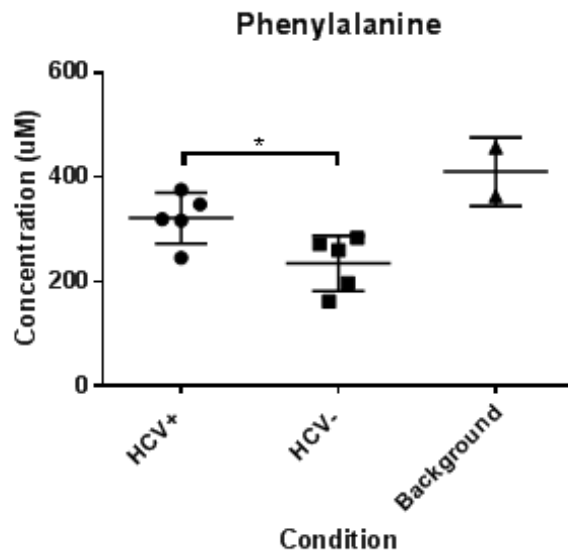


Figure 4.5 – Phenylalanine Metabolism in Huh7.5 Cells Cultured in 2% HS with or without HCV Infection. Huh7.5 cells were cultured in media containing HS for 21 days with or without HCV infection. Prior to collecting the supernatant for analysis, cells are first placed in serum free media and incubated at 37°C. The supernatant was collected after 24 hours and analyzed using NMR. The concentration of phenylalanine in the supernatant was significantly higher in Huh7.5 cells cultured in HS in the presence of HCV. This experiment was conducted in duplicate and repeated 5 times. Each point represents the average value for each experiment. *P<0.05

4.1.1.1.6 Leucine Metabolism

The leucine degradation yields 3-hydroxyisovalerate. Further metabolism of 3-hydroxyisovalerate degradation yields HMG-CoA, a precursor of cholesterol and ketone bodies (Section 3.2.1.2.1). When cells were infected with HCV, there was 20% more leucine present relative to uninfected cells (Figure 4.6A). The reduced metabolism of leucine seen in HCV infected cells was reflected in a 5 fold reduction in 3-hydroxyisovalerate (Figure 4.6B). These results suggested that when cells were infected with HCV, the reduction in leucine degradation leads to the decreased synthesis of metabolites such as acetoacetate.

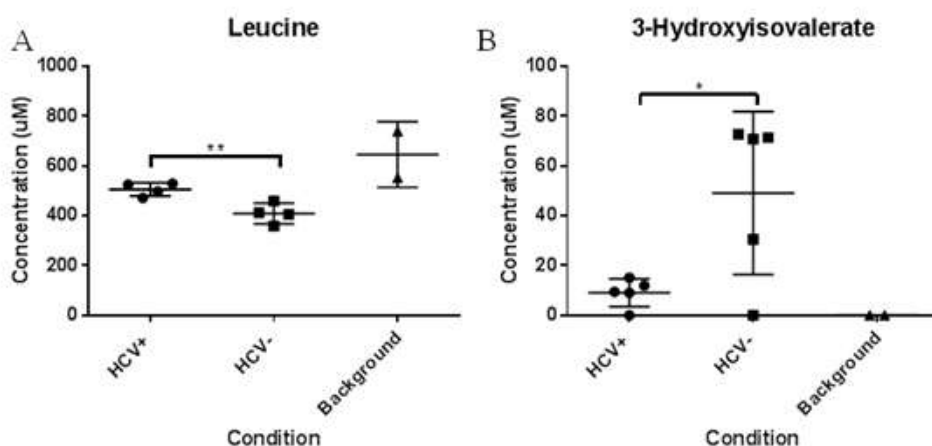


Figure 4.6 – Leucine Metabolism in Huh7.5 Cells Cultured in 2% HS with or without HCV Infection. Huh7.5 cells were cultured in media containing HS for 21 days with or without HCV infection. Prior to collecting the supernatant for analysis, cells are first placed in serum free media and incubated at 37°C. The supernatant was collected after 24 hours and analyzed using NMR. (A) Leucine was significantly higher the supernatant of HCV infected cells compared to uninfected cells (B) There was significantly lower 3-hydroxyisovalerate detected in the supernatant of cells cultured in the presence of HCV infection. This experiment was conducted in duplicates and repeated at least 4 times. Each point represents the average value for each experiment. *P<0.05 **P<0.01

4.1.1.2 Phospholipid Metabolism

O-phosphocholine was detected at significantly difference concentrations in the supernatant taken from HCV infected and uninfected cells. O-phosphocholine is the precursor of PC, the most common phospholipid in cells (Section 3.2.1.4). There was no detectable difference in the concentration of choline detected between HCV infected and uninfected cells (Figure 4.7A). Conversely, there was 15 fold more O-phosphocholine in the media of cells infected with HCV compared to uninfected cells (Figure 4.7B). This result suggests in both infected and uninfected cells, the choline was completely metabolized into O-phosphocholine. However, the presence of O-phosphocholine in the supernatant taken from infected cells may likely be the result of cell death since O-phosphocholine is normally an intracellular metabolite.

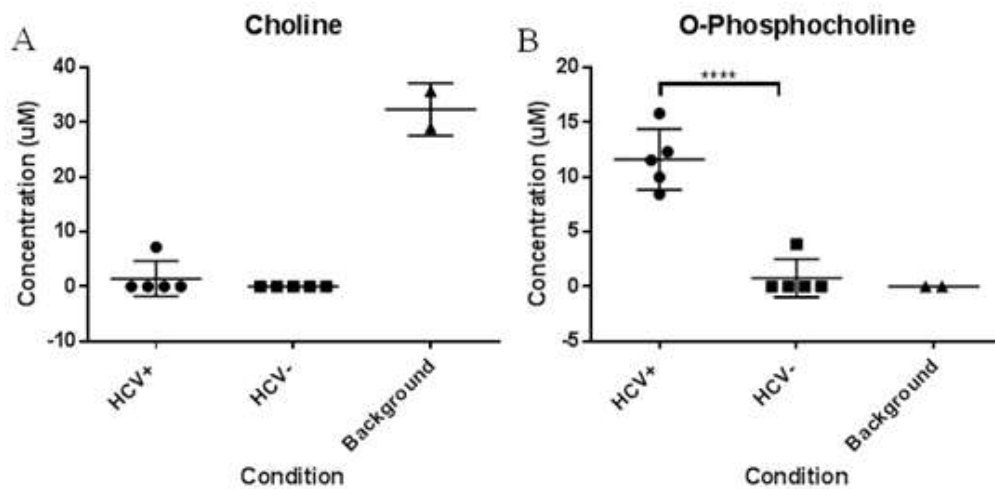


Figure 4.7 – O-phosphocholine Metabolism in Huh7.5 Cells Cultured in 2% HS with or without HCV Infection. Huh7.5 cells were cultured in media containing HS for 21 days with or without HCV infection. Prior to collecting the supernatant for analysis, cells are first placed in serum free media and incubated at 37°C. The supernatant was collected after 24 hours and analyzed using NMR. (A) There is no difference in choline while (B) there was a higher concentration of O-phosphocholine that was detected in the supernatant during HCV infection compared to cells that were not infected. This experiment was conducted in duplicate and repeated 5 times. Each point represents the average value for each experiment. **** P<0.0001

4.1.1.3 Glycolysis

The metabolites associated with glycolysis and OXPHOS were detected in supernatant of HCV infected and uninfected cells. The concentration of glucose was 40% higher in the media of HCV infected cells compared to uninfected cells (Figure 4.8A). The concentration of pyruvate generated by HCV infected or uninfected cells were comparable (Figure 4.8B). However, in uninfected cells, there was 50% more lactate generated relative to HCV infected cells (Figure 4.8C). In addition, there was 25% more acetate detected in HCV infected cells (Figure 4.8D). Acetate is

metabolized into acetyl-CoA which enters the TCA cycle, ketogenesis pathway (276). Taken together, these results suggest that there is an increase in glycolysis in uninfected cells to generate pyruvate or macromolecules. Additionally, the pyruvate is converted into lactate more readily in uninfected cells compared to infected cells.

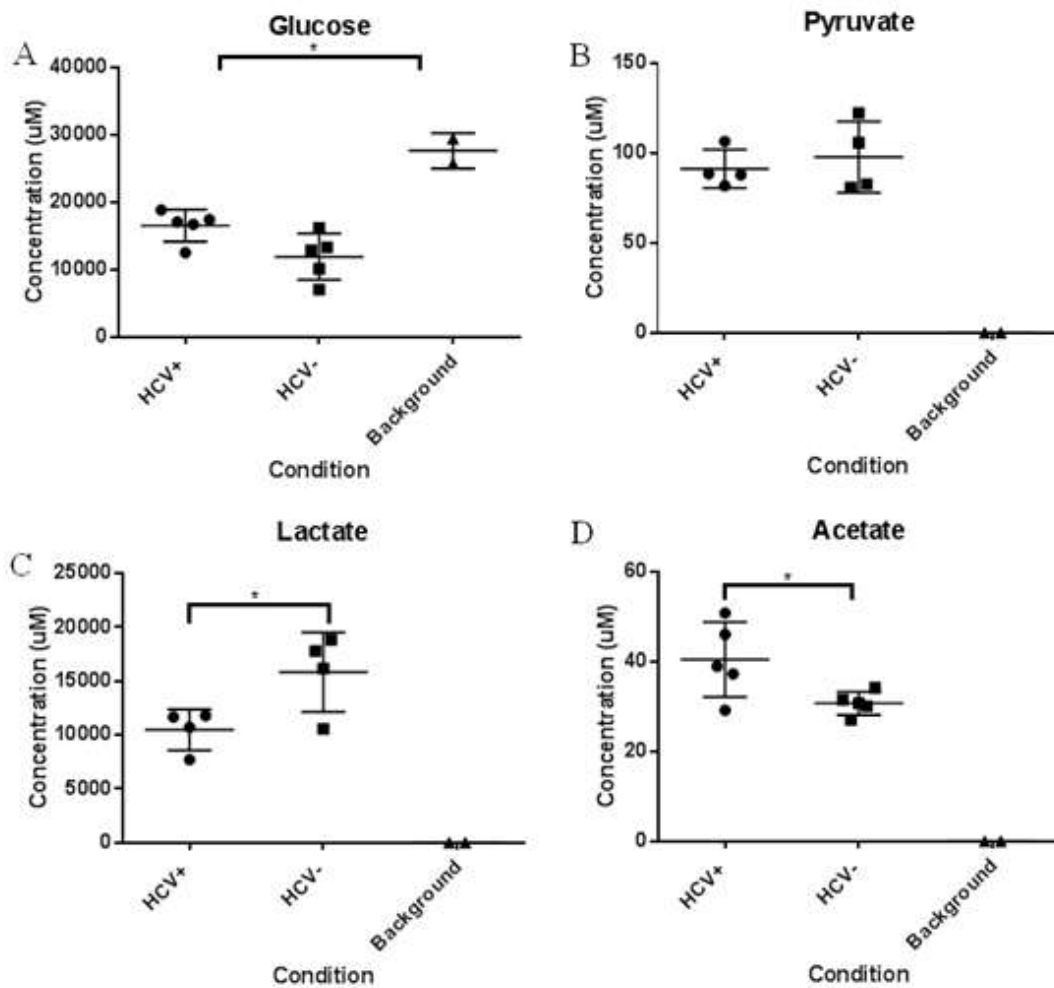


Figure 4.8 – Glucose Metabolism in Huh7.5 Cells Cultured in 2% HS with or without HCV Infection. Huh7.5 cells were cultured in media containing HS for 21 days with or without HCV infection. Prior to collecting the supernatant for analysis, cells are first placed in serum free media and incubated at 37°C. The supernatant was collected after 24 hours and analyzed using NMR. (A) There was significantly more glucose detected in the supernatant of cells that were infected with HCV compared to uninfected cells. (B) There was similar concentration of pyruvate secreted into the supernatant of HCV infected and uninfected cells. (C) There was significantly less lactate that was detected during HCV infection compared to the absence of infection. (D) There was significantly more acetate that was detected in the supernatant of HCV infected cells relative to uninfected cells. This experiment was conducted in duplicate and repeated at least 4 times. Each point represents the average value for each experiment. * P<0.05

4.1.1.4 Ketogenesis

Using NMR analysis on secreted metabolites, ketone bodies were detected in the supernatant of HCV infected and uninfected cells. The ketone bodies are a product of the ketogenesis pathway which is downstream from β -oxidation (Section 3.2.1.6). When cells were infected with HCV, there was an 8.5 fold reduction in acetoacetate and 7 fold reduction in 3-hydroxybutyrate secreted in the media. However, there was no difference in acetone in the media of HCV infected and uninfected cells (Figure 4.9). This result suggests that there was less ketogenesis occurring in HCV infected cells. One possibility leading to the reduction in ketogenesis is decreased β -oxidation in HCV infected cells.

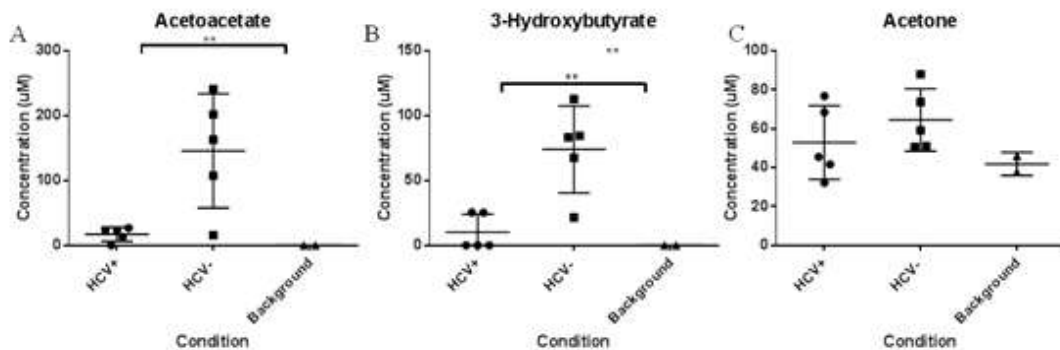


Figure 4.9 – Ketogenesis in Huh7.5 Cells Cultured in 2% HS with or without HCV Infection. Huh7.5 cells were cultured in media containing HS for 21 days with or without HCV infection. Prior to collecting the supernatant for analysis, cells are first placed in serum free media and incubated at 37°C. The supernatant was collected after 24 hours and analyzed using NMR. (A) There was significantly less acetoacetate and (B) 3-hydroxybutyrate during HCV infection compared to the absence of HCV infection. (C) There was no difference in acetone that was detected in the supernatant of HCV infected and uninfected cells. This experiment was conducted in duplicate and repeated 5 times. Each point represents the average value for each experiment. ** P<0.01

4.1.2 Assessing the Metabolic Flux of Huh7.5 Cells during HCV Infection

To determine whether there was a change in the cell's ability to utilize energy producing pathways such as glycolysis, β -oxidation and glutaminolysis, cells were grown in HS media with or without HCV infection. The OCR was then measured using the XFe24 analyzer to measure the dependency on each pathway.

The results show that glycolysis, β -oxidation and glutaminolysis were active in HCV infected and uninfected cells. However, there was no difference in the dependency of glycolysis, β -oxidation and glutaminolysis as means to provide substrates for the TCA cycle and OXPHOS in HCV infected and uninfected cells cultured in HS media (Figure 4.10). Taken together, these results suggest that there is no difference in the mitochondria's ability to utilize glycolysis, β -oxidation and glutaminolysis in HCV infected and uninfected cells. However, this assay does not measure the rates of each pathway that is occurring in HCV infected and uninfected cells.

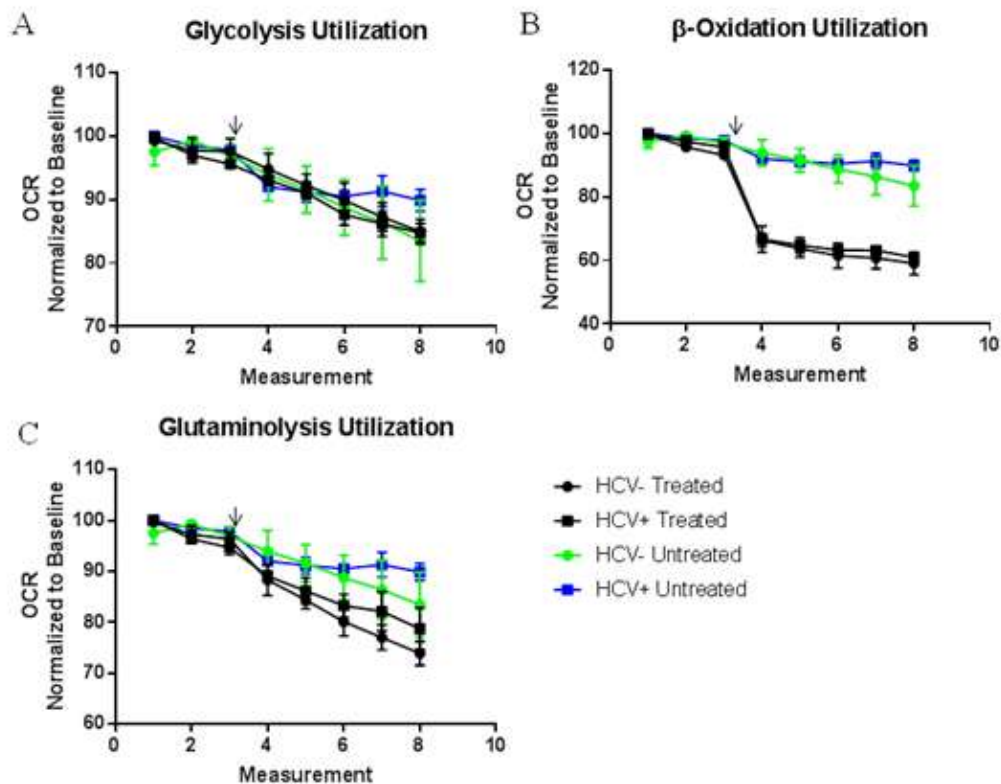


Figure 4.10 – HCV Infected and Uninfected Cells Cultured in 2% HS dependency on Glycolysis, β -oxidation and Glutaminolysis. Huh7.5 cells were grown in HS, with or without HCV infection for 28 days. The metabolic flux was analyzed using the XFe24 analyzer. The first three points were basal measurements then the inhibitor is added after the third timepoint. The results were normalized to untreated cells. (A) The inhibitor UK5099 was added after the third time point to measure dependency on glycolysis to provide pyruvate for the TCA cycle (B) The inhibitor etomoxir was added after the third time point to measure dependency on β -oxidation to provide acetyl CoA for the TCA cycle (C) The inhibitor BPTES was added after the third time point to measure dependency on glutaminolysis to provide α -ketoglutarate for the TCA cycle. This experiment was repeated three times. Each point represents the average value for each experiment. Arrows indicate the addition of inhibitors.

4.1.3 Assessment of the Rate of β -oxidation

To address the limitation of Section 4.1.2, a different assay was used to assess the rates of β -oxidation rather than the cell's ability to utilize different pathways in HCV infected and uninfected cells. The exact rates of β -oxidation were assessed by the XFe24 analyzer from Seahorse Bioscience (Section 2.6.3). To differentiate between the endogenous, maximum and spare capacity for β -oxidation, the inhibitors oligomycin, FCCP and a combination of rotenone and antimycin A was used (Table 2.6). The endogenous β -oxidation is defined as the level of β -oxidation to meet the energetic demand of the cell under baseline conditions. The maximum β -oxidation is defined as the maximum rate of β -oxidation that a cell can achieve. The spare capacity of β -oxidation is defined as the cells ability to respond to energetic demands by increasing the rate of β -oxidation.

In cells grown in the presence of HCV infection, there was a 4 fold decrease in the endogenous β -oxidation compared to uninfected cells. Additionally, the maximum β -oxidation and spare capacity for β -oxidation was 8 and 9 fold lower respectively in infected cells compared to uninfected cells (Figure 4.11). Taken together with the results in Section 4.1.2, the mitochondria in infected and uninfected cells have a similar ability to utilize β -oxidation when glycolysis and glutaminolysis were inhibited. However, when assessing β -oxidation alone, there was a significantly lower rate of β -oxidation in infected cells compared to uninfected cells. Overall, the results from Sections 4.1.1.4 to Sections 4.1.3 suggest an overall reduction in β -oxidation in HCV infected cells compared to uninfected cells.

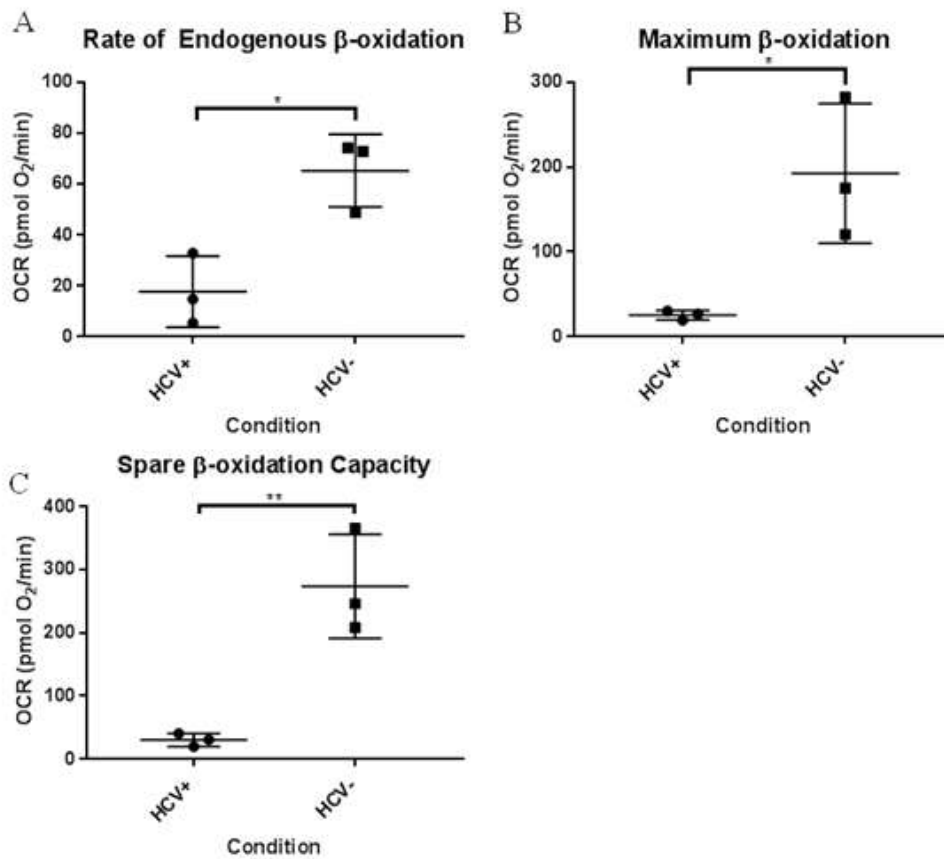


Figure 4.11 – Endogenous β -oxidation, Maximum β -oxidation and Spare Capacity for β -oxidation in Huh7.5 Cells Cultured using 2% HS Supplemented Media with or without HCV Infection. Huh7.5 cells were differentiated in 2% HS supplemented media for 28 days grown cells with or without HCV infection were analyzed using the XFe24 analyzer. The endogenous β -oxidation was calculated by taking the basal OCR and subtracting with the nonmitochondrial respiration rate after rotenone and antimycin A were added. The maximum β -oxidation was calculated by taking the maximal OCR after the addition of FCCP and subtracting with the nonmitochondrial respiration. The spare capacity for β -oxidation was calculated by taking the maximal β -oxidation and subtracting with the basal respiration. (A) There was significantly lower endogenous β -oxidation (B) maximum β -oxidation and (C) spare capacity for β -oxidation in cells that are infected with HCV compared to uninfected cells. This experiment was conducted in triplicates and repeated three times. Each point represents the average value for each experiment. * P<0.05 ** P<0.01

4.2 Assessment of CPT-1 Levels

The previous findings from Section 4.1.1.4 and 4.1.2 suggest that there was a reduction in β -oxidation during HCV infection. To confirm that β -oxidation is reduced during HCV infection, the levels of CPT-1, the transporter that catalyzes the rate limiting step of β -oxidation, was examined in HCV infected and uninfected cells. Cells were first cultured in media supplemented with 2% HS for 21 days with or without HCV infection. Next, the cells were lysed using RIPA buffer and subjected to SDS-PAGE and western blot analysis (Section 2.7). The ratio of the fluorescent intensity between the loading control, β -tubulin and the protein of interest, CPT-1 was determined for HCV infected and uninfected cells. There was approximately 50% less CPT-1 detected in HCV infected cells compared to cells that were not infected with HCV (Figure 4.11). These results suggested that a decrease in CPT-1 in HCV infected cells may lead to a reduction in β -oxidation and accumulation of lipids.

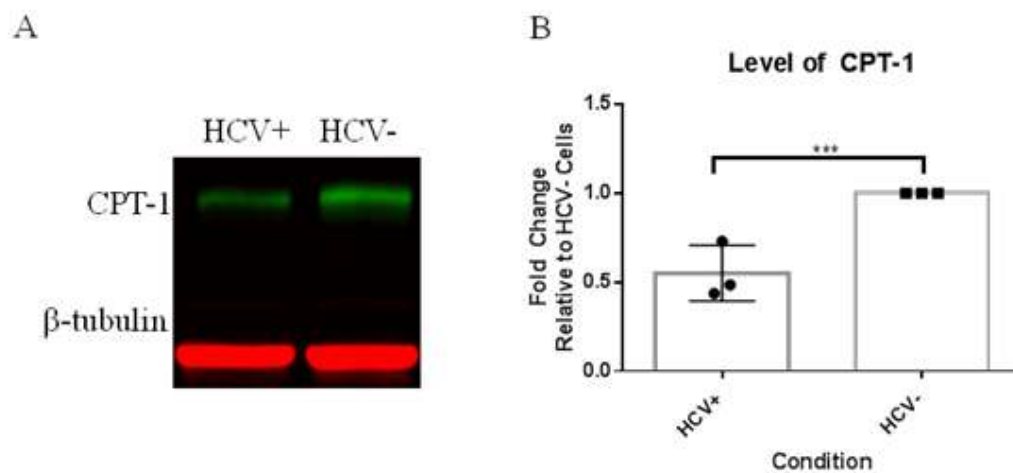


Figure 4.11 – CPT-1 Protein Levels in Huh7.5 Cells Cultured in 2% HS media with or without HCV Infection. Huh7.5 cells were cultured in media containing 2% HS for 21 days with or without HCV infection. After 21 days, cells were lysed using RIPA and 20ug of protein from cell lysates were subjected to SDS-PAGE and Western blot analysis using a Licor approach. (A) CPT-1 is shown in green, which is 82kDa. The loading control, β -tubulin is shown in red, which is 51kDa. (B) The ratio of signal intensity was obtained from CPT-1 and β -tubulin and normalized to uninfected cells. This experiment was repeated three times, each point signifies a single experiment. *** $P < 0.001$

4.3 Assessment of Lipid Content

It was shown previously that β -oxidation and ketogenesis were decreased in HCV infected Huh7.5 cells cultured in media supplemented with 2% HS (Section 4.1 – 4.2). To determine whether HCV infection leads to an increase in lipids, two different approaches were used.

4.3.1 Assessment of Total Lipid Content

To determine the total lipid content within HCV infected and uninfected cells cultured in the presence of 2% HS, lipids were extracted using a 1:1 ratio of chloroform: methanol. The lipids were then separated using a three solvent gradient in an Onyx monolithic silica normal phase column (Section 2.5.2, Lipidomics Core Facility in Edmonton). Using this approach, several groups of lipids such as cholesterol, phospholipids and triglycerides were detected.

4.3.1.1. Triglycerides and Fatty Acid Content

The major constituents of lipid droplets, triglycerides and fatty acids were detected using the HPLC total lipid class analysis. When cells were infected in the presence of HS, there was no difference in the levels of triglyceride compared to the levels found in uninfected cells (Figure 4.12A). However, significantly less fatty acids were detected in HCV infected cells compared to uninfected cells (Figure 4.12B). Taken together these results suggest that there were similar triglyceride content in HCV infected and uninfected cells. However, there was likely a reduction in the breakdown of triglyceride into fatty acid in HCV infected cells compared to uninfected cells. A limitation of using the HPLC total lipid class analysis to determine triglyceride content was the inability to detect small differences in the levels of triglycerides detected. This approach was more suitable in determining the mass of phospholipids and cholesterol in cells (277–279).

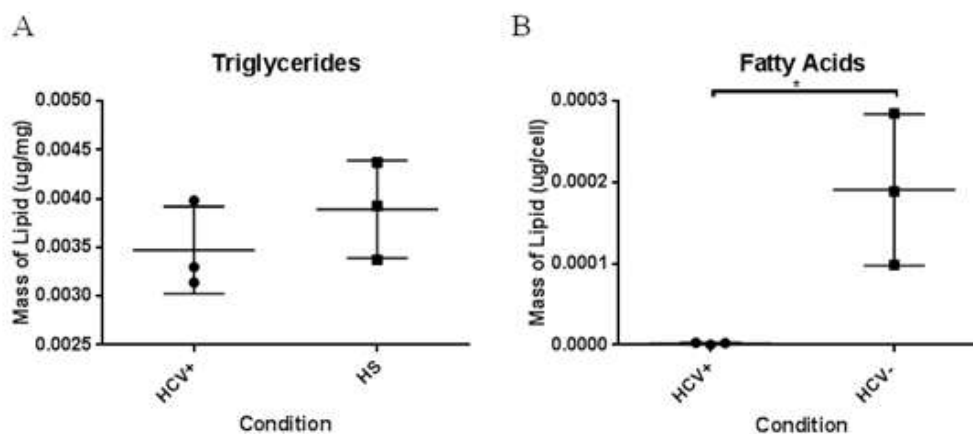


Figure 4.12 – Triglyceride and Fatty Acids Content in Huh7.5 Cells Cultured in 2% HS media with or without HCV Infection. Lipids were extracted from Huh7.5 cells grown in HS, with or without HCV infection for 21 days. The lipids were extracted using a 1:1 ratio of chloroform: methanol. The lipids were then separated using a three solvent gradient in an onyx monolithic silica normal phase column. The mass of lipids were normalized to cell number. (A) There was no significant difference in triglycerides in HCV infected and uninfected cells (B) The mass of fatty acid in HCV infected cells was significantly lower compared to uninfected cells. This experiment was conducted in duplicate and repeated 3 times. Each point represents the average value for each experiment. * P<0.05vb

4.3.1.2 Phospholipid and Cholesterol Content

Using the HPLC total lipid class analysis, the phospholipids PE, PC and sphingomyelin were detected. Additionally, the free cholesterol and the cholesterol esters 16:0, 18:0 and 20:4 were also detected. Collectively, these compounds make up majority of the membrane of the cell and organelles (Section 3.3.1.2.2).

When cells were infected in the presence of HS, there were less phospholipids and cholesterol detected per cell. Specifically, the phospholipids PE, PC and sphingomyelin were 7 fold, 6 fold and 5 fold lower respectively in HCV infected cells

compared to uninfected cells. There was no significant change in DG during HCV infection (Figure 4.13). Free cholesterol was 2.5 fold lower during HCV infection while the cholesterol esters 16:0/18:0 and 20:4 were 2 fold and 3 fold lower respectively in HCV infected cells compared to uninfected cells (Figure 4.14). These results are suggest a decrease in phospholipid and cholesterol content in HCV infected cells compared to uninfected cells.

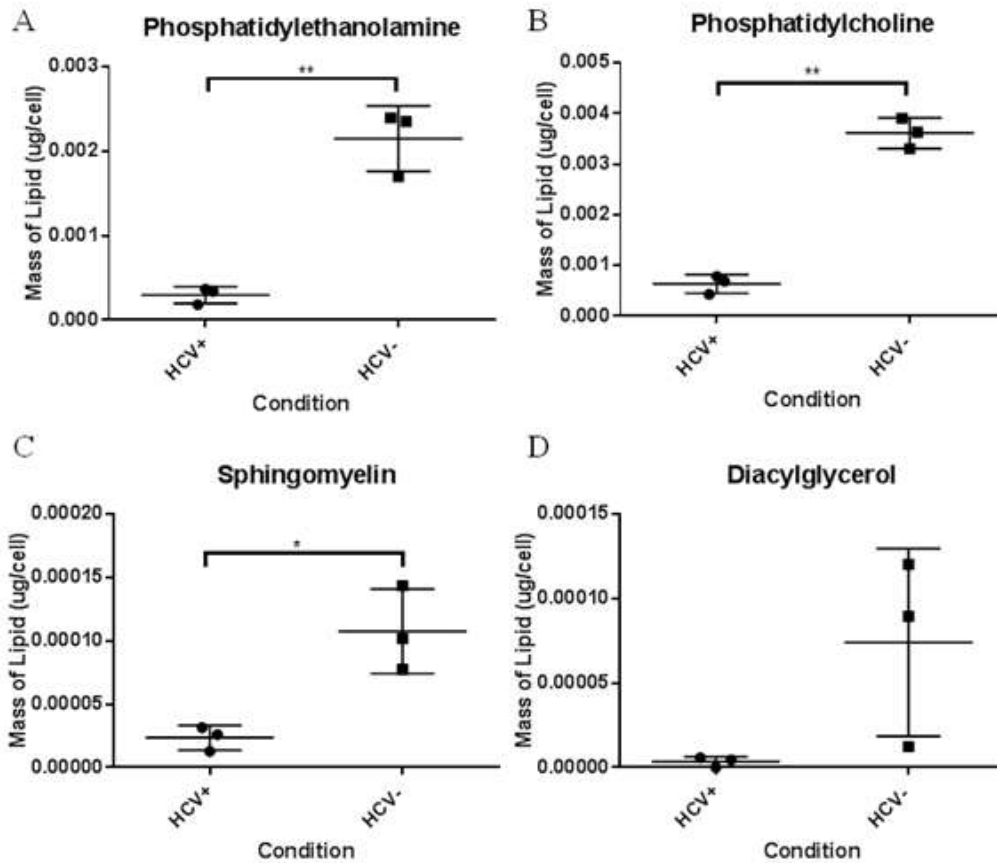


Figure 4.13 – Phospholipid Content in Huh7.5 Cells Cultured in 2% HS supplemented Media with or without HCV Infection. Lipids were extracted from Huh7.5 cells grown in HS media, with or without HCV infection for 21 days. The lipids were extracted using a 1:1 ratio of chloroform: methanol. The lipids were then separated using a three solvent gradient in an onyx monolithic silica normal phase column. The mass of lipids were normalized to cell number. (A) The mass of phosphatidylethanolamine (B) phosphatidylcholine (C) sphingomyelin was significantly lower in cells infected with HCV relative to HCV uninfected cells (D) there was no difference in diacylglycerol in HCV infected and uninfected cells. This experiment was conducted in duplicate and repeated 3 times. Each point represents the average value for each experiment. *P<0.05 ** P<0.01

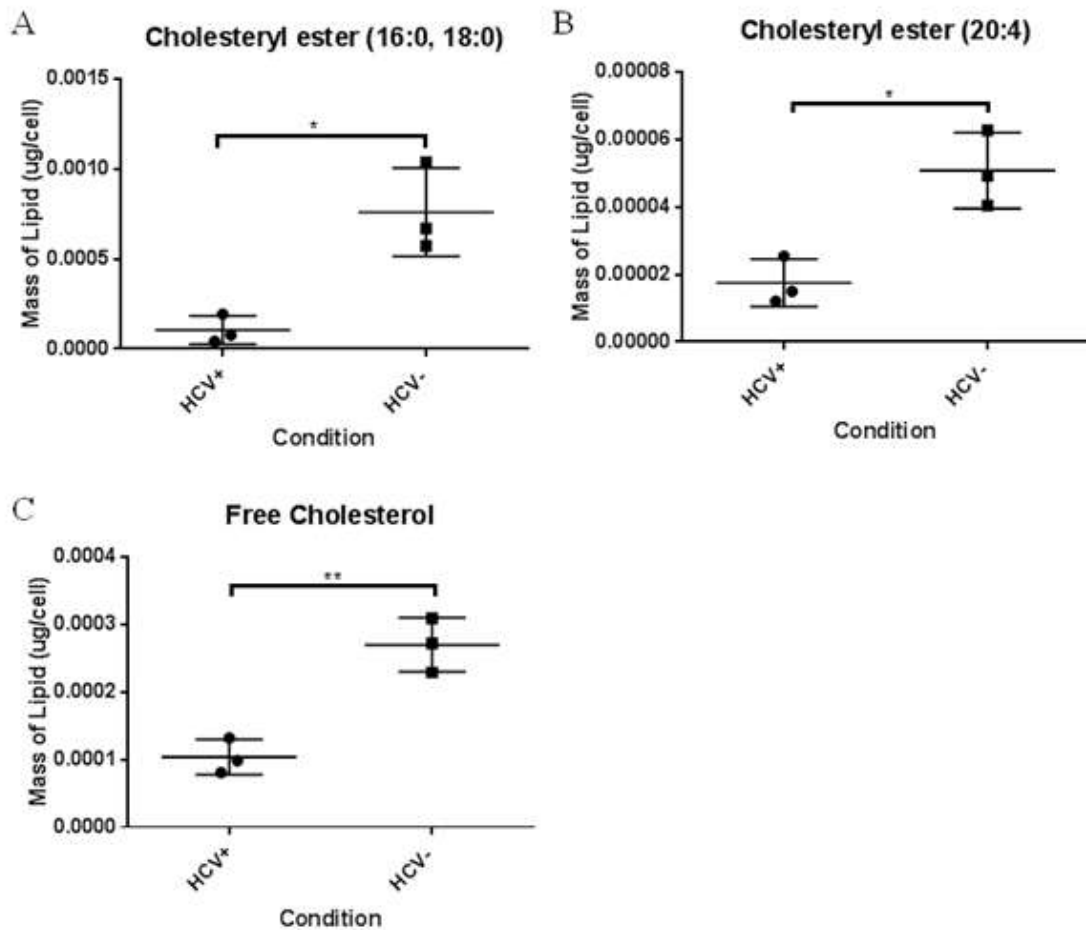


Figure 4.14 –Cholesterol Content in Huh7.5 Cells Cultured in 2% HS media with or without HCV Infection. Lipids were extracted from Huh7.5 cells grown in HS, with or without HCV infection for 21 days. The lipids were extracted using a 1:1 ratio of chloroform: methanol. The lipids were then separated using a three solvent gradient in an onyx monolithic silica normal phase column. The mass of lipids were normalized to cell number. (A) The mass of cholesterol esters 16:0, 18:0 (B) cholesterol esters 20:4 and (C) free cholesterol was significantly lower during HCV infection compared to cells that were not infected with HCV. This experiment was conducted in duplicate and repeated 3 times. Each point represents the average value for each experiment. * P<0.05 **P<0.01

4.3.2 Assessment of Lipid Droplets using Flow Cytometry

In order to address the limitation of the HPLC total lipid class analysis, cells were stained for neutral lipids using Bodipy493/503. Bodipy493/503 was chosen due to the high specificity for lipid droplets compared to other stains such as Nile red while NS5a staining was a marker for HCV infection (280). When comparing the Bodipy 493/503 staining in HCV infected and uninfected cells, there was an average of 50% increased median fluorescence intensity in cells that were HCV infected compared to uninfected cells (Figure 4.14). These results show that there is an accumulation of neutral lipids during HCV infection

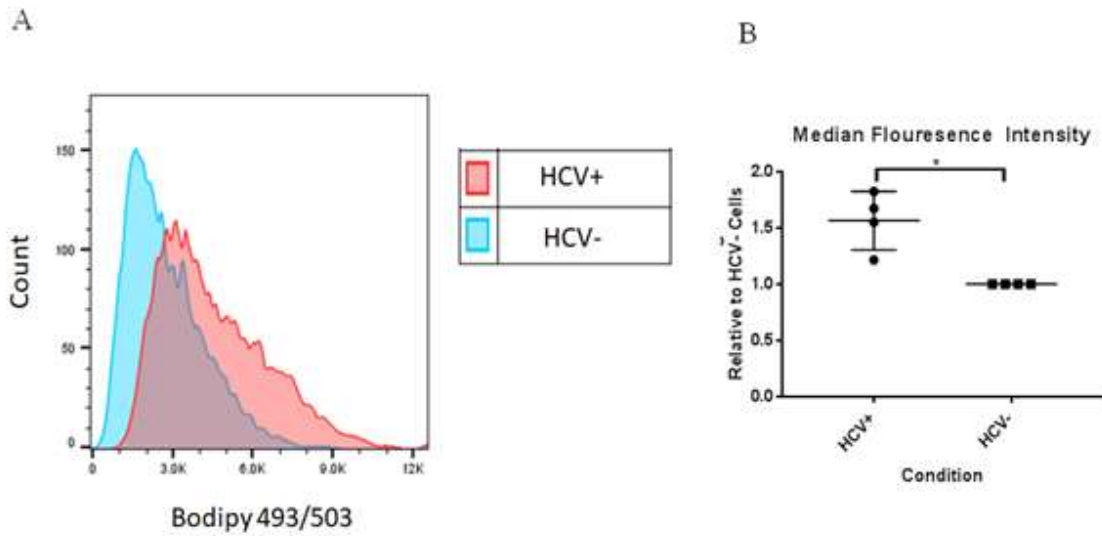


Figure 4.15 – Bodipy493/503 Staining in Huh7.5 Cells Cultured in 2% HS media with or without HCV Infection. Huh7.5 cells were grown in HS, with or without HCV infection for 21 days. Cells were fixed using 4% PFA and permeabilized using the permeabilization buffer from Biolegend. Anti-NS5a 9E10 antibody was used as a marker for HCV infection, the secondary antibody was anti-mouse Alexa647. Neutral lipids were stained using Bodipy493/503. Bodipy493/503 shows a similar emission and excitation wavelengths as Alexa488. (A) There was an increase in the detection of Bodipy493/503 in HCV infected cells compared to (B) uninfected cells. The data shown here was from one experiment. This experiment was representative of 4 other experiments. ** P<0.01

4.4 Effects of Antiviral Therapy on Metabolism in HCV Infected Cells

It has been reported that in a subpopulation of patients who achieve SVR, there is no improvement in liver disease. In fact, it has been reported that steatosis remains unchanged in 50% of the patients who achieved SVR while steatosis worsen in 13% of patients who achieved SVR (281). Additionally, 10% of patients who achieve SVR progress onto more severe liver disease such as fibrosis, cirrhosis and HCC many years after cessation of therapy (282–285). Here, we wanted to examine whether treating cells with Sofosbuvir and eliminating HCV infection would restore levels of ketogenesis to levels present in uninfected cells.

4.4.1 Assessment of HCV RNA following Sofosbuvir Treatment

To determine the optimal concentration of Sofosbuvir to treat HCV infected cells, a dose response curve was generated. Huh7.5 cells that were infected for a minimum of 21 days were treated with a Sofosbuvir concentration of 0.001 μ g/mL, 0.01 μ g/mL, 0.03 μ g/mL, 0.1 μ g/mL, 0.3 μ g/mL, 1 μ g/mL, 3 μ g/mL or 10 μ g/mL. The media was replaced with new media containing Sofosbuvir every 4 days.

Cells treated with a concentration of Sofosbuvir greater than 0.1 μ g/mL showed a reduction in HCV RNA compared to untreated HCV infected cells. At a concentration of 1 μ g/mL or greater with Sofosbuvir, there was a consistent 4 – 5 log reduction in HCV RNA after 12 days of treatment (Figure 4.16A – 4.16C). Despite the consistent 4 – 5 log reduction in HCV RNA, the HCV RNA did not decrease to undetectable levels after 16 days of treatment. Since there was no difference in the reduction of HCV RNA in cells that were treated for 12 and 16 days with

concentrations greater than 1 $\mu\text{g}/\text{mL}$, the treatment regimen chosen for the NMR analysis was 3 $\mu\text{g}/\text{mL}$ for 14 days. The dose response curve was generated from data taken from day 12 of treatment with Sofosbuvir. The inhibitory concentration 50 (IC_{50}) of 38nM obtain from Figure 4.16D was comparable to the IC_{50} of $75 \pm 50\text{nM}$ reported in literature (286).

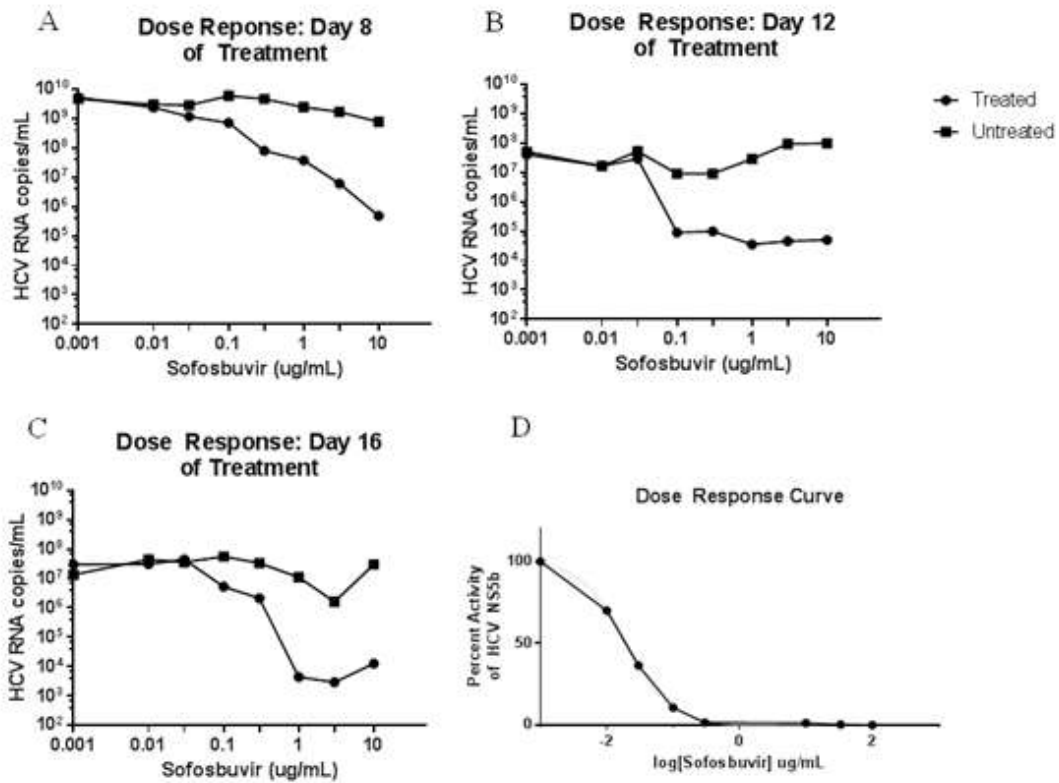


Figure 4.16: HCV Production during Sofosbuvir Treatment in HCV Infected Huh7.5 Cells Cultured in 2% HS. Huh7.5 cells were cultured in media containing HS for 21 days with HCV infection. Cells were treated with Sofosbuvir concentration of 0.001 μ g/mL, 0.01 μ g/mL, 0.03 μ g/mL, 0.1 μ g/mL, 0.3 μ g/mL, 1 μ g/mL, 3 μ g/mL or 10 μ g/mL. Prior to media replacements, a sample was taken to quantify HCV RNA by qPCR. Samples were taken at different time points to determine a dose response. The HCV RNA detected from media taken from cells after (A) 8 days (B) 12 days (C) 16 days of treatment. (D) The dose response curve generated from the previous data. This experiment was conducted in triplicates and conducted once. Each point represents the average of the triplicate.

4.4.2 Assessment of Ketone Body Production after Sofosbuvir Treatment

Cells were cultured in HS media with or without HCV infection for a minimum 21 days. After 21 days, the cells were then treated with 3 μ g/mL of Sofosbuvir for 14 days. Samples of the media were taken after 14 days to quantify the HCV RNA present. Cells were then placed in serum free media for 24 hours. The media was then analyzed using NMR to determine the concentration of acetoacetate secreted.

The quantified HCV RNA confirmed that a 14 day treatment regimen with 3 μ g/mL of Sofosbuvir led to a 4 log reduction in HCV RNA (Figure 4.17A). The secreted metabolites were examined by NMR. Acetoacetate was detected but 3-hydroxybutyrate was not detected. In the media taken from HCV infected cells, there was no significant difference in acetoacetate detected in Sofosbuvir treated and untreated cells. The concentration of acetoacetate secreted in the media of treated HCV infected was significantly lower compared to media taken from uninfected cells (Figure 4.17B). Surprisingly, these results showed that despite treatment with Sofosbuvir, ketogenesis and possibly β -oxidation was not reversed to levels seen in uninfected cells. The lack of reversal in metabolism may be related to the long term effects HCV infection have on the metabolism of hepatocytes. This long term change in metabolism may be one of the factors contributing to the failure to reverse steatosis reported in patients who achieve SVR (281).

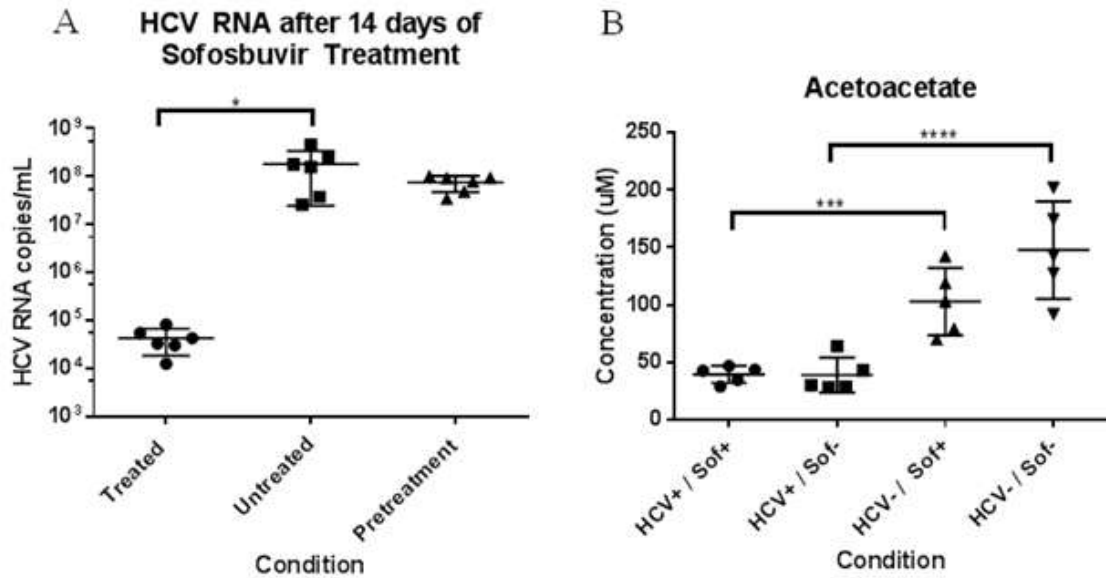


Figure 4.17: HCV RNA and Acetoacetate Production after 3µg/mL Sofosbuvir Treatment for 14 days in Infected Huh7.5 Cells Cultured in 2% HS. Huh7.5 cells were cultured in media containing HS for 21 days with HCV infection. Cells were treated with 3µg/mL of Sofosbuvir for 14 days. After 14 days, samples were collected to quantify HCV RNA by qPCR and cells were placed in serum free media. The supernatant was collected after 24 hours and analyzed using NMR. (A) There was a 4 log reduction in HCV RNA after treatment. (B) There were similar levels of acetoacetate secreted in HCV infected cells regardless if cells were treated with Sofosbuvir or not. This experiment was conducted in duplicates and repeated at least 5 times. Each point represents the average of each experiment. * $P < 0.05$ *** $P < 0.001$ **** $P < 0.0001$. Sof+ indicates treatment with Sofosbuvir. Sof- indicates no treatment. HCV+ indicates infection. HCV- indicates no infection.

4.5 Summary of the Effects of HCV Infection

The metabolomic profile of Huh7.5 cells cultured in media supplemented with 2% HS was examined in the presence or absence of HCV infection. The secretion of a total of 34 metabolites were detected with 16 metabolites that were significantly different between HCV infected and uninfected cells. The metabolites that showed significant difference between HCV infected and uninfected cells included metabolites associated with amino acid metabolism, phospholipid metabolism, glucose metabolism and lipid metabolism (Section 4.1.1). The metabolites detected include acetoacetate and 3-hydroxybutyrate which were 8.5 and 7 fold lower in HCV infected cells compared to uninfected cells. Acetoacetate and 3-hydroxybutyrate are collectively known as ketone bodies. Ketone bodies are products of the ketogenesis pathway that is downstream of β -oxidation. The other pathway downstream of β -oxidation is the TCA cycle. The XFe24 analyzer was used to measure whether there were any differences in the TCA cycle in HCV infected and uninfected cells. The results from Section 4.1.2 showed no difference in the mitochondria's ability to utilize β -oxidation when glycolysis and glutaminolysis were active in HCV infected and uninfected cells. However, the rates of endogenous, maximum and spare capacity for β -oxidation were significantly reduced in HCV infected cells when there were no substrates available for glutaminolysis and glycolysis to occur (Section 4.1.2 and Section 4.1.3). Next, the rate limiting protein of β -oxidation, CPT-1 expression level was examined using SDS-PAGE and Western Blot analysis (Section 4.2). During HCV infection, there was a 50% reduction in the level of CPT-1 compared to cells that were not infected with HCV. The reduction in β -oxidation, ketogenesis (Section 4.1) and CPT-1 (Section 4.2) indicate that there was a quantitative reduction in β -oxidation in HCV infected cells.

There was a reduction in β -oxidation observed during HCV infection and this reduction in β -oxidation was accompanied by an increase in lipid content. The lipid droplet content in HCV infected cells and uninfected cells were measured using Bodipy493/503 since Bodipy493/503 is highly specific towards lipid droplets. The results show a 50% increase in Bodipy493/503 staining in HCV infected cells compared to uninfected cells. These results suggest that HCV infected cells had 50% more lipid droplet content compared to uninfected cells.

Treatment of HCV infected cells with Sofosbuvir did not lead to the restoration of ketogenesis compared to uninfected cells. This lack of reversal may be related to patients who remain steatotic after achieving SVR.

The data in this chapter were consistent with the concept that that impairing β -oxidation may be one of the factors by which HCV causes lipid accumulation and steatosis.

CHAPTER 5: Discussion and Future Directions

Chapter 5: Discussion and Future Directions

5.1 Discussion and Future Directions

There are several mechanisms by which HCV induces steatosis. They include increased lipogenesis, decreased lipid catabolism and decreased lipoprotein secretion (Figure 5.1). SREBP is a transcription factor which is a major activator of lipogenesis. The target genes of SREBP include ATP citrate lyase (ACL), ACC and FAS (210,287–289). These enzymes are involved in the conversion of citrate into acetyl-CoA, conversion of acetyl-CoA into malonyl-CoA and the synthesis of fatty acids using malonyl-CoA (287,289). A series of studies show that abnormally high activation or abundance of SREBP leads to the development of steatosis (208,290–294). One mechanism by which HCV increases lipogenesis is by increasing the activation of SREBP (210–212). Lipogenesis can also occur due to the interaction with HCV RNA and miR-122. By interacting with miR-122, miR-122 cannot target transcripts coding for ACC and FAS for degradation. Lastly, HCV infection decreases translation of ANGPTL3, an inhibitor of extracellular lipases. Increased lipase activity leads to an increase in extracellular fatty acids that are then taken up by the cell (216,217).

HCV infection decreases lipid catabolism by several mechanisms. PPAR α is a transcription factor that controls the expression of genes associated with fatty acid transport and catabolism such as the major fatty acid transporter CPT-1, whose activity is the rate limiting step of β -oxidation (295). Other pathways regulated by PPAR α include β -oxidation and ketogenesis which are the main pathways for the catabolism of fatty acids (216,218,220,295). There have been reports that link a reduction in PPAR α activity with the development of steatosis due to decreased

degradation of triglycerides (296–302). HCV interferes with the PPAR α activity by several mechanisms, possibly contributing to the development of steatosis. First, HCV infection increases miR-27b expression. Increased miR-27b expression leads to reduced translation of transcripts that code for PPAR α . An increase in miR-27a expression reduces levels of another expression factor, RXR. A reduction in RXR decreases heterodimerization with PPAR α and decreased PPAR α activity (216,217,222). The last way HCV infection reduces lipid catabolism is by preventing the degradation of triglycerides within lipid droplets by preventing their interaction with HSL (97).

Another possible mechanism of HCV induced lipid accumulation occurs is by interfering with lipoprotein secretion. HCV infection leads to the inhibition of MTP. MTP functions to lipidate ApoB. The lipidated apoB then interacts with triglycerides to form VLDL which is exported from the cell. A reduction in MTP activity and consequently decreased VLDL secretion might lead to an accumulation of intracellular lipids since less triglyceride is secreted from the cell with VLDL (94,96,223).

In summary, each mechanism by which HCV disturbs lipid metabolism might cause steatosis. The goal of our project was to elucidate elements of the molecular mechanism of steatosis consequent to HCV infection, specifically the effects of HCV infection on lipid catabolism. To examine this, Huh7.5 cells cultured in HS media were used as a model to study the effects of HCV infection on lipid catabolism.

In this model system, hepatocyte-specific functions and lipid metabolism are restored to levels much more similar to that seen *in vivo* compared to the traditional culture system using FBS media (238). Culturing Huh7.5 cells in HS media generates a

lipoprotein profile in the media which is similar to the lipoprotein profile seen in normal sera (Section 3.1) (238). In particular, cells grown in HS media produce HCV that is associated with apoB leading to the formation of virus of lower buoyant density than that of HCV from cells cultured in FBS media (238). This low density of HCV is similar to the density of HCV present in patient sera (74–76,238). Cells grown in HS media have increased transcripts for transcription factors LXR α , PPAR α and PPAR γ (238). LXR α regulates lipogenesis by increasing SREBP1 expression. On the other hand, PPAR α upregulates genes associated with lipid catabolism. Finally, PPAR γ is involved in the storage of fatty acids. The increased expression of these transcripts is reflective of processes that occur in hepatocytes *in vivo* since these pathways are highly active within hepatocytes (303–313). Thus, Huh7.5 cells grown in HS media are more similar to normal hepatocytes due to their secretion of VLDL, increased lipogenesis and their increased lipid catabolism. These cells were chosen to study the effects of HCV infection on these processes. However, we mainly focused on the effects of HCV infection on lipid catabolism.

Prior to using Huh7.5 cells cultured in HS media as a model to study the effects of HCV infection on lipid catabolism, we first wanted to confirm whether there were increased rates of metabolic pathways associated with the increased PPAR α activity in these cells (238). These pathways include β -oxidation and ketogenesis. The protein CPT-1 was also examined since it is the major regulator of fatty acids transport (314). Using the XFe24 analyzer, we showed the mitochondria in cells grown in HS media preferentially use β -oxidation compared to glycolysis. On the other hand, cells in FBS preferentially use glycolysis over β -oxidation. Additionally, we also found a 10 fold increase in the rate of endogenous β -oxidation when culturing cells in HS compared to FBS media (Figure 3.11). Additionally, we found that levels of CPT-1, the

transporter that is the rate limiting step of β -oxidation, was 7 fold higher in cells grown in HS relative to FBS media. In PHH, CPT-1 levels were a 100 fold higher than in cells grown in FBS media. This result implies Huh7.5 cells cultured using HS media were more reflective of PHH's compared to cells grown in FBS media. The activity of ketogenesis was examined using NMR. We found that there was a 21 fold and 8 fold increase in acetoacetate and 3-hydroxybutyrate secreted in cells grown in HS media compared to cells grown in FBS media (Sections 3.2.1.6 to Section 3.3). Overall, the increases in β -oxidation, ketogenesis and CPT-1 activity were observed and are reflective of the increase in PPAR α transcripts in cells grown in HS compared to FBS media (238).

An alternative explanation for the increased ketone bodies generated in cells grown in HS media may partly be explained to the increased degradation of leucine. An intermediate of leucine degradation, 3-hydroxyisovalerate was detected using NMR. The complete metabolism of 3-hydroxyisovalerate yields acetyl-CoA and acetoacetate (315). The acetyl-CoA could enter the ketogenesis pathway while the production of acetoacetate could contribute to the increase in ketone bodies detected during growth in HS media. However, the most likely explanation for the increase in ketone body production is the increase in β -oxidation since the majority of the ketone bodies generated *in vivo* comes from β -oxidation due to the high concentrations of acetyl-Co-A generated when β -oxidation is active (316).

In vivo, the ketogenesis pathway is extremely active at producing ketone bodies that can be used by other organs such as the brain and heart as a source of energy (316–320). Generally, ketogenesis only occurs when β -oxidation is active (316). Since,

there was an increase in both β -oxidation and ketogenesis in cells grown using HS media, these cells may be more reflective of hepatocytes *in vivo*.

Since we were interested in whether there would be lipid accumulation during HCV infection, we wanted to confirm if there was an increase in lipids present in cells grown in HS media compared to FBS media. The major regulators of lipid synthesis and lipid storage reported previously are LXRA and PPAR γ (296,321–324). Expression of both these transcription factors increases when cells are grown in HS media compared to FBS (238). The increase in both these transcription factors could lead to lipid droplet formation. In Section 3.4 we reported that there was a dramatic increase in lipid droplet size when cells were grown in HS media compared to FBS media. This was consistent with the increase in triglycerides present in cells grown in HS compared to FBS media. These results are consistent with data reported previously (238). This increase in lipid content in cells grown in HS is similar to the lipid content that is normally found in hepatocytes (325).

During chronic HCV infection, it is proposed that the downregulation of PPAR α leads to reduced transcription of genes associated with fatty acid oxidation, however, there has been little direct evidence of a reduction in pathways that are regulated by PPAR α during HCV infection (96,216,217,222). Since Huh7.5 cells grown in HS media have increased lipid catabolism, these cells were chosen as a model to study the effects of HCV on the pathways regulated by PPAR α (238). We found that during HCV infection, the rate of β -oxidation was 4 fold lower compared to uninfected cells. Additionally, we observed a 50% reduction in CPT-1 in HCV infected cells compared to uninfected cells. As a consequence of decreased β -oxidation, the levels of ketone bodies such as acetoacetate and 3-hydroxybutyrate secreted by infected cells were 8.5

and 7 fold lower respectively compared to uninfected cells (Section 4.1.1.4 to Section 4.2). These results provide direct evidence that during HCV infection, pathways such as β -oxidation and ketogenesis which are regulated by PPAR α were decreased (216,218–221). The data presented in this thesis are consistent with studies that show decreased expression of mitochondrial trifunctional protein, an enzymatic complex that catalyzes the last three steps in β -oxidation, during HCV infection (96). We also found that during HCV infection there was a reduction in free fatty acids levels in the cells. The reduced production of free fatty acids from triglycerides can be attributed to reduced lipolysis in HCV infected cells (97). A reduction in lipolysis leads to less fatty acids available for β -oxidation. In summary we showed that during HCV infection in our model system there was a significant reduction in β -oxidation, consistent with previously reported data (216–218,220,221). We also show that during HCV infection, there was a 50% increase in lipids such as triglycerides compared to uninfected cells (Section 4.3.2). This accumulation of triglycerides potentially stems from a reduction in lipid catabolism (218,221,296–299,326–328).

In summary, we established that Huh7.5 cells grown in HS media compared to FBS media were a viable model to study lipid catabolism. During HCV infection we find a reduction in β -oxidation and ketogenesis compared to uninfected cells. The reduction in both these pathways leads to accumulation of lipids in HCV infected cells relative to uninfected cells (Figure 5.1).

There are reports that state that achieving SVR is a virological cure but it may not reverse HCV induced liver disease. Around 50% of patients who achieve SVR will have no change in their steatosis severity while 13% will have their steatosis worsen (281). Additionally, 10% of patients who achieve SVR will continue to develop liver

diseases such as fibrosis, cirrhosis and HCC many years after achieving SVR (282–285,329–331). We were interested examining whether this phenomenon can be observed in our cell culture system. Huh7.5 cells grown in HS media were infected with HCV and treated with Sofosbuvir. Following Sofosbuvir treatment, the concentration of ketone bodies secreted was examined using NMR. We found no change in acetoacetate in the media taken from treated and untreated HCV infected cells. Both conditions had lower ketone bodies compared to uninfected cells. These results suggest that short term Sofosbuvir treatment does not lead to the reversal of ketogenesis and β -oxidation. This may be reflective of the persistence and progression of steatosis seen in many patients who achieve SVR.

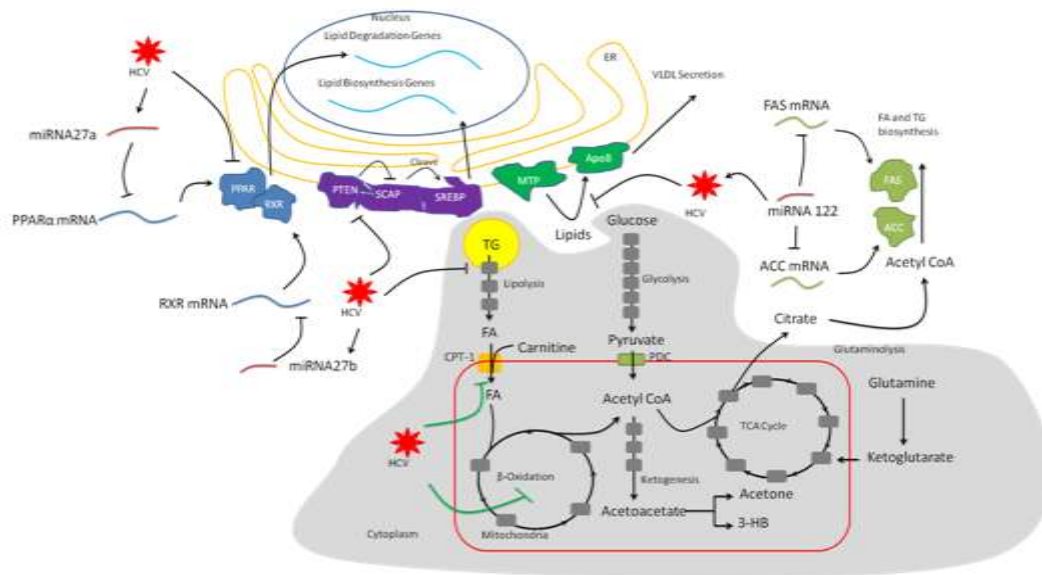


Figure 5.1 – Mechanism of HCV Induced Steatosis. HCV induces steatosis by increased lipogenesis, decreased lipid catabolism and decreased lipoprotein export. Lipogenesis is increased during HCV infection due to increased SREBP activity and increased translation of transcripts for FAS and ACC. Lipid catabolism is decreased by reducing PPAR α activation and translation of PPAR α coding transcripts. Lipoprotein secretion is reduced by the inhibition of MTP during infection. Here, we showed that HCV infection also decreases lipid catabolism by decreased CPT-1 expression and reduced β -oxidation and ketogenesis (gray area). Abbreviations are: phosphate and tensin homolog (PTEN) sterol regulatory element binding protein (SREBP) SREBP cleavage activating protein (SCAP) endoplasmic reticulum (ER) peroxisome proliferator activated receptor α (PPAR α) retinoid X receptor (RXR) microsomal transfer protein (MTP) apolipoprotein B (ApoB) very low density lipoprotein (VLDL) triglycerides (TG) fatty acids (FA) carnitine palmitoyl transferase 1a (CPT-1) pyruvate dehydrogenase complex (PDC) 3-hydroxybutyrate (3-HB) acetyl-CoA carboxylase (ACC) fatty acid synthase (FAS).

There were some unexpected results from the NMR analysis when we were comparing the metabolites secreted by cells grown in HS media or FBS media. O-phosphocholine, an intermediate of the CDP-choline pathway, was detected in the NMR analysis. The concentration of O-phosphocholine was significantly lower in

cells cultured in HS media compared to FBS media. The increase utilization of O-phosphocholine was reflected by the increased synthesis of phospholipids in cells grown in HS media compared to FBS media (Section 3.4.2.2). This increase may be related to the secretion of VLDL (260,261).

Metabolites of glycolysis were also detected. There was no difference in the concentration of glucose detected in the media between cells cultured with HS media and FBS media. However, the concentration of pyruvate was lower in the media in cells cultured in HS media compared to FBS media. The utilization of glycolysis by cells grown in HS media and FBS media was measured using the XFe24 Seahorse analyzer. The results suggests that in HS cultured cells, there was reduced glycolysis as a means for providing substrate for the TCA cycle compared to cells grown in FBS media (Section 3.2.2). Since there was similar utilization of glucose between cells in both culture conditions, it is reasonable to conclude that when cells were cultured in HS media, the intermediates in glycolysis are converted into other molecules such as lipids and glycogen (332,333).

In summary, the changes in these metabolites suggest the cells grown in HS media differ markedly from cells grown in FBS media. From these results, we can conclude that cells grown in HS media use lipid metabolism as a source of energy whereas cells grown in FBS media rely on both glycolysis and β -oxidation of fatty acids as a source of energy.

There were also some unexpected results that arose when identifying the metabolites secreted by HCV infected and uninfected cells. O-phosphocholine, the precursor to PC, was significantly increased during HCV infection (Section 4.1.1.2). The reduction in O-phosphocholine utilization implies that there is a reduction in PC

synthesis during HCV infection. This speculation was confirmed in Section 4.3.1.2 that shows a significant decrease in PC during HCV infection. The reduction in PC synthesis may be related to the reduction in lipoprotein secretion other studies reported (94,96,223,260,261,334).

There was a significant reduction in glucose utilization in cells that were infected with HCV compared to uninfected cells. Similar concentrations of pyruvate were secreted by HCV infected and uninfected cells but the amount of lactate secreted was significantly higher by cells that were not infected with HCV. Additionally, there was a significantly increase in acetate secreted by cells that were infected with HCV compared to uninfected cells (Section 4.1.1.3). In Section 4.1.2 we showed that there was little dependency on glycolysis in both HCV infected and uninfected cells. Taken together these results imply that there was an increase in the conversion of glucose to precursors of lipid, amino acid or nucleotide synthesis in uninfected cells. Additionally, the pyruvate generated in glycolysis was not converted to lactate in uninfected cells compared to infected cells (Figure 1.8). In cells infected with HCV, the pyruvate generated from glycolysis is converted to acetyl-CoA and finally acetate.

One of the limitations of this study was the inability to compare the metabolism between Huh7.5 cells grown in HS media and PHH. By having a comparison between Huh7.5 cells and PHH, a conclusion could be drawn of how reflective cells grown in HS media are of PHH. PHH were not included in this experiment due to the difficulty in culturing them. After a single day of growth in cell culture, the PHH began to lift off from the plates. These cells could not be incubated in serum free media for 24 hours for the NMR analysis without the cells detaching from the tissue culture flask.

Additionally, we could not compare HCV infected PHH with HCV infected Huh7.5 cells grown in HS media since PHH are very difficult to infect with HCV.

The conclusions and key findings of this thesis were:

1. Huh7.5 cells cultured in HS media exhibited different metabolic profiles compared to cells cultured in FBS media. There was decreased glycolysis in cells cultured in HS media compared to FBS media. While pathways associated with lipid metabolism were more active in cells grown in HS media compared to FBS media.
2. Huh7.5 cells cultured in HS media possessed increased lipid catabolism compared to cells cultured in FBS media. There was increased β -oxidation and ketogenesis in cells grown in HS media compared to FBS media. The protein responsible for the rate limiting step for these pathways, CPT-1, was 7 fold greater in cells grown in HS media compared to FBS media. The increase in lipid catabolism in cells grown in HS media made these cells more suitable as a model to study the effects of HCV infection on lipid catabolism compared to cells grown in FBS media.
3. Huh7.5 cells cultured in HS media have larger lipid droplets. This was reflected in the increase in triglycerides observed in cells in cells grown in HS media compared to FBS media.
4. Huh7.5 cells cultured in HS media with HCV infection possessed a different metabolic profile compared to uninfected cells. Many of the changes occurred in pathways associated with phospholipid metabolism and lipid metabolism.
5. In HCV infected cells, there was a reduction in lipid catabolism compared to uninfected cells. There was a reduction in both β -oxidation and ketogenesis in

infected cells compared to uninfected cells. There was 50% less CPT-1 present in infected cells compared to uninfected cells.

6. In HCV infected cells, there was 50% more lipids compared to uninfected cells. The increase in lipids in HCV infected cells was related to the reduction in lipid catabolism.
7. Previous studies report that the reduction in PPAR α expression and activation leads to a reduction in lipid catabolism during HCV infection. The reduction in lipid catabolism is one of the factors that results in lipid accumulation during HCV infection. Here we show that the rate of pathways regulated by PPAR α such as β -oxidation and ketogenesis were reduced during HCV infection. Taken together, these findings contribute to our better understanding of lipid accumulation as a result of HCV infection.
8. Treating HCV infected cells with Sofosbuvir for 14 days does not reverse the levels of ketogenesis to levels seen in uninfected cells. This lack of reversal in ketogenesis may be related to the lack of change in steatosis or worsening of steatosis in some patients who achieve SVR.

With the conclusion of this project, there are several future studies that can be created from the data presented in this thesis. We established that Huh7.5 cells grown in HS media display a lipoprotein profile in the medium similar to human sera, possessed increased lipogenesis and increased lipid catabolism. Huh7.5 cells cultured in HS media has proven indispensable in studying lipid accumulation due to decreased lipid catabolism during HCV infection due to the similarities between these cells and hepatocytes (238). Given that this thesis focuses primarily on lipid catabolism, we

cannot rule out that possibility of increased lipogenesis and decreased lipoprotein secretion as potential contributors of lipid accumulation during HCV infection. There is the possibility of using Huh7.5 cells grown in HS media to study these pathways during HCV infection.

This hepatocyte model may be useful in studying the underlying mechanism of the development of another liver disease, non-alcoholic fatty liver disease (NAFLD). These cells could be used to develop novel treatments that can prevent or ameliorate lipid accumulation seen in NAFLD.

References

References

1. Lavanchy D. The global burden of hepatitis C. *Liver Int Off J Int Assoc Study Liver*. 2009 Jan;29 Suppl 1:74–81.
2. Global Burden Of Hepatitis C Working Group. Global burden of disease (GBD) for hepatitis C. *J Clin Pharmacol*. 2004 Jan;44(1):20–9.
3. Lavanchy D. Evolving epidemiology of hepatitis C virus. *Clin Microbiol Infect*. 2011 Feb;17(2):107–15.
4. WHO | Global hepatitis report, 2017 [Internet]. WHO. [cited 2018 Jan 17]. Available from: <http://www.who.int/hepatitis/publications/global-hepatitis-report2017/en/>
5. Guerra J, Garenne M, Mohamed MK, Fontanet A. HCV burden of infection in Egypt: results from a nationwide survey. *J Viral Hepat*. 2012 Aug 1;19(8):560–7.
6. Hajarizadeh B, Grebely J, Dore GJ. Epidemiology and natural history of HCV infection. *Nat Rev Gastroenterol Hepatol*. 2013 Sep;10(9):553–62.
7. Alter MJ, Kruszon-Moran D, Nainan OV, McQuillan GM, Gao F, Moyer LA, et al. The Prevalence of Hepatitis C Virus Infection in the United States, 1988 through 1994. *N Engl J Med*. 1999 Aug 19;341(8):556–62.
8. Cornberg M, Razavi HA, Alberti A, Bernasconi E, Buti M, Cooper C, et al. A systematic review of hepatitis C virus epidemiology in Europe, Canada and Israel. *Liver Int*. 2011 Jul 1;31:30–60.
9. Esteban JI, Sauleda S, Quer J. The changing epidemiology of hepatitis C virus infection in Europe. *J Hepatol*. 2008 Jan;48(1):148–62.

10. Shobokshi OA, Serebour FE, Skakni L, Al-Saffy YH, Ahdal MN. Hepatitis C genotypes and subtypes in Saudi Arabia. *J Med Virol.* 1999 May;58(1):44–8.
11. Antaki N, Haddad M, Kebbewar K, Abdelwahab J, Hamed O, Aaraj R, et al. The unexpected discovery of a focus of hepatitis C virus genotype 5 in a Syrian province. *Epidemiol Infect.* 2009 Jan;137(1):79–84.
12. Krugman S, Giles JP, Hammond J. Infectious Hepatitis: Evidence for Two Distinctive Clinical, Epidemiological, and Immunological Types of Infection. *JAMA.* 1967 May 1;200(5):365–73.
13. Feinstone SM, Kapikian AZ, Purcell RH, Alter HJ, Holland PV, Zuckerman R by AJ. Transfusion-associated hepatitis not due to viral hepatitis type A or B†. *Rev Med Virol.* 2001 Jan 1;11(1):3–9.
14. Prince A, Grady G, Hazzi C, Brotman B, Kuhns W, Levine R, et al. LONG-INCUBATION POST-TRANSFUSION HEPATITIS WITHOUT SEROLOGICAL EVIDENCE OF EXPOSURE TO HEPATITIS-B VIRUS. *The Lancet.* 1974 Aug 3;304(7875):241–6.
15. Mares Bermúdez J, Plaja Román P, Calico Bosch I, Javier Manchón G, Ortega Aramburu JJ. [Cytomegalovirus disease in immunosuppressed patients]. *An Esp Pediatr.* 1988 Mar;28(3):211–6.
16. Wreghitt TG, Teare EL, Sule O, Devi R, Rice P. Cytomegalovirus Infection in Immunocompetent Patients. *Clin Infect Dis.* 2003 Dec 15;37(12):1603–6.
17. Vine LJ, Shepherd K, Hunter JG, Madden R, Thornton C, Ellis V, et al. Characteristics of Epstein–Barr virus hepatitis among patients with jaundice or acute hepatitis. *Aliment Pharmacol Ther.* 2012 Jul 1;36(1):16–21.

18. Méndez-Sánchez N, Aguilar-Domínguez C, Chávez-Tapia NC, Uribe M. Hepatic manifestations of Epstein-Barr viral infection. *Ann Hepatol.* 2005 Sep;4(3):205–9.
19. Houghton M. Discovery of the hepatitis C virus. *Liver Int.* 2009 Jan 1;29:82–8.
20. Choo QL, Kuo G, Weiner AJ, Overby LR, Bradley DW, Houghton M. Isolation of a cDNA clone derived from a blood-borne non-A, non-B viral hepatitis genome. *Science.* 1989 Apr 21;244(4902):359–62.
21. Kuo G, Choo QL, Alter HJ, Gitnick GL, Redeker AG, Purcell RH, et al. An assay for circulating antibodies to a major etiologic virus of human non-A, non-B hepatitis. *Science.* 1989 Apr 21;244(4902):362–4.
22. Tibbs CJ. Methods of transmission of hepatitis C. *J Viral Hepat.* 1995;2(3):113–9.
23. Dalgard O, Jeansson S, Skaug K, Raknerud N, Bell H. Hepatitis C in the general adult population of Oslo: prevalence and clinical spectrum. *Scand J Gastroenterol.* 2003 Aug;38(8):864–70.
24. Harris RJ, Ramsay M, Hope VD, Brant L, Hickman M, Foster GR, et al. Hepatitis C prevalence in England remains low and varies by ethnicity: an updated evidence synthesis. *Eur J Public Health.* 2012 Apr 1;22(2):187–92.
25. Delarocque-Astagneau E, Pillonel J, De Valk H, Perra A, Laperche S, Desenclos J-C. An Incident Case–Control Study of Modes of Hepatitis C Virus Transmission in France. *Ann Epidemiol.* 2007 Oct;17(10):755–62.
26. Williams IT, Bell BP, Kuhnert W, Alter MJ. Incidence and Transmission Patterns of Acute Hepatitis C in the United States, 1982-2006. *Arch Intern Med.* 2011 Feb 14;171(3):242–8.

27. Sievert W, Altraif I, Razavi HA, Abdo A, Ahmed EA, AlOmair A, et al. A systematic review of hepatitis C virus epidemiology in Asia, Australia and Egypt. *Liver Int.* 2011 Jul 1;31:61–80.
28. Jimenez AP, Eldin NS, Rimlinger F, El-Daly M, El-Hariri H, El-Hoseiny M, et al. HCV iatrogenic and intrafamilial transmission in Greater Cairo, Egypt. *Gut.* 2010 Nov 1;59(11):1554–60.
29. Plancoulaine S, Mohamed MK, Arafa N, Bakr I, Rekacewicz C, Trégouët D-A, et al. Dissection of familial correlations in hepatitis C virus (HCV) seroprevalence suggests intrafamilial viral transmission and genetic predisposition to infection. *Gut.* 2008 Sep 1;57(9):1268–74.
30. Mohamed MK, Abdel-Hamid M, Mikhail NN, Abdel-Aziz F, Medhat A, Magder LS, et al. Intrafamilial transmission of hepatitis C in Egypt. *Hepatology.* 2005 Sep 1;42(3):683–7.
31. Benova L, Mohamoud YA, Calvert C, Abu-Raddad LJ. Vertical Transmission of Hepatitis C Virus: Systematic Review and Meta-analysis. *Clin Infect Dis Off Publ Infect Dis Soc Am.* 2014 Sep 15;59(6):765–73.
32. Chen SL, Morgan TR. The Natural History of Hepatitis C Virus (HCV) Infection. *Int J Med Sci.* 2006 Apr 1;3(2):47–52.
33. Alter HJ, Seeff LB. Recovery, persistence, and sequelae in hepatitis C virus infection: a perspective on long-term outcome. *Semin Liver Dis.* 2000;20(1):17–35.
34. Thimme R, Oldach D, Chang KM, Steiger C, Ray SC, Chisari FV. Determinants of viral clearance and persistence during acute hepatitis C virus infection. *J Exp Med.* 2001 Nov 19;194(10):1395–406.

35. Farci P, Alter HJ, Wong D, Miller RH, Shih JW, Jett B, et al. A long-term study of hepatitis C virus replication in non-A, non-B hepatitis. *N Engl J Med.* 1991 Jul 11;325(2):98–104.
36. Farci P, Alter HJ, Shimoda A, Govindarajan S, Cheung LC, Melpolder JC, et al. Hepatitis C virus-associated fulminant hepatic failure. *N Engl J Med.* 1996 Aug 29;335(9):631–4.
37. Zoulim F, Chevallier M, Maynard M, Trepo C. Clinical consequences of hepatitis C virus infection. *Rev Med Virol.* 2003 Jan 1;13(1):57–68.
38. Ke P-Y, Chen SS-L. Hepatitis C Virus and Cellular Stress Response: Implications to Molecular Pathogenesis of Liver Diseases. *Viruses.* 2012 Oct 19;4(10):2251–90.
39. Bulteel N, Partha Sarathy P, Forrest E, Stanley AJ, Innes H, Mills PR, et al. Factors associated with spontaneous clearance of chronic hepatitis C virus infection. *J Hepatol.* 2016 Aug;65(2):266–72.
40. Stenkvist J, Nyström J, Falconer K, Sönnernborg A, Weiland O. Occasional spontaneous clearance of chronic hepatitis C virus in HIV-infected individuals. *J Hepatol.* 2014 Oct;61(4):957–61.
41. Lauer GM, Walker BD. Hepatitis C Virus Infection. *N Engl J Med.* 2001 Jul 5;345(1):41–52.
42. Okuda M, Hino K, Korenaga M, Yamaguchi Y, Katoh Y, Okita K. Differences in hypervariable region 1 quasispecies of hepatitis C virus in human serum, peripheral blood mononuclear cells, and liver. *Hepatology.* 1999 Jan 1;29(1):217–22.
43. Zignego AL, De Carli M, Monti M, Careccia G, La Villa G, Giannini C, et al. Hepatitis C virus infection of mononuclear cells from peripheral blood and

- liver infiltrates in chronically infected patients. *J Med Virol*. 1995 Sep;47(1):58–64.
44. World Health Assembly 63. Viral hepatitis: report by the Secretariat. 2010 [cited 2016 Nov 22]; Available from: <http://www.who.int/iris/handle/10665/2383>
 45. Manns MP, Wedemeyer H, Cornberg M. Treating viral hepatitis C: efficacy, side effects, and complications. *Gut*. 2006 Sep;55(9):1350–9.
 46. Poynard T, Marcellin P, Lee SS, Niederau C, Minuk GS, Ideo G, et al. Randomised trial of interferon α 2b plus ribavirin for 48 weeks or for 24 weeks versus interferon α 2b plus placebo for 48 weeks for treatment of chronic infection with hepatitis C virus. *The Lancet*. 1998 Oct 31;352(9138):1426–32.
 47. McHutchison JG, Gordon SC, Schiff ER, Shiffman ML, Lee WM, Rustgi VK, et al. Interferon Alfa-2b Alone or in Combination with Ribavirin as Initial Treatment for Chronic Hepatitis C. *N Engl J Med*. 1998 Nov 19;339(21):1485–92.
 48. Manns MP, McHutchison JG, Gordon SC, Rustgi VK, Shiffman M, Reindollar R, et al. Peginterferon alfa-2b plus ribavirin compared with interferon alfa-2b plus ribavirin for initial treatment of chronic hepatitis C: a randomised trial. *The Lancet*. 2001 Sep 22;358(9286):958–65.
 49. McHutchison JG, Manns M, Patel K, Poynard T, Lindsay KL, Trepo C, et al. Adherence to combination therapy enhances sustained response in genotype-1–infected patients with chronic hepatitis C. *Gastroenterology*. 2002 Oct;123(4):1061–9.

50. Fried MW, Shiffman ML, Reddy KR, Smith C, Marinos G, Gonçales FLJ, et al. Peginterferon Alfa-2a plus Ribavirin for Chronic Hepatitis C Virus Infection. *N Engl J Med*. 2002 Sep 26;347(13):975–82.
51. Bidell MR, McLaughlin M, Faragon J, Morse C, Patel N. Desirable Characteristics of Hepatitis C Treatment Regimens: A Review of What We Have and What We Need. *Infect Dis Ther*. 2016 Sep;5(3):299–312.
52. Moradpour D, Penin F. Hepatitis C Virus Proteins: From Structure to Function. In: Bartenschlager R, editor. *Hepatitis C Virus: From Molecular Virology to Antiviral Therapy* [Internet]. Springer Berlin Heidelberg; 2013 [cited 2016 Nov 23]. p. 113–42. (Current Topics in Microbiology and Immunology). Available from: http://link.springer.com/chapter/10.1007/978-3-642-27340-7_5
53. Kwon HJ, Xing W, Chan K, Niedziela-Majka A, Brendza KM, Kirschberg T, et al. Direct Binding of Ledipasvir to HCV NS5A: Mechanism of Resistance to an HCV Antiviral Agent. *PLoS ONE* [Internet]. 2015 Apr 9;10(4). Available from: <https://www.ncbi.nlm.nih.gov/pmc/articles/PMC4391872/>
54. Greig SL. Sofosbuvir/Velpatasvir: A Review in Chronic Hepatitis C. *Drugs*. 2016 Oct 1;76(16):1567–78.
55. Chamorro-de-Vega E, Gimenez-Manzorro A, Rodriguez-Gonzalez CG, Escudero-Vilaplana V, Collado Borrell R, Ibañez-Garcia S, et al. Effectiveness and Safety of Ombitasvir-Paritaprevir/Ritonavir and Dasabuvir With or Without Ribavirin for HCV Genotype 1 Infection for 12 Weeks Under Routine Clinical Practice. *Ann Pharmacother*. 2016 Nov 1;50(11):901–8.
56. Bell AM, Wagner JL, Barber KE, Stover KR. Elbasvir/Grazoprevir: A Review of the Latest Agent in the Fight against Hepatitis C. *Int J Hepatol*. 2016 Jun 15;2016:e3852126.

57. Montgomery M, Ho N, Chung E, Marzella N. Daclatasvir (Daklinza). *Pharm Ther.* 2016 Dec;41(12):751–5.
58. Gritsenko D, Hughes G. Ledipasvir/Sofosbuvir (Harvoni): Improving Options for Hepatitis C Virus Infection. *Pharm Ther.* 2015 Apr;40(4):256–76.
59. Burton DR, Poignard P, Stanfield RL, Wilson IA. Broadly neutralizing antibodies suggest new prospects to counter highly antigenically diverse viruses. *Science.* 2012 Jul 13;337(6091):183–6.
60. Chmielewska AM, Naddeo M, Capone S, Ammendola V, Hu K, Meredith L, et al. Combined Adenovirus Vector and Hepatitis C Virus Envelope Protein Prime-Boost Regimen Elicits T Cell and Neutralizing Antibody Immune Responses. *J Virol.* 2014 May;88(10):5502–10.
61. Abdelwahab KS, Ahmed Said ZN. Status of hepatitis C virus vaccination: Recent update. *World J Gastroenterol.* 2016 Jan 14;22(2):862–73.
62. Wong JAJ-X, Bhat R, Hockman D, Logan M, Chen C, Levin A, et al. Recombinant Hepatitis C Virus Envelope Glycoprotein Vaccine Elicits Antibodies Targeting Multiple Epitopes on the Envelope Glycoproteins Associated with Broad Cross-Neutralization. *J Virol.* 2014 Dec;88(24):14278–88.
63. Stamatakis Z, Coates S, Evans MJ, Wininger M, Crawford K, Dong C, et al. Hepatitis C virus envelope glycoprotein immunization of rodents elicits cross-reactive neutralizing antibodies. *Vaccine.* 2007 Nov 7;25(45):7773–84.
64. Meunier J-C, Gottwein JM, Houghton M, Russell RS, Emerson SU, Bukh J, et al. Vaccine-Induced Cross-Genotype Reactive Neutralizing Antibodies Against Hepatitis C Virus. *J Infect Dis.* 2011 Oct 15;204(8):1186–90.

65. Stamatakis Z, Coates S, Abrignani S, Houghton M, McKeating JA. Immunization of Human Volunteers With Hepatitis C Virus Envelope Glycoproteins Elicits Antibodies That Cross-Neutralize Heterologous Virus Strains. *J Infect Dis*. 2011 Sep 1;204(5):811–3.
66. Gottwein JM, Bukh J. Viral hepatitis: Cell-culture-derived HCV—a promising vaccine antigen. *Nat Rev Gastroenterol Hepatol*. 2013 Sep;10(9):508–9.
67. Akazawa D, Moriyama M, Yokokawa H, Omi N, Watanabe N, Date T, et al. Neutralizing Antibodies Induced by Cell Culture–Derived Hepatitis C Virus Protect Against Infection in Mice. *Gastroenterology*. 2013 Aug;145(2):447–455.e4.
68. Ahlén G, Nyström J, Pult I, Frelin L, Hultgren C, Sällberg M. In Vivo Clearance of Hepatitis C Virus Nonstructural 3/4A–Expressing Hepatocytes by DNA Vaccine–Primed Cytotoxic T Lymphocytes. *J Infect Dis*. 2005 Dec 15;192(12):2112–6.
69. Man John Law L, Landi A, Magee WC, Lorne Tyrrell D, Houghton M. Progress towards a hepatitis C virus vaccine. *Emerg Microbes Infect*. 2013 Nov;2(11):e79.
70. Stoll-Keller F, Barth H, Fafi-Kremer S, Zeisel MB, Baumert TF. Development of hepatitis C virus vaccines: challenges and progress. *Expert Rev Vaccines*. 2009 Mar;8(3):333–45.
71. Shi C, Ploss A. Hepatitis C virus vaccines in the era of new direct-acting antivirals. *Expert Rev Gastroenterol Hepatol*. 2013 Feb 1;7(2):171–85.
72. Pishraft Sabet L, Taheri T, Memarnejadian A, Mokhtari Azad T, Asgari F, Rahimnia R, et al. Immunogenicity of Multi-Epitope DNA and Peptide Vaccine Candidates Based on Core, E2, NS3 and NS5B HCV Epitopes in

- BALB/c Mice. *Hepat Mon* [Internet]. 2014 Oct 15 [cited 2017 Feb 24];14(10). Available from: <http://www.ncbi.nlm.nih.gov/pmc/articles/PMC4238154/>
73. Gastaminza P, Dryden KA, Boyd B, Wood MR, Law M, Yeager M, et al. Ultrastructural and Biophysical Characterization of Hepatitis C Virus Particles Produced in Cell Culture. *J Virol*. 2010 Nov 1;84(21):10999–1009.
 74. André P, Komurian-Pradel F, Deforges S, Perret M, Berland JL, Sodoyer M, et al. Characterization of Low- and Very-Low-Density Hepatitis C Virus RNA-Containing Particles. *J Virol*. 2002 Jul 15;76(14):6919–28.
 75. Calattini S, Fusil F, Mancip J, Thi VLD, Granier C, Gadot N, et al. Functional and Biochemical Characterization of HCV Particles Produced in a Humanized Liver Mouse Model. *J Biol Chem*. 2015 Jul 29;jbc.M115.662999.
 76. Pumeechockchai W, Bevitt D, Agarwal K, Petropoulou T, Langer BCA, Belohradsky B, et al. Hepatitis C virus particles of different density in the blood of chronically infected immunocompetent and immunodeficient patients: Implications for virus clearance by antibody. *J Med Virol*. 2002 Nov;68(3):335–42.
 77. Boyer A, Dumans A, Beaumont E, Etienne L, Roingeard P, Meunier J-C. The Association of Hepatitis C Virus Glycoproteins with Apolipoproteins E and B Early in Assembly Is Conserved in Lipoviral Particles. *J Biol Chem*. 2014 Jul 4;289(27):18904–13.
 78. Fukuhara T, Wada M, Nakamura S, Ono C, Shiokawa M, Yamamoto S, et al. Amphipathic α -Helices in Apolipoproteins Are Crucial to the Formation of Infectious Hepatitis C Virus Particles. *PLOS Pathog*. 2014 Dec 11;10(12):e1004534.

79. Lee J-Y, Acosta EG, Stoeck IK, Long G, Hiet M-S, Mueller B, et al. Apolipoprotein E Likely Contributes to a Maturation Step of Infectious Hepatitis C Virus Particles and Interacts with Viral Envelope Glycoproteins. *J Virol.* 2014 Nov 1;88(21):12422–37.
80. Thimme R, Binder M, Bartenschlager R. Failure of innate and adaptive immune responses in controlling hepatitis C virus infection. *FEMS Microbiol Rev.* 2012 May 1;36(3):663–83.
81. Maniloff J. Identification and classification of viruses that have not been propagated. *Arch Virol.* 1995;140(8):1515–20.
82. Kieft JS, Zhou K, Jubin R, Doudna JA. Mechanism of ribosome recruitment by hepatitis C IRES RNA. *RNA.* 2001 Feb;7(2):194–206.
83. Kao CC, Fan B, Chinnaswamy S, Cai H, Ranjith-Kumar CT, Deval J, et al. Assays for RNA synthesis and replication by the hepatitis C virus. *Front Biol.* 2012 Jun 1;7(3):233–45.
84. McLauchlan J, Lemberg MK, Hope G, Martoglio B. Intramembrane proteolysis promotes trafficking of hepatitis C virus core protein to lipid droplets. *EMBO J.* 2002 Aug 1;21(15):3980–8.
85. Okamoto K, Moriishi K, Miyamura T, Matsuura Y. Intramembrane Proteolysis and Endoplasmic Reticulum Retention of Hepatitis C Virus Core Protein. *J Virol.* 2004 Jun;78(12):6370–80.
86. Oehler V, Filipe A, Montserret R, da Costa D, Brown G, Penin F, et al. Structural Analysis of Hepatitis C Virus Core-E1 Signal Peptide and Requirements for Cleavage of the Genotype 3a Signal Sequence by Signal Peptide Peptidase. *J Virol.* 2012 Aug;86(15):7818–28.

87. Pietschmann T, Lohmann V, Rutter G, Kurpanek K, Bartenschlager R. Characterization of Cell Lines Carrying Self-Replicating Hepatitis C Virus RNAs. *J Virol*. 2001 Feb;75(3):1252–64.
88. Hijikata M, Kato N, Ootsuyama Y, Nakagawa M, Shimotohno K. Gene mapping of the putative structural region of the hepatitis C virus genome by in vitro processing analysis. *Proc Natl Acad Sci U S A*. 1991 Jul 1;88(13):5547–51.
89. Herod MR, Jones DM, McLauchlan J, McCormick CJ. Increasing Rate of Cleavage at Boundary between Non-structural Proteins 4B and 5A Inhibits Replication of Hepatitis C Virus. *J Biol Chem*. 2012 Jan 2;287(1):568–80.
90. Cristofari G, Ivanyi-Nagy R, Gabus C, Boulant S, Lavergne J-P, Penin F, et al. The hepatitis C virus Core protein is a potent nucleic acid chaperone that directs dimerization of the viral (+) strand RNA in vitro. *Nucleic Acids Res*. 2004;32(8):2623–31.
91. de Chassey B, Navratil V, Tafforeau L, Hiet MS, Aublin-Gex A, Agaugué S, et al. Hepatitis C virus infection protein network. *Mol Syst Biol*. 2008 Nov 4;4:230.
92. Barba G, Harper F, Harada T, Kohara M, Goulinet S, Matsuura Y, et al. Hepatitis C virus core protein shows a cytoplasmic localization and associates to cellular lipid storage droplets. *Proc Natl Acad Sci U S A*. 1997 Feb 18;94(4):1200–5.
93. Moriya K, Yotsuyanagi H, Shintani Y, Fujie H, Ishibashi K, Matsuura Y, et al. Hepatitis C virus core protein induces hepatic steatosis in transgenic mice. *J Gen Virol*. 1997;78(7):1527–31.

94. Perlemuter G, Sabile A, Letteron P, Vona G, Topilco A, Chrétien Y, et al. Hepatitis C virus core protein inhibits microsomal triglyceride transfer protein activity and very low density lipoprotein secretion: a model of viral-related steatosis. *FASEB J.* 2002 Feb 1;16(2):185–94.
95. Afzal MS, Zaidi NUSS, Dubuisson J, Rouille Y. Hepatitis C Virus Capsid Protein and Intracellular Lipids Interplay and its Association With Hepatic Steatosis. *Hepat Mon* [Internet]. 2014 Aug 11 [cited 2016 Nov 30];14(8). Available from: <http://www.ncbi.nlm.nih.gov/pmc/articles/PMC4165984/>
96. Amako Y, Munakata T, Kohara M, Siddiqui A, Peers C, Harris M. Hepatitis C Virus Attenuates Mitochondrial Lipid β -Oxidation by Downregulating Mitochondrial Trifunctional-Protein Expression. *J Virol.* 2015 Apr 15;89(8):4092–101.
97. Harris C, Herker E, Farese RV, Ott M. Hepatitis C Virus Core Protein Decreases Lipid Droplet Turnover. *J Biol Chem.* 2011 Dec 9;286(49):42615–25.
98. Boulant S, Vanbelle C, Ebel C, Penin F, Lavergne J-P. Hepatitis C Virus Core Protein Is a Dimeric Alpha-Helical Protein Exhibiting Membrane Protein Features. *J Virol.* 2005 Sep;79(17):11353–65.
99. Boulant S, Montserret R, Hope RG, Ratinier M, Targett-Adams P, Lavergne J-P, et al. Structural Determinants That Target the Hepatitis C Virus Core Protein to Lipid Droplets. *J Biol Chem.* 2006 Aug 4;281(31):22236–47.
100. Vieyres G, Thomas X, Descamps V, Duverlie G, Patel AH, Dubuisson J. Characterization of the Envelope Glycoproteins Associated with Infectious Hepatitis C Virus. *J Virol.* 2010 Oct;84(19):10159–68.

101. Krey T, d'Alayer J, Kikuti CM, Saulnier A, Damier-Piolle L, Petitpas I, et al. The Disulfide Bonds in Glycoprotein E2 of Hepatitis C Virus Reveal the Tertiary Organization of the Molecule. *PLoS Pathog* [Internet]. 2010 Feb [cited 2016 Nov 25];6(2). Available from: <http://www.ncbi.nlm.nih.gov/pmc/articles/PMC2824758/>
102. Clarke D, Griffin S, Beales L, Gelais CS, Burgess S, Harris M, et al. Evidence for the Formation of a Heptameric Ion Channel Complex by the Hepatitis C Virus P7 Protein in Vitro. *J Biol Chem*. 2006 Dec 1;281(48):37057–68.
103. Chandler DE, Penin F, Schulten K, Chipot C. The p7 Protein of Hepatitis C Virus Forms Structurally Plastic, Minimalist Ion Channels. *PLOS Comput Biol*. 2012 Sep 20;8(9):e1002702.
104. Luik P, Chew C, Aittoniemi J, Chang J, Wentworth P, Dwek RA, et al. The 3-dimensional structure of a hepatitis C virus p7 ion channel by electron microscopy. *Proc Natl Acad Sci U S A*. 2009 Aug 4;106(31):12712–6.
105. Wozniak AL, Griffin S, Rowlands D, Harris M, Yi M, Lemon SM, et al. Intracellular proton conductance of the hepatitis C virus p7 protein and its contribution to infectious virus production. *PLoS Pathog*. 2010 Sep 2;6(9):e1001087.
106. Jirasko V, Montserret R, Appel N, Janvier A, Eustachi L, Brohm C, et al. Structural and Functional Characterization of Nonstructural Protein 2 for Its Role in Hepatitis C Virus Assembly. *J Biol Chem*. 2008 Oct 17;283(42):28546–62.
107. Jirasko V, Montserret R, Lee JY, Gouttenoire J, Moradpour D, Penin F, et al. Structural and Functional Studies of Nonstructural Protein 2 of the Hepatitis C Virus Reveal Its Key Role as Organizer of Virion Assembly. *PLoS Pathog*

- [Internet]. 2010 Dec [cited 2016 Nov 25];6(12). Available from:
<http://www.ncbi.nlm.nih.gov/pmc/articles/PMC3002993/>
108. Boson B, Granio O, Bartenschlager R, Cosset F-L. A Concerted Action of Hepatitis C Virus P7 and Nonstructural Protein 2 Regulates Core Localization at the Endoplasmic Reticulum and Virus Assembly. *PLoS Pathog* [Internet]. 2011 Jul [cited 2016 Nov 25];7(7). Available from:
<http://www.ncbi.nlm.nih.gov/pmc/articles/PMC3141040/>
 109. Stapleford KA, Lindenbach BD. Hepatitis C Virus NS2 Coordinates Virus Particle Assembly through Physical Interactions with the E1-E2 Glycoprotein and NS3-NS4A Enzyme Complexes. *J Virol*. 2011 Feb 15;85(4):1706–17.
 110. Ma Y, Anantpadma M, Timpe JM, Shanmugam S, Singh SM, Lemon SM, et al. Hepatitis C Virus NS2 Protein Serves as a Scaffold for Virus Assembly by Interacting with both Structural and Nonstructural Proteins. *J Virol*. 2011 Jan;85(1):86–97.
 111. Popescu C-I, Callens N, Trinel D, Roingeard P, Moradpour D, Descamps V, et al. NS2 Protein of Hepatitis C Virus Interacts with Structural and Non-Structural Proteins towards Virus Assembly. *PLoS Pathog* [Internet]. 2011 Feb [cited 2016 Nov 25];7(2). Available from:
<http://www.ncbi.nlm.nih.gov/pmc/articles/PMC3037360/>
 112. Zhang C, Cai Z, Kim Y-C, Kumar R, Yuan F, Shi P-Y, et al. Stimulation of Hepatitis C Virus (HCV) Nonstructural Protein 3 (NS3) Helicase Activity by the NS3 Protease Domain and by HCV RNA-Dependent RNA Polymerase. *J Virol*. 2005 Jul;79(14):8687–97.
 113. Morikawa K, Lange CM, Gouttenoire J, Meylan E, Brass V, Penin F, et al. Nonstructural protein 3-4A: the Swiss army knife of hepatitis C virus. *J Viral Hepat*. 2011 May 1;18(5):305–15.

114. Wölk B, Sansonno D, Kräusslich H-G, Dammacco F, Rice CM, Blum HE, et al. Subcellular Localization, Stability, and trans-Cleavage Competence of the Hepatitis C Virus NS3-NS4A Complex Expressed in Tetracycline-Regulated Cell Lines. *J Virol*. 2000 Mar;74(5):2293–304.
115. Horner SM, Liu HM, Park HS, Briley J, Gale M. Mitochondrial-associated endoplasmic reticulum membranes (MAM) form innate immune synapses and are targeted by hepatitis C virus. *Proc Natl Acad Sci U S A*. 2011 Aug 30;108(35):14590–5.
116. Gu M, Rice CM. Three conformational snapshots of the hepatitis C virus NS3 helicase reveal a ratchet translocation mechanism. *Proc Natl Acad Sci*. 2010 Jan 12;107(2):521–8.
117. Gouttenoire J, Penin F, Moradpour D. Hepatitis C virus nonstructural protein 4B: a journey into unexplored territory. *Rev Med Virol*. 2010 Mar 1;20(2):117–29.
118. Egger D, Wölk B, Gosert R, Bianchi L, Blum HE, Moradpour D, et al. Expression of Hepatitis C Virus Proteins Induces Distinct Membrane Alterations Including a Candidate Viral Replication Complex. *J Virol*. 2002 Jun;76(12):5974–84.
119. Gosert R, Egger D, Lohmann V, Bartenschlager R, Blum HE, Bienz K, et al. Identification of the Hepatitis C Virus RNA Replication Complex in Huh-7 Cells Harboring Subgenomic Replicons. *J Virol*. 2003 May;77(9):5487–92.
120. Thompson AA, Zou A, Yan J, Duggal R, Hao W, Molina D, et al. Biochemical Characterization of Recombinant Hepatitis C Virus Nonstructural Protein 4B: Evidence for ATP/GTP Hydrolysis and Adenylate Kinase Activity. *Biochemistry (Mosc)*. 2009 Feb 10;48(5):906–16.

121. Yu G-Y, Lee K-J, Gao L, Lai MMC. Palmitoylation and Polymerization of Hepatitis C Virus NS4B Protein. *J Virol*. 2006 Jun;80(12):6013–23.
122. Mutations in the Nonstructural Protein 5a Gene and Response to Interferon in Patients with Chronic Hepatitis C Virus 1b Infection — NEJM [Internet]. [cited 2016 Nov 25]. Available from:
<http://www.nejm.org/doi/full/10.1056/NEJM199601113340203>
123. Tellinghuisen TL, Foss KL, Treadaway J. Regulation of Hepatitis C Virion Production via Phosphorylation of the NS5A Protein. *PLoS Pathog* [Internet]. 2008 Mar [cited 2016 Nov 25];4(3). Available from:
<http://www.ncbi.nlm.nih.gov/pmc/articles/PMC2265800/>
124. Kim S, Welsch C, Yi M, Lemon SM. Regulation of the Production of Infectious Genotype 1a Hepatitis C Virus by NS5A Domain III ∇ . *J Virol*. 2011 Jul;85(13):6645–56.
125. Masaki T, Suzuki R, Murakami K, Aizaki H, Ishii K, Murayama A, et al. Interaction of Hepatitis C Virus Nonstructural Protein 5A with Core Protein Is Critical for the Production of Infectious Virus Particles. *J Virol*. 2008 Aug;82(16):7964–76.
126. Miyanari Y, Hijikata M, Yamaji M, Hosaka M, Takahashi H, Shimotohno K. Hepatitis C Virus Non-structural Proteins in the Probable Membranous Compartment Function in Viral Genome Replication. *J Biol Chem*. 2003 Dec 12;278(50):50301–8.
127. Barth H, Schäfer C, Adah MI, Zhang F, Linhardt RJ, Toyoda H, et al. Cellular Binding of Hepatitis C Virus Envelope Glycoprotein E2 Requires Cell Surface Heparan Sulfate. *J Biol Chem*. 2003 Oct 17;278(42):41003–12.

128. Agnello V, Ábel G, Elfahal M, Knight GB, Zhang Q-X. Hepatitis C virus and other Flaviviridae viruses enter cells via low density lipoprotein receptor. *Proc Natl Acad Sci U S A*. 1999 Oct 26;96(22):12766–71.
129. Scarselli E, Ansuini H, Cerino R, Roccasecca RM, Acali S, Filocamo G, et al. The human scavenger receptor class B type I is a novel candidate receptor for the hepatitis C virus. *EMBO J*. 2002 Oct 1;21(19):5017–25.
130. Zahid MN, Turek M, Xiao F, Dao T, Guérin M, Fofana I, et al. The postbinding activity of scavenger receptor class B type I mediates initiation of hepatitis C virus infection and viral dissemination. *Hepatology*. 2013;57(2):492–504.
131. Dao Thi VL, Granier C, Zeisel MB, Guérin M, Mancip J, Granio O, et al. Characterization of Hepatitis C Virus Particle Subpopulations Reveals Multiple Usage of the Scavenger Receptor BI for Entry Steps. *J Biol Chem*. 2012 Sep 7;287(37):31242–57.
132. Bankwitz D, Steinmann E, Bitzegeio J, Ciesek S, Friesland M, Herrmann E, et al. Hepatitis C virus hypervariable region 1 modulates receptor interactions, conceals the CD81 binding site, and protects conserved neutralizing epitopes. *J Virol*. 2010;84(11):5751–63.
133. Dubuisson J, Cosset F-L. Virology and cell biology of the hepatitis C virus life cycle – An update. *J Hepatol*. 2014 Nov;61(1, Supplement):S3–13.
134. Maillard P, Huby T, Andréo U, Moreau M, Chapman J, Budkowska A. The interaction of natural hepatitis C virus with human scavenger receptor SR-BI/Cla1 is mediated by ApoB-containing lipoproteins. *FASEB J* [Internet]. 2006 Feb 13 [cited 2016 Dec 22]; Available from: <http://www.fasebj.org/content/early/2006/04/01/fj.05-4728fje>

135. Kim S, Ishida H, Yamane D, Yi M, Swinney DC, Fong S, et al. Contrasting roles of mitogen-activated protein kinases in cellular entry and replication of hepatitis C virus: MKNK1 facilitates cell entry. *J Virol*. 2013;87(8):4214–24.
136. Zona L, Lupberger J, Sidahmed-Adrar N, Thumann C, Harris HJ, Barnes A, et al. HRas Signal Transduction Promotes Hepatitis C Virus Cell Entry by Triggering Assembly of the Host Tetraspanin Receptor Complex. *Cell Host Microbe*. 2013 Mar 13;13(3):302–13.
137. Brazzoli M, Bianchi A, Filippini S, Weiner A, Zhu Q, Pizza M, et al. CD81 Is a Central Regulator of Cellular Events Required for Hepatitis C Virus Infection of Human Hepatocytes. *J Virol*. 2008 Sep;82(17):8316–29.
138. Martin DN, Uprichard SL. Identification of transferrin receptor 1 as a hepatitis C virus entry factor. *Proc Natl Acad Sci U S A*. 2013;110(26):10777–82.
139. Sainz J, Barretto N, Martin DN, Hiraga N, Imamura M, Hussain S, et al. Identification of the Niemann-Pick C1-like 1 cholesterol absorption receptor as a new hepatitis C virus entry factor. *Nat Med*. 2012;18(2):281–5.
140. Haid S, Pietschmann T, Pécheur E-I. Low pH-dependent Hepatitis C Virus Membrane Fusion Depends on E2 Integrity, Target Lipid Composition, and Density of Virus Particles. *J Biol Chem*. 2009 Jun 26;284(26):17657–67.
141. Collier KE, Berger KL, Heaton NS, Cooper JD, Yoon R, Randall G. RNA Interference and Single Particle Tracking Analysis of Hepatitis C Virus Endocytosis. *PLoS Pathog* [Internet]. 2009 Dec [cited 2016 Nov 28];5(12). Available from: <http://www.ncbi.nlm.nih.gov/pmc/articles/PMC2790617/>
142. Zhu Y-Z, Qian X-J, Zhao P, Qi Z-T. How hepatitis C virus invades hepatocytes: The mystery of viral entry. *World J Gastroenterol WJG*. 2014 Apr 7;20(13):3457–67.

143. Kielian M, Rey FA. Virus membrane-fusion proteins: more than one way to make a hairpin. *Nat Rev Microbiol.* 2006 Jan;4(1):67–76.
144. Stiasny K, Fritz R, Pangerl K, Heinz FX. Molecular mechanisms of flavivirus membrane fusion. *Amino Acids.* 2011 Nov;41(5):1159–63.
145. Mukhopadhyay S, Kuhn RJ, Rossmann MG. A structural perspective of the flavivirus life cycle. *Nat Rev Microbiol.* 2005 Jan;3(1):13–22.
146. Lavillette D, Pécheur E-I, Donot P, Fresquet J, Molle J, Corbau R, et al. Characterization of Fusion Determinants Points to the Involvement of Three Discrete Regions of Both E1 and E2 Glycoproteins in the Membrane Fusion Process of Hepatitis C Virus. *J Virol.* 2007 Aug;81(16):8752–65.
147. Li H-F, Huang C-H, Ai L-S, Chuang C-K, Chen SS. Mutagenesis of the fusion peptide-like domain of hepatitis C virus E1 glycoprotein: involvement in cell fusion and virus entry. *J Biomed Sci.* 2009 Sep 24;16(1):89.
148. Drummer HE, Boo I, Pountourios P. Mutagenesis of a conserved fusion peptide-like motif and membrane-proximal heptad-repeat region of hepatitis C virus glycoprotein E1. *J Gen Virol.* 2007;88(4):1144–8.
149. Cholesterol uptake and hepatitis C virus entry [Internet]. [cited 2016 Nov 28]. Available from:
<http://www.sciencedirect.com/science/article/pii/S016882781200164X>
150. Jangra RK, Yi M, Lemon SM. Regulation of Hepatitis C Virus Translation and Infectious Virus Production by the MicroRNA miR-122. *J Virol.* 2010 Jul;84(13):6615–25.
151. Li Y, Masaki T, Yamane D, McGivern DR, Lemon SM. Competing and noncompeting activities of miR-122 and the 5' exonuclease Xrn1 in regulation

- of hepatitis C virus replication. *Proc Natl Acad Sci U S A*. 2013 Jan 29;110(5):1881–6.
152. Machlin ES, Sarnow P, Sagan SM. Masking the 5' terminal nucleotides of the hepatitis C virus genome by an unconventional microRNA-target RNA complex. *Proc Natl Acad Sci U S A*. 2011 Feb 22;108(8):3193–8.
 153. Neufeldt CJ, Joyce MA, Levin A, Steenbergen RH, Pang D, Shields J, et al. Hepatitis C Virus-Induced Cytoplasmic Organelles Use the Nuclear Transport Machinery to Establish an Environment Conducive to Virus Replication. *PLOS Pathog*. 2013 Oct 31;9(10):e1003744.
 154. Levin A, Neufeldt CJ, Pang D, Wilson K, Loewen-Dobler D, Joyce MA, et al. Functional Characterization of Nuclear Localization and Export Signals in Hepatitis C Virus Proteins and Their Role in the Membranous Web. *PLOS ONE*. 2014 Dec 8;9(12):e114629.
 155. Neufeldt CJ, Joyce MA, Buuren NV, Levin A, Kirkegaard K, Jr MG, et al. The Hepatitis C Virus-Induced Membranous Web and Associated Nuclear Transport Machinery Limit Access of Pattern Recognition Receptors to Viral Replication Sites. *PLOS Pathog*. 2016 Feb 10;12(2):e1005428.
 156. Targett-Adams P, Boulant S, McLauchlan J. Visualization of double-stranded RNA in cells supporting hepatitis C virus RNA replication. *J Virol*. 2008;82(5):2182–95.
 157. Salloum S, Wang H, Ferguson C, Parton RG, Tai AW. Rab18 Binds to Hepatitis C Virus NS5A and Promotes Interaction between Sites of Viral Replication and Lipid Droplets. *PLOS Pathog*. 2013 Aug 1;9(8):e1003513.

158. Ploen D, Hafirassou ML, Himmelsbach K, Sauter D, Biniossek ML, Weiss TS, et al. TIP47 plays a crucial role in the life cycle of hepatitis C virus. *J Hepatol.* 2013;58(6):1081–8.
159. Vogt DA, Camus G, Herker E, Webster BR, Tsou C-L, Greene WC, et al. Lipid Droplet-Binding Protein TIP47 Regulates Hepatitis C Virus RNA Replication through Interaction with the Viral NS5A Protein. *PLOS Pathog.* 2013 Apr 11;9(4):e1003302.
160. Menzel N, Fischl W, Hueging K, Bankwitz D, Frentzen A, Haid S, et al. MAP-Kinase Regulated Cytosolic Phospholipase A2 Activity Is Essential for Production of Infectious Hepatitis C Virus Particles. *PLOS Pathog.* 2012 Jul 26;8(7):e1002829.
161. Herker E, Harris C, Hernandez C, Carpentier A, Kaehlcke K, Rosenberg AR, et al. Efficient hepatitis C virus particle formation requires diacylglycerol acyltransferase-1. *Nat Med.* 2010;16(11):1295–8.
162. Liefhebber JMP, Hague CV, Zhang Q, Wakelam MJO, McLauchlan J. Modulation of Triglyceride and Cholesterol Ester Synthesis Impairs Assembly of Infectious Hepatitis C Virus. *J Biol Chem.* 2014 Aug 1;289(31):21276–88.
163. Phan T, Kohlway A, Dimberu P, Pyle AM, Lindenbach BD. The Acidic Domain of Hepatitis C Virus NS4A Contributes to RNA Replication and Virus Particle Assembly. *J Virol.* 2011 Feb;85(3):1193–204.
164. Gouklani H, Bull RA, Beyer C, Coulibaly F, Gowans EJ, Drummer HE, et al. Hepatitis C Virus Nonstructural Protein 5B Is Involved in Virus Morphogenesis. *J Virol.* 2012 May;86(9):5080–8.

165. Jones DM, Patel AH, Targett-Adams P, McLauchlan J. The Hepatitis C Virus NS4B Protein Can trans-Complement Viral RNA Replication and Modulates Production of Infectious Virus. *J Virol.* 2009 Mar;83(5):2163–77.
166. Chang K-S, Jiang J, Cai Z, Luo G. Human Apolipoprotein E Is Required for Infectivity and Production of Hepatitis C Virus in Cell Culture. *J Virol.* 2007 Dec;81(24):13783–93.
167. Gastaminza P, Cheng G, Wieland S, Zhong J, Liao W, Chisari FV. Cellular Determinants of Hepatitis C Virus Assembly, Maturation, Degradation, and Secretion. *J Virol.* 2008 Mar;82(5):2120–9.
168. Sun H-Y, Lin C-C, Lee J-C, Wang S-W, Cheng P-N, Wu I-C, et al. Very low-density lipoprotein/lipo-viro particles reverse lipoprotein lipase-mediated inhibition of hepatitis C virus infection via apolipoprotein C-III. *Gut.* 2013 Aug 1;62(8):1193–203.
169. Huang H, Sun F, Owen DM, Li W, Chen Y, Gale M, et al. Hepatitis C virus production by human hepatocytes dependent on assembly and secretion of very low-density lipoproteins. *Proc Natl Acad Sci.* 2007 Apr 3;104(14):5848–53.
170. Bartenschlager R, Penin F, Lohmann V, André P. Assembly of infectious hepatitis C virus particles. *Trends Microbiol.* 2011 Feb;19(2):95–103.
171. Scheel TKH, Rice CM. Understanding the hepatitis C virus life cycle paves the way for highly effective therapies. *Nat Med.* 2013 Jul 1;19(7):837–49.
172. Chang M-L. Metabolic alterations and hepatitis C: From bench to bedside. *World J Gastroenterol.* 2016 Jan 28;22(4):1461–76.
173. Lonardo A, Adinolfi LE, Loria P, Carulli N, Ruggiero G, Day CP. Steatosis and hepatitis C virus: Mechanisms and significance for hepatic and extrahepatic disease. *Gastroenterology.* 2004 Feb;126(2):586–97.

174. Smith BW, Adams LA. Non-alcoholic fatty liver disease. *Crit Rev Clin Lab Sci.* 2011 Jun 1;48(3):97–113.
175. Mitochondrial injury, oxidative stress, and antioxidant gene expression are induced by hepatitis C virus core protein [Internet]. [cited 2017 Mar 2]. Available from:
<http://www.sciencedirect.com/science/article/pii/S0016508502212214>
176. Bigger CB, Brasky KM, Lanford RE. DNA Microarray Analysis of Chimpanzee Liver during Acute Resolving Hepatitis C Virus Infection. *J Virol.* 2001 Aug;75(15):7059–66.
177. Bigger CB, Guerra B, Brasky KM, Hubbard G, Beard MR, Luxon BA, et al. Intrahepatic Gene Expression during Chronic Hepatitis C Virus Infection in Chimpanzees. *J Virol.* 2004 Dec;78(24):13779–92.
178. Su AI, Pezacki JP, Wodicka L, Brideau AD, Supekova L, Thimme R, et al. Genomic analysis of the host response to hepatitis C virus infection. *Proc Natl Acad Sci U S A.* 2002 Nov 26;99(24):15669–74.
179. Syed GH, Amako Y, Siddiqui A. Hepatitis C Virus Hijacks Host Lipid Metabolism. *Trends Endocrinol Metab TEM.* 2010 Jan;21(1):33.
180. Mueckler M. Family of glucose-transporter genes. Implications for glucose homeostasis and diabetes. *Diabetes.* 1990 Jan;39(1):6–11.
181. Puri D. *Textbook of Medical Biochemistry.* Elsevier Health Sciences; 2014. 735 p.
182. Lunt SY, Heiden MG. Aerobic Glycolysis: Meeting the Metabolic Requirements of Cell Proliferation. *Annu Rev Cell Dev Biol.* 2011;27(1):441–64.

183. Mehta SH. Prevalence of Type 2 Diabetes Mellitus among Persons with Hepatitis C Virus Infection in the United States. *Ann Intern Med.* 2000 Oct 17;133(8):592.
184. Mehta SH, Brancati FL, Strathdee SA, Pankow JS, Netski D, Coresh J, et al. Hepatitis C virus infection and incident type 2 diabetes. *Hepatology.* 2003 Jul 1;38(1):50–6.
185. Negro F, Alaei M. Hepatitis C virus and type 2 diabetes. *World J Gastroenterol WJG.* 2009 Apr 7;15(13):1537–47.
186. Banerjee S, Saito K, Ait-Goughoulte M, Meyer K, Ray RB, Ray R. Hepatitis C Virus Core Protein Upregulates Serine Phosphorylation of Insulin Receptor Substrate-1 and Impairs the Downstream Akt/Protein Kinase B Signaling Pathway for Insulin Resistance. *J Virol.* 2008 Mar;82(6):2606–12.
187. Bose SK, Shrivastava S, Meyer K, Ray RB, Ray R. Hepatitis C Virus Activates the mTOR/S6K1 Signaling Pathway in Inhibiting IRS-1 Function for Insulin Resistance. *J Virol.* 2012 Jun;86(11):6315–22.
188. Bose SK, Ray R. Hepatitis C virus infection and insulin resistance. *World J Diabetes.* 2014 Feb 15;5(1):52–8.
189. Pal S, Polyak SJ, Bano N, Qiu WC, Carithers RL, Shuhart M, et al. Hepatitis C virus induces oxidative stress, DNA damage and modulates the DNA repair enzyme NEIL1. *J Gastroenterol Hepatol.* 2010 Mar;25(3):627–34.
190. Mangia A, Ripoli M. Insulin resistance, steatosis and hepatitis C virus. *Hepatol Int.* 2013 Aug 27;7(Suppl 2):782–9.
191. Bartz R, Li W-H, Venables B, Zehmer JK, Roth MR, Welti R, et al. Lipidomics reveals that adiposomes store ether lipids and mediate phospholipid traffic,. *J Lipid Res.* 2007 Apr 1;48(4):837–47.

192. Martin S, Parton RG. Lipid droplets: a unified view of a dynamic organelle. *Nat Rev Mol Cell Biol.* 2006 May;7(5):373–8.
193. Kuerschner L, Moessinger C, Thiele C. Imaging of Lipid Biosynthesis: How a Neutral Lipid Enters Lipid Droplets. *Traffic.* 2008 Mar 1;9(3):338–52.
194. Stone SJ, Levin MC, Zhou P, Han J, Walther TC, Farese RV. The Endoplasmic Reticulum Enzyme DGAT2 Is Found in Mitochondria-associated Membranes and Has a Mitochondrial Targeting Signal That Promotes Its Association with Mitochondria. *J Biol Chem.* 2009 Feb 20;284(8):5352–61.
195. Ducharme NA, Bickel PE. Minireview: Lipid Droplets in Lipogenesis and Lipolysis. *Endocrinology.* 2008 Mar 1;149(3):942–9.
196. Brasaemle DL. Thematic review series: Adipocyte Biology. The perilipin family of structural lipid droplet proteins: stabilization of lipid droplets and control of lipolysis. *J Lipid Res.* 2007 Dec 1;48(12):2547–59.
197. Saltiel AR, Kahn CR. Insulin signalling and the regulation of glucose and lipid metabolism. *Nature.* 2001 Dec 13;414(6865):799–806.
198. Habegger KM, Heppner KM, Geary N, Bartness TJ, DiMarchi R, Tschöp MH. The metabolic actions of glucagon revisited. *Nat Rev Endocrinol.* 2010 Dec;6(12):689–97.
199. Eehalt R, Füllekrug J, Pohl J, Ring A, Herrmann T, Stremmel W. Translocation of long chain fatty acids across the plasma membrane – lipid rafts and fatty acid transport proteins. *Mol Cell Biochem.* 2006 Mar 1;284(1–2):135–40.
200. Schaffer JE, Lodish HF. Expression cloning and characterization of a novel adipocyte long chain fatty acid transport protein. *Cell.* 1994 Nov 4;79(3):427–36.

201. Guo Y, Cordes KR, Farese RV, Walther TC. Lipid droplets at a glance. *J Cell Sci.* 2009 Mar 15;122(6):749–52.
202. Chapter 22. Oxidation of Fatty Acids: Ketogenesis | Harper's Illustrated Biochemistry, 29e | AccessMedicine | McGraw-Hill Medical [Internet]. [cited 2016 Nov 29]. Available from:
<http://accessmedicine.mhmedical.com/content.aspx?bookid=389§ionid=40142498&jumpsectionID=40144367>
203. Chowdhury GMI, Jiang L, Rothman DL, Behar KL. The contribution of ketone bodies to basal and activity-dependent neuronal oxidation in vivo. *J Cereb Blood Flow Metab Off J Int Soc Cereb Blood Flow Metab.* 2014 Jul;34(7):1233–42.
204. Rakhshandehroo M, Knoch B, Müller M, Kersten S. Peroxisome Proliferator-Activated Receptor Alpha Target Genes. *PPAR Res.* 2010 Sep 26;2010:e612089.
205. Xu HE, Stanley TB, Montana VG, Lambert MH, Shearer BG, Cobb JE, et al. Structural basis for antagonist-mediated recruitment of nuclear co-repressors by PPAR α . *Nature.* 2002 Feb 7;415(6873):813–7.
206. Pathophysiology of lipid droplet proteins in liver diseases [Internet]. [cited 2016 Nov 30]. Available from:
<http://www.sciencedirect.com/science/article/pii/S0014482715301282>
207. SREBP transcription factors: master regulators of lipid homeostasis [Internet]. [cited 2016 Nov 30]. Available from:
<http://www.sciencedirect.com/science/article/pii/S0300908404001658>

208. Horton JD, Goldstein JL, Brown MS. SREBPs: activators of the complete program of cholesterol and fatty acid synthesis in the liver. *J Clin Invest*. 2002 May 1;109(9):1125–31.
209. Lee JN, Ye J. Proteolytic Activation of Sterol Regulatory Element-binding Protein Induced by Cellular Stress through Depletion of Insig-1. *J Biol Chem*. 2004 Oct 22;279(43):45257–65.
210. McRae S, Iqbal J, Sarkar-Dutta M, Lane S, Nagaraj A, Ali N, et al. The Hepatitis C Virus-induced NLRP3 Inflammasome Activates the Sterol Regulatory Element-binding Protein (SREBP) and Regulates Lipid Metabolism. *J Biol Chem*. 2016 Feb 12;291(7):3254–67.
211. Hepatitis C Virus Induces Proteolytic Cleavage of Sterol Regulatory Element Binding Proteins and Stimulates Their Phosphorylation via Oxidative Stress [Internet]. [cited 2016 Nov 30]. Available from: <http://jvi.asm.org/content/81/15/8122.full>
212. Oem J-K, Jackel-Cram C, Li Y-P, Zhou Y, Zhong J, Shimano H, et al. Activation of sterol regulatory element-binding protein 1c and fatty acid synthase transcription by hepatitis C virus non-structural protein 2. *J Gen Virol*. 2008;89(5):1225–30.
213. Luna JM, Scheel TKH, Danino T, Shaw KS, Mele A, Fak JJ, et al. Hepatitis C virus RNA functionally sequesters miR-122. *Cell*. 2015 Mar 12;160(6):1099–110.
214. Wen J, Friedman JR. miR-122 regulates hepatic lipid metabolism and tumor suppression. *J Clin Invest*. 2012 Aug 1;122(8):2773–6.

215. Moore KJ, Rayner KJ, Suárez Y, Fernández-Hernando C. microRNAs and cholesterol metabolism. *Trends Endocrinol Metab TEM*. 2010 Dec;21(12):699–706.
216. Singaravelu R, Chen R, Lyn RK, Jones DM, O'Hara S, Rouleau Y, et al. Hepatitis C virus induced up-regulation of microRNA-27: A novel mechanism for hepatic steatosis. *Hepatology*. 2014 Jan 1;59(1):98–108.
217. Shrivastava S, Steele R, Ray R, Ray RB. MicroRNAs: Role in hepatitis C virus pathogenesis. *Genes Dis*. 2015 Mar;2(1):35–45.
218. Dharancy S, Malapel M, Perlemuter G, Roskams T, Cheng Y, Dubuquoy L, et al. Impaired expression of the peroxisome proliferator-activated receptor alpha during hepatitis C virus infection. *Gastroenterology*. 2005 Feb;128(2):334–42.
219. Fujita N, Kaito M, Kai M, Sugimoto R, Tanaka H, Horiike S, et al. Effects of bezafibrate in patients with chronic hepatitis C virus infection: combination with interferon and ribavirin. *J Viral Hepat*. 2006 Jul 1;13(7):441–8.
220. Tsutsumi T, Suzuki T, Shimoike T, Suzuki R, Moriya K, Shintani Y, et al. Interaction of hepatitis C virus core protein with retinoid X receptor α modulates its transcriptional activity. *Hepatology*. 2002 Apr 1;35(4):937–46.
221. Cheng Y, Dharancy S, Malapel M, Desreumaux P. Hepatitis C virus infection down-regulates the expression of peroxisome proliferator-activated receptor α and carnitine palmitoyl acyl-CoA transferase 1A. *World J Gastroenterol*. 2005 Dec 28;11(48):7591–6.
222. Shirasaki T, Honda M, Shimakami T, Horii R, Yamashita T, Sakai Y, et al. MicroRNA-27a Regulates Lipid Metabolism and Inhibits Hepatitis C Virus Replication in Human Hepatoma Cells. *J Virol*. 2013 May;87(9):5270–86.

223. Domitrovich AM, Felmlee DJ, Siddiqui A. Hepatitis C Virus Nonstructural Proteins Inhibit Apolipoprotein B100 Secretion. *J Biol Chem*. 2005 Dec 2;280(48):39802–8.
224. Warburg O. On the Origin of Cancer Cells. *Science*. 1956 Feb 24;123(3191):309–14.
225. Hedeskov CJ. Early effects of phytohaemagglutinin on glucose metabolism of normal human lymphocytes. *Biochem J*. 1968 Nov;110(2):373–80.
226. Brand K. Glutamine and glucose metabolism during thymocyte proliferation. Pathways of glutamine and glutamate metabolism. *Biochem J*. 1985 Jun 1;228(2):353–61.
227. Fantin VR, St-Pierre J, Leder P. Attenuation of LDH-A expression uncovers a link between glycolysis, mitochondrial physiology, and tumor maintenance. *Cancer Cell*. 2006 Jun 13;9(6):425–34.
228. Moreno-Sánchez R, Rodríguez-Enríquez S, Marín-Hernández A, Saavedra E. Energy metabolism in tumor cells. *FEBS J*. 2007 Mar 1;274(6):1393–418.
229. Zu XL, Guppy M. Cancer metabolism: facts, fantasy, and fiction. *Biochem Biophys Res Commun*. 2004 Jan 16;313(3):459–65.
230. DeBerardinis RJ, Mancuso A, Daikhin E, Nissim I, Yudkoff M, Wehrli S, et al. Beyond aerobic glycolysis: Transformed cells can engage in glutamine metabolism that exceeds the requirement for protein and nucleotide synthesis. *Proc Natl Acad Sci U S A*. 2007 Dec 4;104(49):19345–50.
231. Hume DA, Weidemann MJ. Role and regulation of glucose metabolism in proliferating cells. *J Natl Cancer Inst*. 1979 Jan;62(1):3–8.

232. Vander Heiden MG, Cantley LC, Thompson CB. Understanding the Warburg Effect: The Metabolic Requirements of Cell Proliferation. *Science*. 2009 May 22;324(5930):1029–33.
233. Portais JC, Voisin P, Merle M, Canioni P. Glucose and glutamine metabolism in C6 glioma cells studied by carbon 13 NMR. *Biochimie*. 1996 Jan 1;78(3):155–64.
234. Kato T, Furusaka A, Miyamoto M, Date T, Yasui K, Hiramoto J, et al. Sequence analysis of hepatitis C virus isolated from a fulminant hepatitis patient. *J Med Virol*. 2001 Jul;64(3):334–9.
235. Nakabayashi H, Taketa K, Miyano K, Yamane T, Sato J. Growth of Human Hepatoma Cell Lines with Differentiated Functions in Chemically Defined Medium. *Cancer Res*. 1982 Sep 1;42(9):3858–63.
236. Lohmann V, Körner F, Koch J-O, Herian U, Theilmann L, Bartenschlager R. Replication of Subgenomic Hepatitis C Virus RNAs in a Hepatoma Cell Line. *Science*. 1999 Jul 2;285(5424):110–3.
237. Blight KJ, McKeating JA, Rice CM. Highly Permissive Cell Lines for Subgenomic and Genomic Hepatitis C Virus RNA Replication. *J Virol*. 2002 Dec;76(24):13001–14.
238. Steenbergen RHG, Joyce MA, Thomas BS, Jones D, Law J, Russell R, et al. Human serum leads to differentiation of human hepatoma cells, restoration of very-low-density lipoprotein secretion, and a 1000-fold increase in HCV Japanese fulminant hepatitis type 1 titers. *Hepatology*. 2013 Dec 1;58(6):1907–17.
239. Singaravelu R, Lyn RK, Srinivasan P, Delcorde J, Steenbergen RH, Tyrrell DL, et al. Human serum activates CIDEB-mediated lipid droplet enlargement

- in hepatoma cells. *Biochem Biophys Res Commun*. 2013 Nov 15;441(2):447–52.
240. Meex SJR, Andreo U, Sparks JD, Fisher EA. Huh-7 or HepG2 cells: which is the better model for studying human apolipoprotein-B100 assembly and secretion? *J Lipid Res*. 2011 Jan;52(1):152–8.
241. Ling J, Lewis J, Douglas D, Kneteman NM, Vance DE. Characterization of lipid and lipoprotein metabolism in primary human hepatocytes. *Biochim Biophys Acta BBA - Mol Cell Biol Lipids*. 2013 Feb;1831(2):387–97.
242. Lindenbach B. Measuring HCV Infectivity Produced in Cell Culture and In Vivo. In: Tang H, editor. *Hepatitis C [Internet]*. Humana Press; 2009 [cited 2017 Jun 27]. p. 329–36. (Methods in Molecular Biology™). Available from: http://dx.doi.org/10.1007/978-1-59745-394-3_24
243. Smith PK, Krohn RI, Hermanson GT, Mallia AK, Gartner FH, Provenzano MD, et al. Measurement of protein using bicinchoninic acid. *Anal Biochem*. 1985 Oct 1;150(1):76–85.
244. Carleton HM, Drury RAB, Wallington EA. *Carleton's Histological technique*. Oxford University Press; 1980. 536 p.
245. Morris SM. Regulation of enzymes of the urea cycle and arginine metabolism. *Annu Rev Nutr*. 2002;22:87–105.
246. Wyss M, Kaddurah-Daouk R. Creatine and Creatinine Metabolism. *Physiol Rev*. 2000 Jul 1;80(3):1107–213.
247. Meister A. *Advances in Enzymology and Related Areas of Molecular Biology*. John Wiley & Sons; 2009. 511 p.

248. Shoulders MD, Raines RT. COLLAGEN STRUCTURE AND STABILITY. *Annu Rev Biochem.* 2009;78:929–58.
249. KEGG PATHWAY: Valine, leucine and isoleucine degradation - Reference pathway [Internet]. [cited 2017 Mar 22]. Available from: http://www.genome.jp/kegg-bin/show_pathway?map00280
250. Shimomura Y, Honda T, Shiraki M, Murakami T, Sato J, Kobayashi H, et al. Branched-Chain Amino Acid Catabolism in Exercise and Liver Disease. *J Nutr.* 2006 Jan 1;136(1):250S–253S.
251. Crown SB, Marze N, Antoniewicz MR. Catabolism of Branched Chain Amino Acids Contributes Significantly to Synthesis of Odd-Chain and Even-Chain Fatty Acids in 3T3-L1 Adipocytes. *PLOS ONE.* 2015 Dec 28;10(12):e0145850.
252. Wilson JM, Fitschen PJ, Campbell B, Wilson GJ, Zanchi N, Taylor L, et al. International Society of Sports Nutrition Position Stand: beta-hydroxy-beta-methylbutyrate (HMB). *J Int Soc Sports Nutr.* 2013 Feb 2;10:6.
253. Zanchi NE, Gerlinger-Romero F, Guimarães-Ferreira L, Filho MA de S, Felitti V, Lira FS, et al. HMB supplementation: clinical and athletic performance-related effects and mechanisms of action. *Amino Acids.* 2011 Apr 1;40(4):1015–25.
254. Kohlmeier M. *Nutrient Metabolism: Structures, Functions, and Genes.* Academic Press; 2015. 899 p.
255. Dahlhoff C, Desmarchelier C, Sailer M, Fürst RW, Haag A, Ulbrich SE, et al. Hepatic Methionine Homeostasis Is Conserved in C57BL/6N Mice on High-Fat Diet Despite Major Changes in Hepatic One-Carbon Metabolism. *PLoS*

- ONE [Internet]. 2013 Mar 5 [cited 2017 Mar 22];8(3). Available from:
<http://www.ncbi.nlm.nih.gov/pmc/articles/PMC3589430/>
256. Finkelstein JD. Methionine metabolism in liver diseases. *Am J Clin Nutr.* 2003 May 1;77(5):1094–5.
257. Mato JM, Martínez-Chantar ML, Lu SC. Methionine metabolism and liver disease. *Annu Rev Nutr.* 2008;28:273–93.
258. Brosnan ME, MacMillan L, Stevens JR, Brosnan JT. Division of labour: how does folate metabolism partition between one-carbon metabolism and amino acid oxidation? *Biochem J.* 2015 Dec 1;472(2):135–46.
259. Phosphatidylcholine biosynthesis and lipoprotein metabolism [Internet]. [cited 2017 Mar 22]. Available from:
<http://www.sciencedirect.com/science/article/pii/S138819811100179X>
260. Yao ZM, Vance DE. The active synthesis of phosphatidylcholine is required for very low density lipoprotein secretion from rat hepatocytes. *J Biol Chem.* 1988 Feb 25;263(6):2998–3004.
261. Vance JE, Vance DE. The role of phosphatidylcholine biosynthesis in the secretion of lipoproteins from hepatocytes. *Can J Biochem Cell Biol Rev Can Biochim Biol Cell.* 1985 Aug;63(8):870–81.
262. Huwiler A, Kolter T, Pfeilschifter J, Sandhoff K. Physiology and pathophysiology of sphingolipid metabolism and signaling. *Biochim Biophys Acta BBA - Mol Cell Biol Lipids.* 2000 May 31;1485(2–3):63–99.
263. Hannun YA. *Sphingolipid-Mediated Signal Transduction.* Springer Science & Business Media; 2013. 316 p.

264. Ohvo-Rekilä H, Ramstedt B, Leppimäki P, Peter Slotte J. Cholesterol interactions with phospholipids in membranes. *Prog Lipid Res.* 2002 Jan;41(1):66–97.
265. Chen Y, Guillemin GJ. Kynurenine Pathway Metabolites in Humans: Disease and Healthy States. *Int J Tryptophan Res IJTR.* 2009 Jan 8;2:1–19.
266. Srivastava S. Emerging therapeutic roles for NAD⁺ metabolism in mitochondrial and age-related disorders. *Clin Transl Med [Internet].* 2016 Jul 27 [cited 2017 Apr 12];5. Available from: <http://www.ncbi.nlm.nih.gov/pmc/articles/PMC4963347/>
267. Rodgers JT, Lerin C, Haas W, Gygi SP, Spiegelman BM, Puigserver P. Nutrient control of glucose homeostasis through a complex of PGC-1 α and SIRT1. *Nature.* 2005 Mar 3;434(7029):113–8.
268. Nemoto S, Fergusson MM, Finkel T. SIRT1 Functionally Interacts with the Metabolic Regulator and Transcriptional Coactivator PGC-1 α . *J Biol Chem.* 2005 Apr 22;280(16):16456–60.
269. Liu Y, Dentin R, Chen D, Hedrick S, Ravnskjaer K, Schenk S, et al. A fasting inducible switch modulates gluconeogenesis via activator/coactivator exchange. *Nature.* 2008 Nov 13;456(7219):269–73.
270. Wilson BJ, Tremblay AM, Deblois G, Sylvain-Drolet G, Giguère V. An Acetylation Switch Modulates the Transcriptional Activity of Estrogen-Related Receptor α . *Mol Endocrinol.* 2010 Jul 1;24(7):1349–58.
271. Yoon JC, Puigserver P, Chen G, Donovan J, Wu Z, Rhee J, et al. Control of hepatic gluconeogenesis through the transcriptional coactivator PGC-1. *Nature.* 2001 Sep 13;413(6852):131–8.

272. Mootha VK, Handschin C, Arlow D, Xie X, Pierre JS, Sihag S, et al. *Errα and Gabpa/b specify PGC-1α-dependent oxidative phosphorylation gene expression that is altered in diabetic muscle.* *Proc Natl Acad Sci U S A.* 2004 Apr 27;101(17):6570–5.
273. Huss JM, Torra IP, Staels B, Giguère V, Kelly DP. *Estrogen-related receptor alpha directs peroxisome proliferator-activated receptor alpha signaling in the transcriptional control of energy metabolism in cardiac and skeletal muscle.* *Mol Cell Biol.* 2004 Oct;24(20):9079–91.
274. Mougios V. *Exercise Biochemistry. Human Kinetics; 2006. 362 p.*
275. Tessari P, Vettore M, Millionini R, Puricelli L, Orlando R. *Effect of liver cirrhosis on phenylalanine and tyrosine metabolism: Curr Opin Clin Nutr Metab Care.* 2010 Jan;13(1):81–6.
276. KEGG PATHWAY: Glycolysis / Gluconeogenesis [Internet]. [cited 2017 Apr 13]. Available from: http://www.genome.jp/kegg-bin/show_pathway?ec00010+6.2.1.1
277. Descalzo AM, Insani EM, Pensel NA. *Light-scattering detection of phospholipids resolved by HPLC.* *Lipids.* 2003 Sep 1;38(9):999–1003.
278. Nissen HP, Kreysel HW. *The use of HPLC for the determination of lipids in biological materials.* *Chromatographia.* 1990 Dec 1;30(11–12):686–90.
279. Lin J-T. *HPLC Separation of Acyl Lipid Classes.* *J Liq Chromatogr Relat Technol.* 2007 Jun 1;30(14):2005–20.
280. Gocze PM, Freeman DA. *Factors underlying the variability of lipid droplet fluorescence in MA-10 leydig tumor cells.* *Cytometry.* 1994 Oct 1;17(2):151–8.

281. Castéra L, Hézode C, Roudot-Thoraval F, Lonjon I, Zafrani E-S, Pawlotsky J-M, et al. Effect of antiviral treatment on evolution of liver steatosis in patients with chronic hepatitis C: indirect evidence of a role of hepatitis C virus genotype 3 in steatosis. *Gut*. 2004 Mar;53(3):420–4.
282. Poynard T, Moussalli J, Munteanu M, Thabut D, Lebray P, Rudler M, et al. Slow regression of liver fibrosis presumed by repeated biomarkers after virological cure in patients with chronic hepatitis C. *J Hepatol*. 2013 Oct 1;59(4):675–83.
283. Maylin S, Martinot–Peignoux M, Moucari R, Boyer N, Ripault M, Cazals–Hattem D, et al. Eradication of Hepatitis C Virus in Patients Successfully Treated for Chronic Hepatitis C. *Gastroenterology*. 2008 Sep 1;135(3):821–9.
284. and YAL, Friedman SL. Reversal, maintenance or progression: What happens to the liver after a virologic cure of hepatitis C? *Antiviral Res*. 2014 Jul;0:23–30.
285. Welsch C, Efinger M, Wagner M von, Herrmann E, Zeuzem S, Welzel TM, et al. Ongoing liver inflammation in patients with chronic hepatitis C and sustained virological response. *PLOS ONE*. 2017 Feb 14;12(2):e0171755.
286. Lam AM, Murakami E, Espiritu C, Steuer HMM, Niu C, Keilman M, et al. PSI-7851, a Pronucleotide of β -d-2'-Deoxy-2'-Fluoro-2'-C-Methyluridine Monophosphate, Is a Potent and Pan-Genotype Inhibitor of Hepatitis C Virus Replication. *Antimicrob Agents Chemother*. 2010 Aug;54(8):3187–96.
287. Oh S-Y, Park S-K, Kim J-W, Ahn Y-H, Park S-W, Kim K-S. Acetyl-CoA Carboxylase β Gene Is Regulated by Sterol Regulatory Element-binding Protein-1 in Liver. *J Biol Chem*. 2003 Aug 1;278(31):28410–7.

288. Sterol regulation of human fatty acid synthase promoter I requires nuclear factor-Y- and Sp-1-binding sites [Internet]. [cited 2017 Jul 7]. Available from: <http://www.pnas.org/content/97/8/3948.full>
289. Amemiya-Kudo M, Shimano H, Hasty AH, Yahagi N, Yoshikawa T, Matsuzaka T, et al. Transcriptional activities of nuclear SREBP-1a, -1c, and -2 to different target promoters of lipogenic and cholesterologenic genes. *J Lipid Res.* 2002 Aug 1;43(8):1220–35.
290. Shimomura I, Shimano H, Korn BS, Bashmakov Y, Horton JD. Nuclear Sterol Regulatory Element-binding Proteins Activate Genes Responsible for the Entire Program of Unsaturated Fatty Acid Biosynthesis in Transgenic Mouse Liver. *J Biol Chem.* 1998 Dec 25;273(52):35299–306.
291. Shimano H, Horton JD, Hammer RE, Shimomura I, Brown MS, Goldstein JL. Overproduction of cholesterol and fatty acids causes massive liver enlargement in transgenic mice expressing truncated SREBP-1a. *J Clin Invest.* 1996 Oct 1;98(7):1575–84.
292. Jeon T-I, Osborne TF. SREBPs: Metabolic Integrators in Physiology and Metabolism. *Trends Endocrinol Metab.* 2012 Feb;23(2):65–72.
293. Leavens KF, Easton RM, Shulman GI, Previs SF, Birnbaum MJ. Akt2 is required for hepatic lipid accumulation in models of insulin resistance. *Cell Metab.* 2009 Nov;10(5):405–18.
294. Shimomura I, Bashmakov Y, Horton JD. Increased levels of nuclear SREBP-1c associated with fatty livers in two mouse models of diabetes mellitus. *J Biol Chem.* 1999 Oct 15;274(42):30028–32.
295. Serviddio G, Giudetti AM, Bellanti F, Priore P, Rollo T, Tamborra R, et al. Oxidation of Hepatic Carnitine Palmitoyl Transferase-I (CPT-I) Impairs Fatty

- Acid Beta-Oxidation in Rats Fed a Methionine-Choline Deficient Diet. PLoS ONE [Internet]. 2011 Sep 1 [cited 2017 Jul 7];6(9). Available from: <http://www.ncbi.nlm.nih.gov/pmc/articles/PMC3164715/>
296. Souza-Mello V. Peroxisome proliferator-activated receptors as targets to treat non-alcoholic fatty liver disease. *World J Hepatol.* 2015 May 18;7(8):1012–9.
 297. Seo YS, Kim JH, Jo NY, Choi KM, Baik SH, Park J-J, et al. PPAR agonists treatment is effective in a nonalcoholic fatty liver disease animal model by modulating fatty-acid metabolic enzymes. *J Gastroenterol Hepatol.* 2008 Jan 1;23(1):102–9.
 298. Sambasiva Rao M, Reddy JK. PPAR α in the pathogenesis of fatty liver disease. *Hepatology.* 2004 Oct 1;40(4):783–6.
 299. Pawlak M, Lefebvre P, Staels B. Molecular mechanism of PPAR α action and its impact on lipid metabolism, inflammation and fibrosis in non-alcoholic fatty liver disease. *J Hepatol.* 2015 Mar 1;62(3):720–33.
 300. Co-regulation of Tissue-specific Alternative Human Carnitine Palmitoyltransferase I β Gene Promoters by Fatty Acid Enzyme Substrate [Internet]. [cited 2017 Jul 7]. Available from: <http://www.jbc.org/content/273/49/32901.long>
 301. Fatty Acids Activate Transcription of the Muscle Carnitine Palmitoyltransferase I Gene in Cardiac Myocytes via the Peroxisome Proliferator-activated Receptor α [Internet]. [cited 2017 Jul 7]. Available from: <http://www.jbc.org/content/273/37/23786.long>
 302. Montagner A, Polizzi A, Fouché E, Ducheix S, Lippi Y, Lasserre F, et al. Liver PPAR α is crucial for whole-body fatty acid homeostasis and is protective against NAFLD. *Gut.* 2016 Feb 1;gutjnl-2015-310798.

303. Nguyen P, Leray V, Diez M, Serisier S, Bloc'h JL, Siliart B, et al. Liver lipid metabolism. *J Anim Physiol Anim Nutr.* 2008 Jun 1;92(3):272–83.
304. Li AC, Glass CK. PPAR- and LXR-dependent pathways controlling lipid metabolism and the development of atherosclerosis. *J Lipid Res.* 2004 Dec 1;45(12):2161–73.
305. Gervois P, Torra IP, Fruchart J-C, Staels B. Regulation of Lipid and Lipoprotein Metabolism by PPAR Activators. *Clin Chem Lab Med.* 2005;38(1):3–11.
306. Varga T, Czimmerer Z, Nagy L. PPARs are a unique set of fatty acid regulated transcription factors controlling both lipid metabolism and inflammation. *Biochim Biophys Acta.* 2011 Aug;1812(8):1007–22.
307. Burri L, Thoresen GH, Berge RK. The Role of PPAR Activation in Liver and Muscle [Internet]. *PPAR Research.* 2010 [cited 2017 Jul 9]. Available from: <https://www.hindawi.com/journals/ppar/2010/542359/>
308. Wang Y-X. PPARs: diverse regulators in energy metabolism and metabolic diseases. *Cell Res.* 2010 Jan 26;20(2):124–37.
309. Braissant O, Fougère F, Scotto C, Dauça M, Wahli W. Differential expression of peroxisome proliferator-activated receptors (PPARs): tissue distribution of PPAR-alpha, -beta, and -gamma in the adult rat. *Endocrinology.* 1996 Jan 1;137(1):354–66.
310. Cook WS, Yeldandi AV, Rao MS, Hashimoto T, Reddy JK. Less Extrahepatic Induction of Fatty Acid β -Oxidation Enzymes by PPAR α . *Biochem Biophys Res Commun.* 2000 Nov 11;278(1):250–7.

311. Kersten S, Seydoux J, Peters JM, Gonzalez FJ, Desvergne B, Wahli W. Peroxisome proliferator-activated receptor α mediates the adaptive response to fasting. *J Clin Invest*. 1999 Jun 1;103(11):1489–98.
312. Xu X, So J-S, Park J-G, Lee A-H. Transcriptional Control of Hepatic Lipid Metabolism by SREBP and ChREBP. *Semin Liver Dis*. 2013 Nov;33(04):301–11.
313. Shao W, Espenshade PJ. Expanding Roles for SREBP in Metabolism. *Cell Metab*. 2012 Oct 3;16(4):414–9.
314. Kersten S. Integrated physiology and systems biology of PPAR α . *Mol Metab*. 2014 Jul 1;3(4):354–71.
315. Cole JT. Metabolism of BCAAs. In: Rajendram R, Preedy VR, Patel VB, editors. *Branched Chain Amino Acids in Clinical Nutrition* [Internet]. Springer New York; 2015 [cited 2017 Jun 15]. p. 13–24. (Nutrition and Health). Available from: http://link.springer.com/chapter/10.1007/978-1-4939-1923-9_2
316. Cotter DG, Schugar RC, Crawford PA. Ketone body metabolism and cardiovascular disease. *Am J Physiol - Heart Circ Physiol*. 2013 Apr 15;304(8):H1060–76.
317. J D McGarry, Foster and DW. Regulation of Hepatic Fatty Acid Oxidation and Ketone Body Production. *Annu Rev Biochem*. 1980;49(1):395–420.
318. Robinson AM, Williamson DH. Physiological roles of ketone bodies as substrates and signals in mammalian tissues. *Physiol Rev*. 1980 Jan 1;60(1):143–87.
319. George F. Cahill J. Fuel Metabolism in Starvation. *Annu Rev Nutr*. 2006;26(1):1–22.

320. Johnson RH, Walton JL, Krebs HA, Williamson DH. POST-EXERCISE KETOSIS. *The Lancet*. 1969 Dec 27;294(7635):1383–5.
321. Repa JJ, Liang G, Ou J, Bashmakov Y, Lobaccaro J-MA, Shimomura I, et al. Regulation of mouse sterol regulatory element-binding protein-1c gene (SREBP-1c) by oxysterol receptors, LXR α and LXR β . *Genes Dev*. 2000 Nov 15;14(22):2819–30.
322. Talukdar S, Hillgartner FB. The mechanism mediating the activation of acetyl-coenzyme A carboxylase- α gene transcription by the liver X receptor agonist T0-901317. *J Lipid Res*. 2006 Nov 1;47(11):2451–61.
323. Wójcicka G, Jamroz-Wiśniewska A, Horoszewicz K, Beltowski J. Liver X receptors (LXRs). Part I: structure, function, regulation of activity, and role in lipid metabolism. *Postepy Hig Med Doswiadczalnej Online*. 2007 Dec 3;61:736–59.
324. Cha J-Y, Repa JJ. The Liver X Receptor (LXR) and Hepatic Lipogenesis THE CARBOHYDRATE-RESPONSE ELEMENT-BINDING PROTEIN IS A TARGET GENE OF LXR. *J Biol Chem*. 2007 Jan 5;282(1):743–51.
325. Reddy JK, Rao MS. Lipid Metabolism and Liver Inflammation. II. Fatty liver disease and fatty acid oxidation. *Am J Physiol - Gastrointest Liver Physiol*. 2006 May 1;290(5):G852–8.
326. Hashimoto T, Cook WS, Qi C, Yeldandi AV, Reddy JK, Rao MS. Defect in Peroxisome Proliferator-activated Receptor α -inducible Fatty Acid Oxidation Determines the Severity of Hepatic Steatosis in Response to Fasting. *J Biol Chem*. 2000 Sep 15;275(37):28918–28.
327. Yan F, Wang Q, Xu C, Cao M, Zhou X, Wang T, et al. Peroxisome Proliferator-Activated Receptor α Activation Induces Hepatic Steatosis,

Suggesting an Adverse Effect. PLoS ONE [Internet]. 2014 Jun 13 [cited 2017 Jul 8];9(6). Available from:
<http://www.ncbi.nlm.nih.gov/pmc/articles/PMC4057124/>

328. Eslam M, Khattab MA, Harrison SA. Peroxisome proliferator-activated receptors and hepatitis C virus. *Ther Adv Gastroenterol*. 2011 Nov;4(6):419–31.
329. Ponziani FR, Mangiola F, Binda C, Zocco MA, Siciliano M, Grieco A, et al. Future of liver disease in the era of direct acting antivirals for the treatment of hepatitis C. *World J Hepatol*. 2017 Mar 8;9(7):352–67.
330. de MATTOS AA, MARCON P dos S, de ARAÚJO FSB, CORAL GP, TOVO CV. HEPATOCELLULAR CARCINOMA IN A NON-CIRRHOTIC PATIENT WITH SUSTAINED VIROLOGICAL RESPONSE AFTER HEPATITIS C TREATMENT. *Rev Inst Med Trop São Paulo*. 2015;57(6):519–22.
331. Toyoda H, Kumada T, Tada T, Kiriyama S, Tanikawa M, Hisanaga Y, et al. Risk factors of hepatocellular carcinoma development in non-cirrhotic patients with sustained virologic response for chronic hepatitis C virus infection. *J Gastroenterol Hepatol*. 2015 Jul 1;30(7):1183–9.
332. Rui L. Energy Metabolism in the Liver. *Compr Physiol*. 2014 Jan;4(1):177–97.
333. Berg JM, Tymoczko JL, Stryer L. Glycogen Metabolism. 2002 [cited 2017 Jun 16]; Available from: <https://www.ncbi.nlm.nih.gov/books/NBK21190/>
334. Mirandola S, Bowman D, Hussain MM, Alberti A. Hepatic steatosis in hepatitis C is a storage disease due to HCV interaction with microsomal triglyceride transfer protein (MTP). *Nutr Metab*. 2010 Feb 23;7:13.

Appendix

Appendix

Compound	HS cultured cells compared to FBS cultured cells (μM)			Pathway or Reaction	EC. Number
	HS	FBS	P Value		
2-Oxoisocaproate	33.1 \pm 6.767	50.92 \pm 4.57	0.0606	Valine Degradation	1.2.1.25
				2-Oxoisovalerate Decarboxylation to Isobutanoyl-CoA	1.2.4.4
				Leucine Degradation	1.2.1.- 2.6.1.6
3-Hydroxybutyrate	74.03 \pm 15.01	9.4 \pm 9.4	0.0065	Ketogenesis	1.1.1.30
				Ketolysis	
3-Hydroxyisovalerate	49.12 \pm 14.65	0 \pm 0	0.0100	Leucine Biosynthesis	No data
3-Methyl-2-oxovalerate	45 \pm 7.682	68.1 \pm 5.053	0.0362	Isoleucine Degradation	2.6.1.42 2.6.1.-
				Valine Degradation	2.6.1.42
				Acetone degradation I	4.1.1.4
Acetoacetate	145.9 \pm 39.35	6.8 \pm 4.576	0.0079	Ketogenesis and Ketolysis pathways	2.8.3.5 4.1.3.4 1.1.1.30
				Leucine degradation	4.1.3.4
				Tyrosine degradation	3.7.1.2
				Ethanol Degradation II, IV	6.2.1.1 1.2.1.3
				Oxidative Ethanol Degradation III	6.2.1.1 1.2.1.3
Acetate	30.76 \pm 1.148	31.58 \pm	0.8259	Ethanol Degradation II, IV	6.2.1.1 1.2.1.3
				Oxidative Ethanol Degradation III	6.2.1.1 1.2.1.3

		3.432		Acetate Conversion to Acetyl Co-A	6.2.1.1
				Heparan Sulfate Biosynthesis	3.1.1.-
Acetone	64.56 ± 7.2	66.52 ± 11.74	0.8900	Acetone Degradation I	1.14.14.1
					1.1.1.80
				Ketogenesis	4.1.1.4
Alanine	587.8 ± 57.99	638 ± 151.5, n=5	0.7650	tRNA Charging	6.1.1.7
				γ-glutamyl Cycle	2.3.2.2
				Leukotriene Biosynthesis	2.3.2.2
				S-methyl-5-thio-α-D-ribose 1-phosphate Degradation	2.6.1.88
				L-kynurenine Degradation	3.7.1.3
				Tryptophan Degradation to 2-amino-3-carboxymuconate Semialdehyde	3.7.1.3
				Molybdenum Cofactor Biosynthesis	2.8.1.7
				Thio-molybdenum Cofactor Biosynthesis	2.8.1.9
				Alanine Biosynthesis and Degradation	2.6.1.2
Glycine Biosynthesis	2.6.1.44				
Arginine	108.2 ± 50.75	282.9 ± 32	0.0196	Citrulline-Nitric Oxide Cycle	1.14.13.39
				Creatine Biosynthesis	2.1.4.1
				Putrescine Biosynthesis II	4.1.1.19
				tRNA Charging	6.1.1.19
				urea Cycle	3.5.3.1
				Citrulline-Nitric Oxide Cycle	4.3.2.1

Choline	2.411 ± 2.411	2.411 ± 2.411	0.3466	Creatine Biosynthesis	1.1.99.1
				Kennedy pathway	2.7.1.32
				Phospholipases	3.1.4.4
Ethanol	1387 ± 665	1408 ± 314.5	0.9783	Ethanol Degradation II, IV	1.11.1.6 1.1.1.1
				Oxidative Ethanol Degradation III	RXN66-2
Formate	294.3 ± 10.54	252.1 ± 54.73	0.4714	Folate Transformations	6.3.4.3
				Folate Polyglutamylation	6.3.4.3
				Cholesterol Biosynthesis	cytochrome P450 51A1
				Estradiol Biosynthesis	cytochrome P450 2A6
				Fatty Acid α -oxidation	3.1.2.10
				Formaldehyde Oxidation	3.1.2.12
				Tryptophan Degradation to 2-amino-3-carboxymuconate Semialdehyde	3.5.1.9
				Methylthiopropionate Biosynthesis	1.13.11.53
				S-methyl-5-thio- α -D-ribose 1-phosphate Degradation	1.13.11.54
				Tetrahydrobiopterin de novo Biosynthesis	3.5.4.16
Glucose	11932 ± 1550	15147 ± 2387	0.2913	GDP-Glucose Biosynthesis II	2.7.1.2 2.7.1.1
				Glycolysis	2.7.1.2
				Trehalose Degradation	2.7.1.2
				UDP-N-acetyl-D-galactosamine Biosynthesis II	2.7.1.2
				Glycogenolysis	3.2.1.33
				Lactose Degradation III	3.2.1.23
				Trehalose Degradation	3.2.1.28

					5.1.3.3
				Sucrose Degradation	5.1.3.3
Glutamate	-	-	-	Folate Polyglutamylation	6.3.2.17
				GABA Shunt	4.1.1.15
				Glutamate Dependent Acid Resistance	4.1.1.15
				Glutamine Biosynthesis	6.3.1.2
				Glutathione Biosynthesis	6.3.2.1
				L-glutamine tRNA Biosynthesis	RXN-9386
				Malate-Aspartate Shuttle	2.6.1.1
				Asparagine Biosynthesis	2.6.1.1
					6.3.5.4
				Asparagine Degradation	2.6.1.1
				Ornithine de novo Biosynthesis	2.7.2.11
				Proline Biosynthesis	2.7.2.11
				Serine Biosynthesis	2.6.1.52
				tRNA Charging	6.1.1.17
				4-aminobutyrate Degradation	2.6.1.19
				β -alanine Degradation	2.6.1.19
				4-hydroxy-2-nonenal Detoxification	3.4.19.9
				Glutathione-mediated Detoxification	3.4.19.9
				Glutamate Removal from Folates	3.4.19.9
				4-hydroxybenzoate Biosynthesis	2.6.1.5
				Tyrosine Degradation	2.6.1.5
				5-aminoimidazole Ribonucleotide Biosynthesis	6.3.5.3

					2.4.2.14
				γ -glutamyl Cycle	3.5.2.9
				Glutamine Degradation/ Glutamate Biosynthesis	3.5.1.2
				Guanosine Ribonucleotides de novo Biosynthesis	6.3.5.2
				Histidine Degradation	2.1.2.5
				L-cysteine Degradation II	2.6.1.3
				L-glutamine tRNA Biosynthesis	6.3.5.7
				Leucine Degradation	2.6.1.6
				Lysine Degradation I (Saccharopine Pathway)	2.6.1.39
					1.5.1.9
				Lysine Degradation II (Pipecolate Pathway)	2.6.1.39
					RXN66-565
				NAD Biosynthesis from 2- amino-3-carboxymuconate Semialdehyde	6.3.5.1
				Proline Degradation	1.2.1.88
				UMP Biosynthesis	6.3.5.5
				UTP and CTP de novo Biosynthesis	6.3.4.2
				UTP and CTP Dephosphorylation I, II	6.3.4.2
Glutamine	1062 \pm 172.1	1038 \pm 92.74	0.9031	5-aminoimidazole Ribonucleotide Biosynthesis	2.4.2.14
					6.3.5.3
				Asparagine Biosynthesis	6.3.5.4
				Glutamine Degradation/ Glutamate Biosynthesis	3.5.1.2
					3.5.1.38
				Asparagine Degradation	3.5.1.38
				Guanosine Ribonucleotides de novo Biosynthesis	6.3.5.2
L-glutamine tRNA	6.3.5.7				

				Biosynthesis	
				NAD Biosynthesis from 2-amino-3-carboxymuconate Semialdehyde	6.3.5.1
				tRNA Charging	6.1.1.18
				UMP Biosynthesis	6.3.5.5
				UTP and CTP de novo Biosynthesis	6.3.4.2
				Glutamine Biosynthesis	6.3.4.1
				UDP-N-acetyl-D-Glucosamine Biosynthesis II	2.6.1.16
Glycerol	18602 ± 16884	2070 ± 900.1	0.3660	Triacylglycerol Degradation	3.1.1.23
				CDP-diacylglycerol Biosynthesis	2.7.1.30
				Glycerol degradation	2.7.1.30
Glycine	201.8 ± 43.62	375.7 ± 37.64	0.0166	5-aminoimidazole Ribonucleotide Biosynthesis	6.3.4.13
				Bile Acid Biosynthesis, Neutral Pathway	2.3.1.65
				Bupropion Degradation	RXN66-185
				Creatine Biosynthesis	2.1.4.1
				Glutathione Biosynthesis	6.3.2.3
				Tetrapyrrole Biosynthesis	2.3.1.37
				Glutathione-mediated Detoxification	3.4.11.2
				4-hydroxy-2-nonenal Detoxification	3.4.11.2
				γ-glutamyl cycle	3.4.13.18
				Superpathway of Choline Degradation to L-serine	RXN66-577
				Glycine Betaine Degradation	RXN66-577
				L-carnitine Biosynthesis	RXN-9896
				Leukotriene Biosynthesis	3.4.13.19
				Folate Transformations	2.1.2.1

				Folate Polyglutamylation	2.1.2.1
				dTMP de novo Biosynthesis	2.1.2.1
				Serine Biosynthesis	2.1.2.1
				Glycine Betaine Degradation	2.1.2.1
				Superpathway of Choline Degradation to L-serine	2.1.2.1
				Glycine Biosynthesis	2.6.1.44
				Glycine Cleavage	1.4.4.2
Histidine	145.7 ± 12.39	157.7 ± 15.71	0.5631	Carnosine Biosynthesis	6.3.2.11
				Homocarnosine Biosynthesis	6.3.2.11
				Histidine Degradation	4.3.1.3
				Histidine Degradation	6.1.1.21
				γ-glutamyl Cycle	2.3.2.2
				Leukotriene Biosynthesis	2.3.2.2
				S-methyl-5-thio-α-D-ribose 1-phosphate Degradation	2.6.1.88
				Histamine Biosynthesis	4.1.1.22
Isoleucine	560.5 ± 31.88	607.9 ± 45.8	0.4203	tRNA Charging	6.1.1.15
				Leukotriene Biosynthesis	2.3.2.2
				γ-Glutamyl Cycle	2.3.2.2
				S-methyl-5-thio-α-D-ribose 1-phosphate Degradation	2.6.1.88
				Isoleucine Degradation	2.6.1.42
Lactate	15947 ± 1430	15426 ± 3464	0.8928	Methylglyoxal Degradation I and VI	1.1.2.4 3.1.2.6 1.1.5-
Leucine	382.3 ±	452.4 ±	0.2122	Leucine Degradation	2.6.1.42 2.6.1.6

	31.67	40.85		tRNA Charging	6.1.1.4
				γ -glutamyl Cycle	2.3.2.2
				Leukotriene Biosynthesis	2.3.2.2
				S-methyl-5-thio- α -D-ribose 1-phosphate Degradation	2.6.1.88
Lysine	532.8 \pm 31.74	573 \pm 44.53	0.4839	Lysine Degradation I (Saccharopine Pathway)	1.5.1.8
				Lysine Degradation II (Pipicolate Pathway)	RXN66-565
				tRNA Charging	6.1.1.6
				Leukotriene Biosynthesis	2.3.2.2
				γ -glutamyl Cycle	2.3.2.2
				S-methyl-5-thio- α -D-ribose 1-phosphate Degradation	2.6.1.88
Methanol	20.44 \pm 1.426	20.41 \pm 1.556	0.9878	N/A	N/A
Methionine	106.4 \pm 11.1	142.7 \pm 9.139	0.0354	S-adenosyl-L-methionine Biosynthesis	2.5.1.6
				Methionine Degradation	2.5.1.6
				S-methyl-5-thio- α -D-ribose 1-phosphate Degradation	2.6.1.88
				tRNA Charging	6.1.1.10
				γ -glutamyl Cycle	2.3.2.2
				Leukotriene Biosynthesis	2.3.2.2
				7-(3-amino-3-carboxypropyl)-wyosine Biosynthesis	4.1.3.44
				Folate Transformations	2.1.1.13
				Methionine Salvage	2.1.1.13
				Superpathway of Choline Degradation to L-serine	2.1.1.5
				Methionine Salvage	2.1.1.5
					2.1.1.10
				Glycine Betaine Degradation	2.1.1.5

				Lipoate Biosynthesis and Incorporation	2.8.1.8
O-Phosphocholine	0.777 8 ± 0.777	5.456 ± 1.47	0.0227	Phosphatidylcholine Biosynthesis	2.7.7.15
					2.7.1.32
				Phospholipases	3.1.4.3
				Sphingomyelin Metabolism/ Ceramide Salvage	3.1.4.12
Phenylalanine	234.9 ± 23.62	273 ± 25.74	0.3079	Phenylalanine Degradation	1.14.16.1
				tRNA Charging	6.1.1.20
				S-methyl-5-thio- α -D-ribose 1-phosphate Degradation	2.6.1.88
				γ -glutamyl Cycle	2.3.2.2
				Leukotriene Biosynthesis	2.3.2.2
Proline	606.9 ± 138.1	141.4 ± 41.36	0.0121	Proline Degradation	1.5.5.2
				tRNA Charging	6.1.1.15
				Proline Biosynthesis	1.5.1.2
Pyroglutamate	1548 ± 128.1	1625 ± 187.5	0.7457	γ -glutamyl Cycle	3.5.2.9
					2.3.2.4
Pyruvate	97.96 ± 9.939	1015 ± 122.8	0.0003	7- (3-amino- 3- carboxypropyl)- Wyosine Biosynthesis	4.1.3.44
				Gluconeogenesis	6.4.1.1
				Pyruvate Decarboxylation to Acetyl-CoA	1.2.4.1
				4-hydroxyproline Degradation	4.1.3.16
				Glutathione-mediated Detoxification	4.4.1.6
				L-cysteine Degradation I	2.7.1.40
				L-cysteine Degradation II	3.13.1-
				L-serine Degradation	2.8.1.2
				Methylglyoxal Degradation I	3.5.99.10
				Alanine Biosynthesis	1.5.-

				Degradation	
				Glycine Degradation	1.1.2.4
				Alanine Biosynthesis/ Degradation	2.6.1.2
				Glycine Biosynthesis	2.6.1.44
				Lactate Fermentation	1.1.1.27
Threonine	595.6 ± 26.51	617.9 ± 34.7	0.6227	Threonine Degradation	4.3.1.19
				tRNA Charging	6.1.1.3
				γ-glutamyl Cycle	2.3.2.2
				Leukotriene Biosynthesis	2.3.2.2
				S-methyl-5-thio-α-D-ribose 1-phosphate Degradation	2.6.1.88
Tryptophan	16.96 ± 11.31	45.57 ± 12.51	0.1283	Tryptophan Degradation to 2-amino-3- carboxymuconate Semialdehyde	1.13.11.11- 52
				Serotonin and Melatonin Biosynthesis	1.14.16.4
				tRNA Charging	6.1.1.2
				Tryptophan Degradation X	4.1.1.28
Tyrosine	451 ± 25.72	443.5 ± 30.42	0.8554	(S)-Reticuline Biosynthesis	4.1.1.25
				4-hydroxybenzoate Biosynthesis	2.6.1.57
				Tyrosine Degradation	2.6.1.57
				Catecholamine Biosynthesis	1.14.16.2
				L-dopachrome Biosynthesis	1.14.18.1
				tRNA Charging	6.1.1.1
Valine	604.6 ± 38.59	666.5 ± 50.76	0.3597	tRNA Charging	6.1.1.9
				Valine Degradation	2.6.1.42
				γ-glutamyl cycle	2.3.2.2
				Leukotriene Biosynthesis	2.3.2.2
				S-methyl-5-thio-α-D-ribose 1-phosphate Degradation	2.6.1.88

Table A.1 – Metabolites Secreted by Huh7.5 Cells Cultured in 2% HS Supplemented or 10% FBS Supplemented Media. Huh7.5 cells were differentiated in media containing HS for 21 days then placed in serum free media. The supernatant was collected after 24 hours and analyzed using NMR. The concentration was reported in μM with the standard deviation. A student t test was used to determine statistical significance. Significant results were defined as a $p < 0.05$ and are highlighted in orange. The pathways that consume or produce the metabolites are listed. The EC number is a classification of the chemical reaction that is catalyzed by an enzyme. The suspected dominant pathway is highlighted in green.

Compound	Concentration of metabolites detected in HCV infected and uninfected cells grown in HS (μM)		
	HCV+	HCV-	P value T Test
2-Oxoisocaproate	43.62 \pm 1.693	33.1 \pm 6.76	0.1699
3-Hydroxybutyrate	10.14 \pm 6.212	74.03 \pm 15.01	0.0043
3-Hydroxyisovalerate	9.1 \pm 2.522	49.12 \pm 14.65	0.0274
3-Methyl-2-oxovalerate	53.72 \pm 2.812	45 \pm 7.682	0.3174
Acetoacetate	17.12 \pm 4.874	145.9 \pm 39.35	0.0117
Acetate	40.51 \pm 3.734	30.76 \pm 1.148	0.0371
Acetone	52.98 \pm 8.451	64.56 \pm 7.2	0.3275
Alanine	373.9 \pm 41.76	587.8 \pm 57.99	0.0172
Arginine	244.1 \pm 19.62	108.2 \pm 50.75	0.0371
Choline	1.444 \pm 1.444	0 \pm 0	0.3466
Ethanol	1171 \pm 536.8	1387 \pm 665	0.8088
Formate	211.6 \pm 5.457	294.3 \pm 10.54	0.0001
Glucose	16552 \pm 1062	11932 \pm 1550	0.0393
Glutamate	43.29 \pm 27.29	0 \pm 0	0.1514
Glutamine	1197 \pm 134.1	1062 \pm 172.1	0.5531
Glycerol	1060 \pm 520.2	18602 \pm 16884	0.3391
Glycine	354.9 \pm 17.97	201.8 \pm 43.62	0.0118
Histidine	163.5 \pm 10.58	145.7 \pm 12.39	0.3067
Isoleucine	631.7 \pm 32.4	560.5 \pm 31.88	0.1561

Lactate	10570 ± 742.2	15947 ± 1430	0.0103
Leucine	474.3 ± 33.69	382.3 ± 31.67	0.0818
Lysine	604.1 ± 34.34	532.8 ± 31.74	0.1660
Methanol	19.32 ± 1.381	20.44 ± 1.426	0.5875
Methionine	155.7 ± 7.281	106.4 ± 11.1	0.0059
O-Phosphocholine	11.63 ± 1.244	0.7778 ± 0.7778	<0.0001
Phenylalanine	321.5 ± 21.76	234.9 ± 23.62	0.0272
Proline	211.7 ± 35.06	606.9 ± 138.1	0.0242
Pyroglutamate	211.7 ± 35.06	606.9 ± 138.1	0.0242
Pyruvate	1576 ± 128.7	1548 ± 128.2	0.8829
Threonine	198.9 ± 107.6	264.8 ± 167.1	0.7485
Tryptophan	47.61 ± 13.27	16.96 ± 11.31	0.1167
Tyrosine	433.6 ± 17.49	451 ± 25.72	0.5920
Valine	692.2 ± 30.66	604.6 ± 38.59	0.1133

Table A.2 – Metabolites Secreted by Huh7.5 Cells Cultured in 2% HS Supplemented or 10% FBS Supplemented Media. Huh7.5 cells were cultured in media containing HS for 21 days with or without HCV infection. Prior to collecting the supernatant for analysis, cells are first placed in serum free media and incubated at 37°C. The supernatant was collected after 24 hours and analyzed using NMR. The concentration was reported in µM with the standard deviation. A student t test was used to determine statistical significance. Significant results were defined as a p<0.05 and are highlighted in orange.

